

1 **European pollen-based REVEALS land-cover reconstructions for the** 2 **Holocene: methodology, mapping and potentials**

3
4 Esther Githumbi^{1,2}, Ralph Fyfe³, Marie-Jose Gaillard², Anna-Kari Trondman^{2,4}, Florence Mazier⁵, Anne-
5 Birgitte Nielsen⁶, Anneli Poska^{1,7}, Shinya Sugita⁸, Jessie Woodbridge³, Julien Azuara⁹, Angelica
6 Feurdean^{10,11}, Roxana Grindean^{11,12}, Vincent Lebreton⁹, Laurent Marquer¹³, Nathalie Nebout-
7 Combourieu⁹, Miglè Stančikaitė¹⁴, Ioan Tanțău¹¹, Spassimir Tonkov¹⁵, Lyudmila Shumilovskikh¹⁶, and
8 LandClimII data contributors¹⁷⁺.

9
10 ¹Department of Physical Geography and Ecosystem Science, University of Lund, 22362 Lund, Sweden

11 ²Department of Biology and Environmental Science, Linnaeus University, 39182 Kalmar, Sweden

12 ³School of Geography, Earth and Environmental Sciences, University of Plymouth, PL4 8AA Plymouth, United Kingdom

13 ⁴Division of Education Affairs, Swedish University of Agricultural Science (SLU), 23456 Alnarp, Sweden

14 ⁵Environmental Geography Laboratory, GEODE UMR 5602 CNRS, Université de Toulouse Jean Jaurès, 31058 Toulouse,
15 France

16 ⁶Department of Geology, Lund University, 22100 Lund, Sweden

17 ⁷Department of Geology, Tallinn University of Technology, 19086 Tallinn, Estonia

18 ⁸Institute of Ecology, Tallinn University of Technology, 10120 Tallinn, Estonia

19 ⁹Département Homme et Environnement, UMR 7194 Histoire Naturelle de l'Homme Préhistorique, 75013 Paris, France

20 ¹⁰Senckenberg Biodiversity and Climate Research Centre (BiK-F), 60325 Frankfurt am Main, Germany

21 ¹¹Department of Geology, Faculty of Biology and Geology, Babeş-Bolyai University, 400084 Cluj-Napoca, Romania

22 ¹² Institute of Archaeology and History of Arts, Romanian Academy, Cluj-Napoca, 400015, Romania

23 ¹³Department of Botany, University of Innsbruck, 6020 Innsbruck, Austria

24 ¹⁴Institute of Geology and Geography, Vilnius University, Vilnius, LT-03101 Vilnius, Lithuania

25 ¹⁵Department of Botany, Sofia University St. Kliment Ohridski, 1164 Sofia, Bulgaria

26 ¹⁶Department of Palynology and Climate Dynamics, Georg-August-University, 37073 Göttingen, Germany

27 ¹⁷⁺Team list

28 +A full list of authors appears at the end of the paper.

29

30 *Correspondence to:* Esther Githumbi (esther.githumbi@lnu.se)

31 **Abstract.** Quantitative reconstructions of past land-cover are necessary to determine the processes involved in climate-human-
32 land interactions. We present the first temporally continuous and most spatially extensive pollen-based land-cover
33 reconstruction for Europe over the Holocene (last 11,700 cal yr BP). We describe how vegetation cover has been quantified
34 from pollen records at a 1°x1° spatial scale using the ‘Regional Estimates of VEgetation Abundance from Large Sites’
35 (REVEALS) model. REVEALS calculates estimates of past regional vegetation cover in proportions or percentages.
36 REVEALS has been applied to 1128 pollen records across Europe and part of the Eastern Mediterranean-Black Sea-Caspian-
37 Corridor (30°-75°N, 25°W-50°E) to reconstruct the percentage cover of 31 plant taxa assigned to 12 plant functional types
38 (PFTs) and 3 land-cover types (LCTs). A new synthesis of relative pollen productivities (RPPs) for European plant taxa was
39 performed for this reconstruction. It includes multiple RPP values (≥ 2 values) for 39 taxa, and single values for 15 taxa (total
40 of 54 taxa). To illustrate this, we present distribution maps for five taxa (*Calluna vulgaris*, *Cerealia-t*, *Picea abies*, deciduous
41 *Quercus t.* and evergreen *Quercus t.*) and three land-cover types (open land-OL, evergreen trees-ET and summer-green trees-
42 ST) for eight selected time windows. The reliability of the REVEALS reconstructions and issues related to the interpretation
43 of the results in terms of landscape openness and human-induced vegetation change are discussed. This is followed by a review
44 of the current use of this reconstruction and its future potential utility and development. REVEALS data quality are primarily
45 determined by pollen count data (pollen count/sample, pollen identification and chronology) and site type/number (lake or
46 bog, large or small, 1 site vs multiple sites) used for REVEALS analysis (for each grid cell). A large number of sites with high
47 quality pollen count data will produce more reliable land-cover estimates with lower standard errors compared to a low number
48 of sites with lower quality pollen count data. The REVEALS data presented here can be downloaded from
49 <https://doi.pangaea.de/10.1594/PANGAEA.937075> (Fyfe et al., 2022).

50

51 **1 Introduction**

52 The reconstruction of past land cover at global, continental and sub-continental scales is essential for the evaluation of climate
53 models, land-use scenarios and the study of past climate – land cover interactions. Vegetation plays a significant role within
54 the climate system through biogeochemical and biogeophysical feedbacks and forcings (Foley, 2005; Gaillard et al., 2015,
55 2010b, 2018; Strandberg et al., 2014). Land use has modified the land cover of Europe over Holocene timescales at local,
56 regional and continental scales (Roberts et al., 2018; Trondman et al., 2015; Woodbridge et al., 2018). Concerted efforts have
57 been made to model land-use and land-cover change (LULCC) over Holocene time scales (e.g. HYDE 3.2 (Klein Goldewijk
58 et al., 2017) and KK10 (Kaplan et al., 2011)). KK10 has been used to assess the impact of the scale of deforestation between
59 6000 and 200 cal yr BP in Europe on regional climate in the modelling study of Strandberg et al (2014). The KK10-inferred
60 land-cover change resulted in cooling or warming of regional climate by 1° to 2° depending on the season (winter or summer)
61 and/or geographical location. Major changes in the forest cover of Europe over the Holocene may therefore have had a
62 significant impact on past regional climate, particularly those driven by deforestation since the start of agriculture during the
63 Neolithic period, the timing of which varies in different parts of Europe (Fyfe et al., 2015; Gaillard et al., 2015; Hofman-
64 Kamińska et al., 2019; Nosova et al., 2018; Pinhasi et al., 2005; de Vareilles et al., 2021). Estimating past land-cover change
65 can enable quantification of the scale at which human impact on terrestrial ecosystems perturbed the climate system. This in
66 turn allows us to consider when environmental changes moved beyond the envelope of natural variability (Ruddiman, 2003;
67 Ruddiman et al., 2016). We focus here on the role of LULCC in the climate system; anthropogenic land-cover change can
68 have broader consequences for other processes and lead to changes in erosion and fluvial systems (Downs and Piégay, 2019),
69 biodiversity (Barnosky et al., 2012), nutrient cycling (Guiry et al., 2018; McLauchlan et al., 2013), habitat exploitation by
70 megafauna (Hofman-Kamińska et al., 2019), and wider ecosystem functioning (Ellis, 2015; Stephens et al., 2019).

71 The Earth System Modelling (ESM) community use LULCC model scenarios, along with dynamic vegetation models, to
72 understand interactions between different components of the earth system in the past (Gilgen et al., 2019; He et al., 2014;
73 Hibbard et al., 2010; Smith et al., 2016). Disagreement between LULCC scenarios suggests that their evaluation is needed
74 using independent, empirical datasets (Gaillard et al., 2010a). Pollen-based reconstruction of past land cover represents
75 probably the best empirical data for this purpose, as fossil pollen is a direct proxy for past vegetation, and fossil pollen records
76 are ubiquitous across the continent of Europe (Gaillard et al., 2010a, 2018). The Landscape Reconstruction Algorithm (LRA)
77 with its two models Regional Estimates of VEgetation Abundance from Large Sites (REVEALS) (Sugita, 2007a) and LOcal
78 VEgetation Estimates (LOVE) (Sugita, 2007b) is the only current land-cover reconstruction approach based on pollen data that
79 effectively reduces the biases caused by the non-linear pollen-vegetation relationship due to differences in sedimentary
80 archives, basin size, inter-taxonomic differences in pollen productivity and dispersal characteristics, and spatial scales.
81 REVEALS and LOVE are mechanistic models that transform pollen count data to produce quantitative reconstructions of
82 regional (spatial scale $\geq 10^4$ km²) and local (spatial scale = relevant source area of pollen *sensu* Sugita (1993), \geq ca. 1-5 km
83 radius) vegetation cover, respectively (Sugita, 2007a; 2007b). The REVEALS model was first tested and validated in southern

84 Sweden (Hellman et al., 2008a, 2008b) and later in other parts of Europe and the world (Mazier et al., 2012; Soepboer et al.,
85 2010; Sugita et al., 2010).

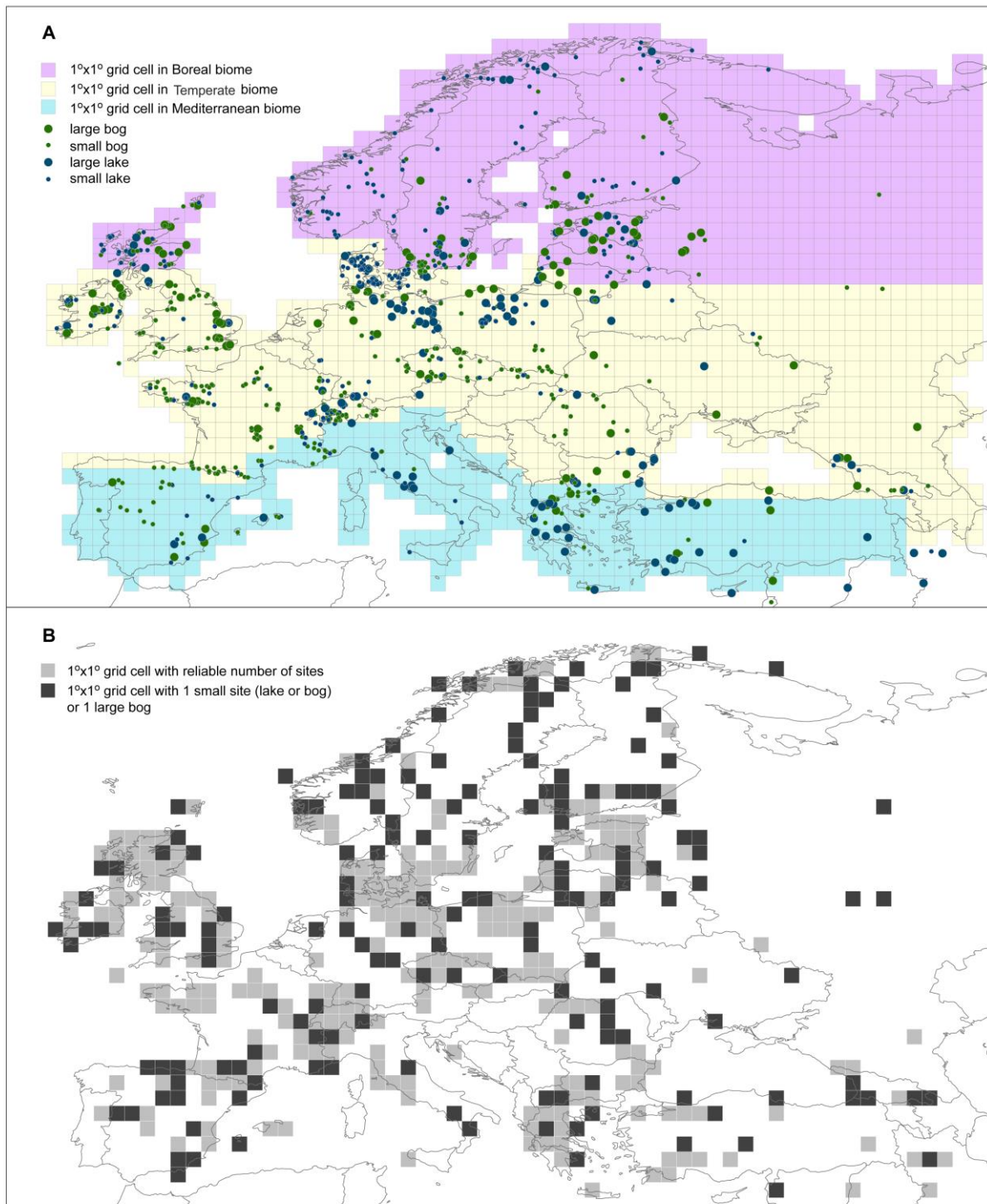
86 The first pollen-based REVEALS reconstruction of plant cover over the Holocene covering a large part of Europe (Trondman
87 et al., 2015) was used for the assessment of LULCC scenarios (Kaplan et al., 2017), and helped to evaluate climate model
88 simulations using LULCC scenarios (Strandberg et al., 2014). A comparison between REVEALS-based open land cover from
89 pollen records and Holocene deforestation simulated by HYDE 3.1 and KK10 showed that the REVEALS reconstructions
90 were more similar to KK10 than HYDE 3.1 scenarios (Kaplan et al., 2017). Therefore, estimates of past plant cover from fossil
91 pollen assemblages are essential to both test and constrain LULCC models, and also provide alternative inputs to Earth System
92 Models (ESMs), Regional Climate Models (RCMs) and ecosystem models (Gaillard et al., 2018; Harrison et al., 2020). This
93 allows improved assessments of biogeophysical and biogeochemical forcings on climate due to LULCC over the Holocene
94 (Gaillard et al., 2010; Harrison et al., 2020; Ruddiman et al., 2016; Strandberg et al., 2014).

95 Europe is of particular interest as one of the global regions that has experienced major human-induced land-cover
96 transformations. Europe has large N-S and W-E gradients in modern and historical climate and land use (Marquer et al., 2014,
97 2017). Early agriculture dates from the start of the Holocene in the SE Mediterranean region (Palmisano et al., 2019; Roberts
98 et al., 2019; Shennan, 2018), and human impact on vegetation across most of Europe is characterized by early land-cover
99 changes through agriculture and the use of fire (Feurdean et al., 2020; Marquer et al., 2014; Strandberg et al., 2014; Trondman
100 et al., 2015). There is therefore a clear need to extend quantitative vegetation reconstruction to the whole of Europe, including
101 for the first time the Mediterranean region and additional areas of eastern Europe. The increase in the spatial coverage of sites
102 and temporal scale to the entire Holocene to capture transient vegetation change at sub-millennial time scales is vital to capture
103 information on the transformation of the biosphere by human actions. Europe has a deep history of pollen data production
104 (Edwards et al., 2017) and an open-access repository for pollen records (the European Pollen Database (EPD)) as well as
105 regional pollen repositories (list of databases and access links in section 2.2 and the Data Availability section). These data
106 repositories result in abundant pollen records that can be used for data-driven reconstructions of past vegetation patterns at
107 continental scales. Pollen based vegetation reconstructions for Europe have used community-level approaches (Huntley, 1990),
108 biomization methods (Davis et al., 2015; Prentice et al., 1996), modern analogue techniques (MAT; Zanon et al., 2018), and
109 pseudobiomization (Fyfe et al., 2010, 2015; Woodbridge et al., 2014). These approaches capture the major trends in vegetation
110 patterns over the course of the Holocene (Roberts et al., 2018; Sun et al., 2020) and biomization methods have proved useful
111 for evaluation of climate model results (Prentice and Webb III, 1998). The results of these forms of pollen data manipulation
112 either classify pollen data into discrete classes (e.g. biomization, pseudobiomization) or are semi-quantitative, capturing
113 relative change through time based on all pollen taxa within a sample. They cannot achieve reconstructions of the cover of
114 evergreen versus summer-green trees, for example, or the cover of individual tree and herb taxa. Although useful in
115 summarising palynological change over time based on entire pollen assemblages, such outputs are of limited use when
116 differentiation of plant functional types (PFTs) is necessary (Strandberg et al., 2014). Forest cover over the Holocene inferred
117 from pollen records using these approaches differs from forest cover obtained with REVEALS (Hellman et al., 2008a; Roberts

118 et al., 2018); these differences confirm that REVEALS corrects biases resulting from the non-linearity of the pollen-vegetation
119 relationship.

120 In this paper we present the results of the second generation of REVEALS-based reconstruction of plant cover over the
121 Holocene in Europe, after the first reconstruction published by Trondman et al. (2015). This second generation reconstruction
122 is, to date, the most spatially and temporally complete estimate of plant cover for Europe across the Holocene. As with the
123 Trondman et al. (2015) reconstruction, this new dataset is specifically designed to be used in climate modelling. It is performed
124 at a spatial scale of $1^{\circ} \times 1^{\circ}$ (ca. 100 km \times 100 km) across 30° - 75° N, 25° W- 50° E (Europe and part of the Eastern Mediterranean-
125 Black Sea-Caspian-Corridor) (Fig. 1). The number of pollen records used (1128), the area covered and time length (entire
126 Holocene) are a significant advance on the results presented in Trondman et al. (2015), which used 636 pollen records covering
127 NW Europe (including Poland and the Czech Republic but excluding western Russia and the Mediterranean area), and
128 produced estimates for five time windows (in cal yr BP, hereafter abbreviated BP): 6200-5700, 4200-3700, 700-350, 350-100
129 BP and 100 BP to present. Marquer et al. (2014, 2017) produced continuous REVEALS reconstructions over the entire
130 Holocene, however, only for transects of individual sites (19 pollen records) and groups of grid cells around them.

131



133 2 Methods

134 2.1 REVEALS model and parameters

135 The REVEALS model (Sugita, 2007a) is a generalized version of the R-Value model of Davis (Davis, 1963). The development
136 of pollen-vegetation modelling from the R-Value model, via the ERV models of Andersen (Andersen, 1970) and Parsons and
137 Prentice (Parsons and Prentice, 1981) through to the REVEALS model is described in detail in numerous earlier papers
138 (Broström et al., 2004; Bunting et al., 2013b; Sugita, 1993, 2007a).

139 Using simulations, Sugita (2007a) showed that “large lakes” represent regional vegetation, i.e. between-lake differences in
140 pollen assemblages are very small, which was the case for lakes ≥ 50 ha in the simulations (Sugita, 2007a). Tests using modern
141 pollen data from surface lake sediments have shown that pollen assemblages from lakes ≥ 50 ha are appropriate to estimate
142 regional plant cover using the REVEALS model (e.g. tests by Hellman et al. (2008a and b) in southern Sweden and by Sugita
143 et al. (2010) in northern America).

144 The REVEALS model (equation 1) calculates estimates of regional vegetation abundance in proportions or percentage cover
145 using fossil pollen counts from “large lakes” (Sugita, 2007a).

$$146 \hat{V}_i = \frac{n_{i,k} / \hat{\alpha}_i \int_R^{Z_{\max}} g_i(z) dz}{\sum_{j=1}^m \left(\frac{n_{j,k}}{\hat{\alpha}_j \int_R^{Z_{\max}} g_j(z) dz} \right)} = \frac{n_{i,k} / \hat{\alpha}_i K_i}{\sum_{j=1}^m (n_{j,k} / \hat{\alpha}_j K_j)} \quad (1)$$

- 147 • \hat{V}_i is the estimate of the regional vegetation abundance for taxon i (proportion or percentage).
- 148 • $n_{i,k}$ is the pollen count of taxon i at site k .
- 149 • $\hat{\alpha}_i$ is the estimate of pollen productivity (relative pollen productivity, RPP) for taxon i .
- 150 • z is the distance between the centre of the sedimentary basin and the pollen source.
- 151 • $g_i(z)$ is the pollen dispersal/deposition function for taxon i expressed as a function of distance z . Fall speed of pollen
152 (FSP), wind speed and atmospheric conditions are parameters needed to calculate this function.
- 153 • R is the radius of the sedimentary basin.
- 154 • Z_{\max} is the maximum distance within which most pollen originates (i.e. the maximum spatial extent of the regional
155 vegetation).
- 156 • m is the total number of taxa included,
- 157 • $K_i = \int_R^{Z_{\max}} g_i(z) dz$ is the “pollen dispersal-deposition coefficient” of taxon i from the border of the study site
158 (distance from the pollen sample corresponding to the radius R of the lake) to Z_{\max} .

160 The assumptions of the REVEALS model are listed in Sugita (2007a). Using simulations Sugita (2007a) demonstrated that, in
161 theory, the model can also be applied to pollen records from multiple “small lakes” (< 50 ha), i.e. lakes for which between lake
162 differences in pollen assemblages can be large. However, the REVEALS estimates using pollen records from “small lakes”
163 generally have larger standard errors (SE) than those based on pollen data from large lakes. The latter was demonstrated for
164 empirical pollen records from large lakes versus small sites (lakes and bogs) by Trondman et al. (2016) in southern Sweden
165 and Mazier et al. (2012) in the Czech Republic. Although the application of the model to pollen data from bogs violates the
166 model assumption that no plants grow on the basin, REVEALS can be applied using models of pollen dispersal and deposition
167 for lakes or bogs. The Prentice model (Prentice, 1985; 1988) describes deposition of pollen at a single point in a deposition
168 basin and is suitable for pollen records from bogs. Sugita (1993) developed the “Prentice-Sugita model” that describes pollen
169 deposition in a lake, i.e. on its entire surface with subsequent mixing in the water body before deposition at the lake bottom.
170 The original versions of both models use the Sutton model of pollen dispersal, i.e. a Gaussian plume model from a ground-
171 level source under neutral atmospheric conditions (Sutton, 1953). A Lagrangian stochastic model of dispersion has also been
172 introduced as an alternative for the description of pollen dispersal in models of the pollen-vegetation relationship in general,
173 and in the REVEALS model in particular (Theuerkauf et al., 2012, 2016). It is difficult, in both theory and practice, to eliminate
174 the effects of pollen coming from plants growing on sedimentary basins (e.g. Poaceae and Cyperaceae in bogs) on regional
175 vegetation reconstruction. Previous studies have assessed the impacts of the violation of this assumption on REVEALS
176 outcomes (Mazier et al., 2012; Sugita et al., 2010; Trondman et al., 2016, 2015). An empirical study in southern Sweden
177 (Trondman et al., 2016) indicated that REVEALS estimates based on pollen records from multiple small sites (lakes and/or
178 bogs) are similar to the REVEALS estimates based on pollen records from large lakes in the same region. The results also
179 suggested that increasing the number of pollen records significantly decreased the standard error of the REVEALS estimates,
180 as expected based on simulations (Sugita, 2007a). It is therefore appropriate to use pollen records from small bogs to increase
181 the number of pollen records included in a REVEALS reconstruction, following the protocol of the first generation REVEALS
182 reconstruction for Europe (Mazier et al., 2012; Trondman et al., 2015). However, REVEALS estimates of plant cover using
183 pollen assemblages from large bogs only should be interpreted with great caution (Mazier et al., 2012; see also section 4,
184 Discussion).

185 The inputs needed to run the REVEALS model are: original pollen counts; relative pollen productivity estimates (RPPs) and
186 their standard deviation; fall speed of pollen (FSP); basin type (lake or bog); size of basin (radius); maximum extent of regional
187 vegetation; wind speed (m/s); and atmospheric conditions. FSP can be calculated using measurements of the pollen grains and
188 Stokes’ law (Gregory, 1973). RPPs of major plant taxa can be estimated using datasets of modern pollen assemblages and
189 related vegetation, and the Extended R-Value model (e.g. Mazier et al., 2008). RPPs exist for a large number of European
190 plant taxa, and syntheses of FSPs and RPPs were published earlier by Broström et al. (2008) and Mazier et al. (2012). The
191 latter was used in the “first generation” REVEALS reconstruction (Trondman et al., 2015). A new synthesis of European RPPs

192 was performed for this “second generation” reconstruction (Appendices A, B, and C). Preparation of data from individual
193 pollen records, and the values of model parameters used, are described below (sections 2.2 and 2.3).

194 **2.2 Pollen records – data compilation and preparation**

195 1143 pollen records from 29 European countries and the Eastern Mediterranean-Black Sea-Caspian-Corridor were obtained
196 from databases and individual data contributors. The contributing databases include: the European Pollen Database (Fyfe et
197 al., 2009; Giesecke et al., 2014); the Alpine Palynological database (ALPADABA; Institute of Plant Sciences, University of
198 Bern; now also archived in EPD); the Czech Quaternary palynological database (PALYCZ; Kuneš et al., 2009); PALEOPYR
199 (Lerigoleur et al., 2015); and datasets compiled within synthesis projects from the Mediterranean region (Fyfe et al., 2018;
200 Roberts et al., 2019) and the Eastern Mediterranean-Black Sea-Caspian-Corridor (EMBSecBIO project; Marinova et al., 2018)
201 (see Fig. 1 for map and Data availability section for data location and team list for individual pollen data contributors). We
202 followed the protocols and criteria published in Mazier et al. (2012) and Trondman et al. (2015) for selection of pollen records
203 and application of the REVEALS model. Available pollen records were filtered based on criteria including basin type (to
204 exclude archaeological sites and marine records) and quality of chronological control (excluding sites with poor age-depth
205 models or fewer than three radiocarbon dates). This resulted in 1128 pollen records from lakes and bogs, both small and large.
206 The rationale behind the use of pollen records from small sites is based on the knowledge that REVEALS estimates based on
207 pollen records from multiple sites provide statistically validated approximations of the regional cover of plant taxa (e.g.
208 Trondman et al., 2016; see details under section 2.1 on the REVEALS model).

209 The taxonomy and nomenclature of pollen morphological types from the 1128 pollen records were harmonised. The pollen
210 morphological types were then consistently assigned to one of 31 RPP taxa (Table 1; see section 2.3 and Appendices A-C for
211 details on the RPP dataset used in this study), following the protocol outlined in Trondman et al. (2015: SI-2 with examples of
212 harmonization between pollen-morphological types and RPP taxa). This process takes into account plant morphology, biology,
213 and ecology of the species that are included in each pollen morphological type. Consequently, RPP-harmonized pollen count
214 data were produced for each of the 1128 pollen records. It should be noted that the EMBSecBIO data does not contain pollen
215 counts from cultivars, i.e. pollen from cereals and cultivated trees were deleted from the pollen records (Marinova et al., 2018).
216 Therefore, the cover of agricultural land (represented by cereals in this reconstruction) will always be zero in the Eastern
217 Mediterranean-Black Sea-Caspian-Corridor in grid cells with only pollen records from EMBSecBIO, even though agriculture
218 did occur in the region from the early Neolithic.

219 For the application of REVEALS, an age-depth model (in cal yr BP) is required for each pollen record. We used the author’s
220 original published model, the model available in the contributing database or, where necessary, a new age-depth model was
221 constructed following the approach in Trondman et al. (2015). The age-depth model for each pollen record is used to aggregate
222 RPP-harmonised pollen count data into 25 time windows throughout the Holocene following a standard time division used in
223 Mazier et al. (2012) and Trondman et al. (2015), which were later adopted by the Past Global Changes (PAGES) LandCover6k
224 working group (Gaillard et al., 2018). The first three time windows (present–100 BP (where present is the year of coring), 100–

225 350 BP; 350-700 BP) capture the major human-induced land-cover changes since the Early Middle Ages. Subsequent time
226 windows are contiguous 500-year long intervals (e.g. 700-1200 BP, 1200-1700 BP, 1700-2200 BP, etc.) with the oldest interval
227 representing the start of the Holocene (11200-11700 BP). The use of 500-year long time windows is motivated by the necessity
228 to obtain sufficiently large pollen counts for reliable REVEALS reconstructions. Since the size of the error on the REVEALS
229 estimate partly depends on the size of the pollen count (Sugita, 2007a), the length of the time window should be a reasonable
230 compromise to ensure both a useful time resolution of the reconstruction and an acceptable reliability of the REVEALS
231 estimate of plant cover (Trondman et al., 2015).

232 **Table 1: Land-cover types (LCTs) and Plant Functional Types (PFTs) according to Wolf et al. (2008) and their corresponding pollen**
 233 **morphological types. Fall speed of pollen (FSP) and the mean relative pollen productivity (RPP) estimates from the new RPP**
 234 **synthesis (see section 2.3 and Appendices A-C for details) with their standard errors in brackets (see text for more explanations).**
 235 ***The FSP values of evergreen *Quercus t.* and Mediterranean Ericaceae according to the original study (Mazier, unpublished) are**
 236 **0.015 and 0.051, respectively (see Appendix B, Table B.3). The value of 0.035 (FSP of deciduous *Quercus t.*) and 0.038 (FSP of boreal-**
 237 **temperate Ericaceae) were used instead (see discussion in section 4.2 for explanation). , t = type e.g. evergreen *Quercus t.* RPP used**
 238 **in this study are relative to grass pollen productivity where Poaceae = 1 (indicated in bold).**

Land-cover types (LCTs)	PFT	PFT definition	Plant taxa/Pollen-morphological types	FSP (m/s)	RPP (SD)
Evergreen trees (ET)	TBE1	Shade-tolerant evergreen trees	<i>Picea abies</i>	0.056	5.437 (0.097)
	TBE2	Shade-tolerant evergreen trees	<i>Abies alba</i>	0.12	6.875 (1.442)
	IBE	Shade-intolerant evergreen trees	<i>Pinus sylvestris</i>	0.031	6.058 (0.237)
	MTBE	Mediterranean shade-tolerant broadleaved evergreen trees	<i>Phillyrea</i>	0.015	0.512 (0.076)
			<i>Pistacia</i>	0.03	0.755 (0.201)
			Evergreen <i>Quercus t.</i>	0.035*	11.043 (0.261)
	TSE	Tall shrub, evergreen	<i>Juniperus communis</i>	0.016	2.07 (0.04)
	MTSE	Mediterranean broadleaved tall shrubs, evergreen	Ericaceae	0.038*	4.265 (0.094)
<i>Buxus sempervirens</i>			0.032	1.89 (0.068)	
Summer green trees (ST)	IBS	Shade-intolerant summer-green trees	<i>Alnus glutinosa</i>	0.021	13.562 (0.293)
			<i>Betula</i>	0.024	5.106 (0.303)
	TBS	Shade-tolerant summer-green trees	<i>Carpinus betulus</i>	0.042	4.52 (0.425)
			<i>Carpinus orientalis</i>	0.042	0.24 (0.07)
			<i>Castanea sativa</i>	0.01	3.258 (0.059)
			<i>Corylus avellana</i>	0.025	1.71 (0.1)
			<i>Fagus sylvatica</i>	0.057	5.863 (0.176)
			<i>Fraxinus</i>	0.022	1.044 (0.048)
			Deciduous <i>Quercus t.</i>	0.035	4.537 (0.086)
			<i>Tilia</i>	0.032	1.21 (0.116)
	<i>Ulmus</i>	0.032	1.27 (0.05)		
TSD	Tall shrub, summer-green	<i>Salix</i>	0.022	1.182 (0.077)	
Open land (OL)	LSE	Low shrub, evergreen	<i>Calluna vulgaris</i>	0.038	1.085 (0.029)
	GL	Grassland - all herbs	<i>Artemisia</i>	0.025	3.937 (0.146)
			Amaranthaceae/Chenopodiaceae	0.019	4.28 (0.27)
			Cyperaceae	0.035	0.962 (0.05)
			<i>Filipendula</i>	0.006	3 (0.285)
			Poaceae	0.035	1 (0)
			<i>Plantago lanceolata</i>	0.029	2.33 (0.201)
			<i>Rumex acetosa-t</i>	0.018	3.02 (0.278)
	AL	Agricultural land - cereals	Cerealia-t	0.06	1.85 (0.380)
			<i>Secale cereale</i>	0.06	3.99 (0.320)

239

240 2.3 Model parameter setting

241 For the purpose of this study, a new synthesis of the RPP values available for European plant taxa was performed in 2018-
242 2019 based on the latest synthesis by Mazier et al. (2012) and additional RPP studies published since then (Appendix A-C).
243 This synthesis provides new alternative RPP datasets for Europe, including or excluding plant taxa with dominant entomophily,
244 and with the important addition of plant taxa from the Mediterranean area (Appendix A, Table A1). The selection of RPP
245 studies, RPP values (shown in Appendix B, Tables B1 and B2) and calculation of mean RPP and their standard error (SD) for
246 Europe are explained in Appendix C. The location of studies included in the RPP synthesis is shown in Fig. C1 and related
247 information is provided in Table C1. The synthesis includes a total of 54 taxa for which RPP values are available (Tables B1
248 and B2), 39 taxa from studies in boreal and temperate Europe, and 15 taxa from studies in Mediterranean Europe of which
249 seven include exclusively sub-Mediterranean and Mediterranean taxa: *Buxus sempervirens*, *Carpinus orientalis*, *Castanea*
250 *sativa*, Ericaceae (Mediterranean species), *Phillyrea*, *Pistacia* and evergreen *Quercus* type. RPP values are available from both
251 boreal/temperate and Mediterranean Europe for seven taxa: i.e. Poaceae (reference taxon), *Acer*, *Corylus avellana*, Apiaceae,
252 *Artemisia*, *Plantago lanceolata* and Rubiaceae (Table B2). Table A1 presents the new RPP dataset for the 54 plant taxa and,
253 for comparison, the mean RPP values from Mazier et al. (2012) and from the recent synthesis by Wieczorek & Herzs Schuh
254 (2020). Moreover, comparison with the RPP values of three studies not used in our synthesis is shown in Table A2. For the
255 REVEALS reconstructions presented in this paper, we excluded strictly entomophilous taxa, which resulted in a total of 31
256 taxa (Table 1). The excluded taxa are Compositae (Asteraceae) SF Cichorioideae, *Leucanthemum (Anthemis)-t.*, *Potentilla-t.*,
257 *Ranunculus acris-t.*, and Rubiaceae. We included entomophilous taxa that are known to be characterised by some anemophily,
258 e.g. *Artemisia*, Amaranthaceae/Chenopodiaceae, Rubiaceae, and *Plantago lanceolata*. We excluded plant taxa with only one
259 RPP value except Chenopodiaceae, *Urtica*, *Juniperus*, and *Ulmus*, and the seven exclusively sub-Mediterranean and
260 Mediterranean taxa mentioned above.

261 The FSP values (Tables 1 and A1) for boreal and temperate plant taxa were obtained from the literature (Broström et al., 2008;
262 Mazier et al., 2012); these values were in turn extracted from Gregory (1973) for trees, and calculated based on pollen
263 measurements and Stokes' law for herbs (Broström et al., 2004). FSPs for Mediterranean taxa (*Buxus sempervirens*, *Castanea*
264 *sativa*, Ericaceae (Mediterranean species), *Phillyrea*, *Pistacia*, and *Quercus* evergreen type) were obtained by using pollen
265 measurements and Stokes' law (Mazier et al., unpublished); the FSP of *Carpinus betulus* (Mazier et al., 2012) was used for
266 *Carpinus orientalis* (Grindean et al., 2019).

267 The site radius was obtained from original publications where possible. Sites in the EMBSeCBIO were classified as small
268 (0.01-1 km²), medium (1.1-50 km²) or large (50.1-500 km²). These were assigned radii of 399m, 2921m and 10000 m,
269 respectively. Where a site's radius could not be determined from publication, it was geolocated in Google Earth and the area
270 of the site was measured. A radius value was extracted assuming that a site shape is circular (Mazier et al., 2012). A constant
271 wind speed of 3 m/s, assumed to correspond approximatively to the modern mean annual wind speed in Europe, was used
272 following Trondman et al. (2015). Z_{\max} (maximum extent of the regional vegetation) was set to 100 km. Z_{\max} and wind speed

273 influence on REVEALS estimates has been evaluated earlier in simulation and empirical studies (Gaillard et al., 2008; Mazier
274 et al., 2012; Sugita, 2007a), which support the values used for these parameters. Atmospheric conditions are assumed to be
275 neutral (Sugita, 2007a).

276 **2.4 Implementation of REVEALS**

277 REVEALS was implemented using the REVEALS function within the LRA R-package of Abraham et al. (2014) (see Code
278 availability, section 6). The function enables the use of deposition models for bogs (Prentice's model) and lakes (Sugita's
279 model), and two dispersal models (a Gaussian plume model, and a Lagrangian stochastic model taken from the DISCOVER
280 package (Theuerkauf et al., 2016)). Within this study, the Gaussian plume model was applied. The REVEALS model was run
281 on all pollen records within each $1^\circ \times 1^\circ$ grid cell across Europe. The REVEALS function is applied to lake and bog sites
282 separately within each $1^\circ \times 1^\circ$ grid cell, and combines results (if there is more than one pollen record per cell) to produce a
283 single mean cover estimate (in proportion) and mean standard error (SE) for each taxon. The formulation of the SE is found
284 in Appendix A of Sugita (2007a). The REVEALS SE accounts for the standard deviations on the relative pollen productivities
285 for the individual pollen taxa (Table 1) and the number of pollen grains counted in the sample (Sugita, 2007a). The uncertainties
286 of the averaged REVEALS estimates of plant taxa for a grid cell are calculated using the delta method (Stuart and Ord., 1994),
287 and expressed as the SEs derived from the sum of the within- and between-site variations of the REVEALS results in the grid
288 cell. The delta method is a mathematical solution to the problem of calculating the mean of individual SEs (see Li et al., 2020,
289 Appendix C, for formula and further details). Results of the REVEALS function are extracted by time window, producing 25
290 matrices of mean REVEALS land-cover estimates and 25 matrices of corresponding mean SEs for each of the 31 RPP taxa
291 and each grid cell. The 31 RPP taxa are also assigned to 12 plant functional types (PFTs) and three land-cover types (LCTs)
292 (Table 1), and their mean REVEALS estimates calculated. These PFTs follow Trondman et al. (2015), with the addition of
293 two PFTs for Mediterranean vegetation not reconstructed in earlier studies: Mediterranean shade-tolerant broadleaved
294 evergreen trees (MTBE) and Mediterranean broadleaved tall shrubs, evergreen (MTSE). The mean SE for LCTs and PFTs
295 including more than one plant taxon are calculated using the delta method (Stuart and Ord., 1994), as described above.

296 **2.5 Mapping of the REVEALS estimates**

297 To illustrate the information that the new REVEALS reconstruction provides, we present and describe (section 3) maps of the
298 REVEALS estimates (% cover) and their associated SEs for the three LCTs (Fig. 2 to 4) and five taxa for eight selected time
299 windows: the five taxa are *Cerealia-t* and *Picea abies* (Fig. 5 and 6), *Calluna vulgaris*, deciduous *Quercus* type (t.), and
300 evergreen *Quercus* t. (Fig. D1-D3). The selection of the five taxa and eight time windows is motivated essentially by notable
301 changes in the spatial distribution of these taxa through time, with higher resolution for recent times characterised by the largest
302 and most rapid human-induced changes in vegetation cover. For visualisation purposes, the estimates are mapped in nine %
303 cover classes. These fractions are the same for the three LCTs (Figures 2-4), and the mapped output can therefore be directly
304 compared. In contrast, the colour scales used for the five taxa vary between maps depending on the abundance of the PFT/taxon

305 (Fig. 5 and 6, D1-D3). Different taxa thus have different scales and maps cannot be directly compared. We visualise uncertainty
306 in our data by plotting the SE as a circle inside each grid cell; it is the coefficient of variation (CV, i.e. the standard error
307 divided by the REVEALS estimate). Circles are scaled to fill the grid cell if the SE is equal or greater than the mean REVEALS
308 estimate (i.e. $CV \geq 1$). Grid-based REVEALS results that are based on pollen records from just one large bog, or single small
309 bogs or lakes, provide lower quality results (see section 2.1 on the REVEALS model, and discussion section 4.1). The quality
310 of REVEALS land-cover estimates by grid cell and time window is provided in Table GC_quality_by_TW (see section 5, Data
311 availability). The percentage scale ranges we use here are different from those used in the maps of Trondman et al. (2015) and,
312 therefore, the data visualisation cannot be directly compared.

313 **3 Results**

314 The complete REVEALS land cover reconstruction dataset includes mean REVEALS values (in proportions) and their related
315 mean SE for 31 individual tree and herb taxa, twelve PFTs and three LCTs for each grid cell in 25 consecutive time windows
316 of the Holocene (11.7 k BP to present). Here, results are illustrated by maps of the three LCTs (Fig. 2-4) and five taxa (Fig. 5-
317 6, D1-D3). The presented maps are not part of the published dataset archived in the PANGAEA online public database (see
318 Data availability, section 5), they are examples of how the data can be visually presented and what they can be used for.

319 **3.1 Land-cover types**

320 The three land-cover types are evergreen trees (ET), summer-green trees (ST) and open land (OL). ET includes six PFTs which
321 are composed of nine pollen-morphological types (from here after referred to as taxa). ST includes three PFTs which are
322 composed of twelve taxa while OL includes three PFTs that are in turn composed of ten taxa (Table 1).

323 **3.1.1 Open Land (OL)**

324 At the start of the Holocene, open land (OL) (Fig. 2) has higher cover in western Europe where it generally exceeds 80%
325 compared with central Europe where it is more typically ~60%. There is a general decline in OL cover through the early
326 Holocene. At 5700-6200 BP most grid cells in central Europe have the lowest OL cover values between 10-50%. In western
327 Europe, whilst OL is generally reduced, several grid cells on the Atlantic fringe of northern Scotland persistently maintain 80-
328 90% OL cover. OL increases from the mid-Holocene, and by 2700-3200 BP the United Kingdom, France, Germany and the
329 Mediterranean region have grid cells recording OL values >70%. In central, northern and eastern Europe grid cells OL values
330 vary between 10 - 70% at 2700-3200 BP. Time windows from the last two millennia show a consistent increase in OL with
331 values >60% across most of central, southern and western Europe and 20-70% in northern Europe.



333 **Figure 1. Grid-based REVEALS estimates of Open Land (OL) cover for eight Holocene time windows. Percentage cover of open**
334 **land in 10% intervals represented by increasingly darker shades of green from 20%. Grey cells: cells without pollen data for the**
335 **time window, but with pollen data in other time windows. Circles in grid cells represent the coefficient of variation (CV; the standard**
336 **error divided by the REVEALS estimate). When $SE \geq$ REVEALS estimate, the circle fills the entire grid cell and the REVEALS**
337 **estimate is not different from zero. This occurs mainly where REVEALS estimates are low.**

338 **3.1.2 Evergreen Trees (ET)**

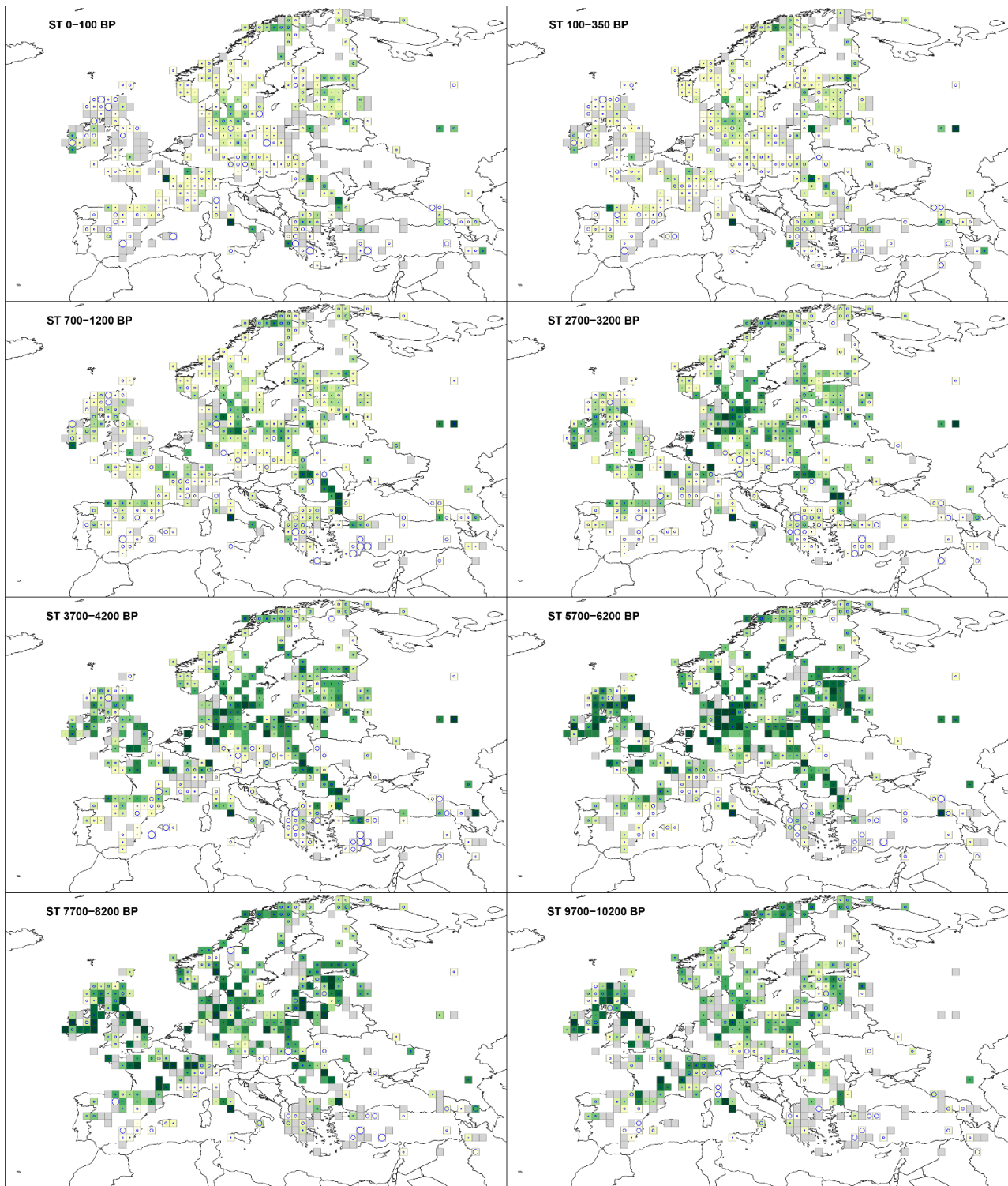
339 The cover of evergreen trees (ET) (Fig. 3) at 9700-10200 BP is <30% across Europe, and by 7700-8200 BP fewer than 30 grid
340 cells show ET >50%. ET cover slowly increases through the early Holocene and at 5700-6200 BP groups of grid cells in
341 southern Europe record >80%, while in northern Europe ET cover ranges between 10% and 60%. There is a consistent increase
342 in ET cover over Europe during the mid- and late-Holocene with ET cover peaking at 2700-3200 BP before starting to decline.
343 Across western parts of Europe, including the United Kingdom, western France, Denmark, and the Netherlands ET never
344 exceeds 20% cover.



346 **Figure 2. Grid-based REVEALS estimates of Evergreen Tress (ET) cover for eight Holocene time windows. Percentage cover of**
347 **Evergreen Trees in 10% intervals represented by increasingly darker shades of green from 20%. Grey cells: cells without pollen**
348 **data for the time window, but with pollen data in other time windows. Circles in grid cells represent the coefficient of variation (CV;**
349 **the standard error divided by the REVEALS estimate). When $SE \geq$ REVEALS estimate, the circle fills the entire grid cell and the**
350 **REVEALS estimate is not different from zero. This occurs mainly where REVEALS estimates are low.**

351 **3.1.3 Summer-green Trees (ST)**

352 The cover of summer-green trees (ST) (Fig. 4) in the early Holocene at 9700-10200 BP is >40% across Europe. A small
353 number (<10) of grid cells in northern, western, central and southern Europe have cover >60%. This significantly increases
354 towards 5700-6200 BP, at which time ST cover is >60% in central Europe, and 40-60% in northern Europe. ST cover remains
355 <20% in southern Europe. From 5700-6200 BP there is a steady decline in ST cover across Europe. At 2700-3200 BP only
356 central Europe has ST cover >50% while values are <50% for the rest of Europe. There is a consistent decline over the last
357 two millennia BP. Most of Europe has ST cover <30% in the two last time windows (100-350 BP and 100 BP-present), except
358 for a group of grid cells in the southern Baltic states and scattered records elsewhere.



360 **Figure 3. Grid-based REVEALS estimates of Summer-green Trees (ST) cover for eight Holocene time windows. Percentage cover**
361 **of ST in 10% intervals represented by increasingly darker shades of green from 20%. Grey cells: cells without pollen data for the**
362 **time window, but with pollen data in other time windows. Circles in grid cells represent the coefficient of variation (CV; the standard**
363 **error divided by the REVEALS estimate). When $SE \geq$ REVEALS estimate, the circle fills the entire grid cell and the REVEALS**
364 **estimate is not different from zero. This occurs mainly where REVEALS estimates are low.**

365 **3.2 Selected taxa**

366 In terms of PFTs, Cerealia-type (t.) is assigned to agricultural land (AL), *Picea abies* to shade tolerant evergreen trees (TBE1:
367 *Picea abies* is the only taxon in this PFT), *Calluna vulgaris* to low evergreen shrubs (LSE: *Calluna vulgaris* is the only taxon
368 in this PFT), deciduous *Quercus* t. to shade tolerant summer-green trees (TBS), and evergreen *Quercus* t. to Mediterranean
369 shade-tolerant broadleaved evergreen trees (MTBE) (Table 1).

370 **3.2.1 Cerealia-type**

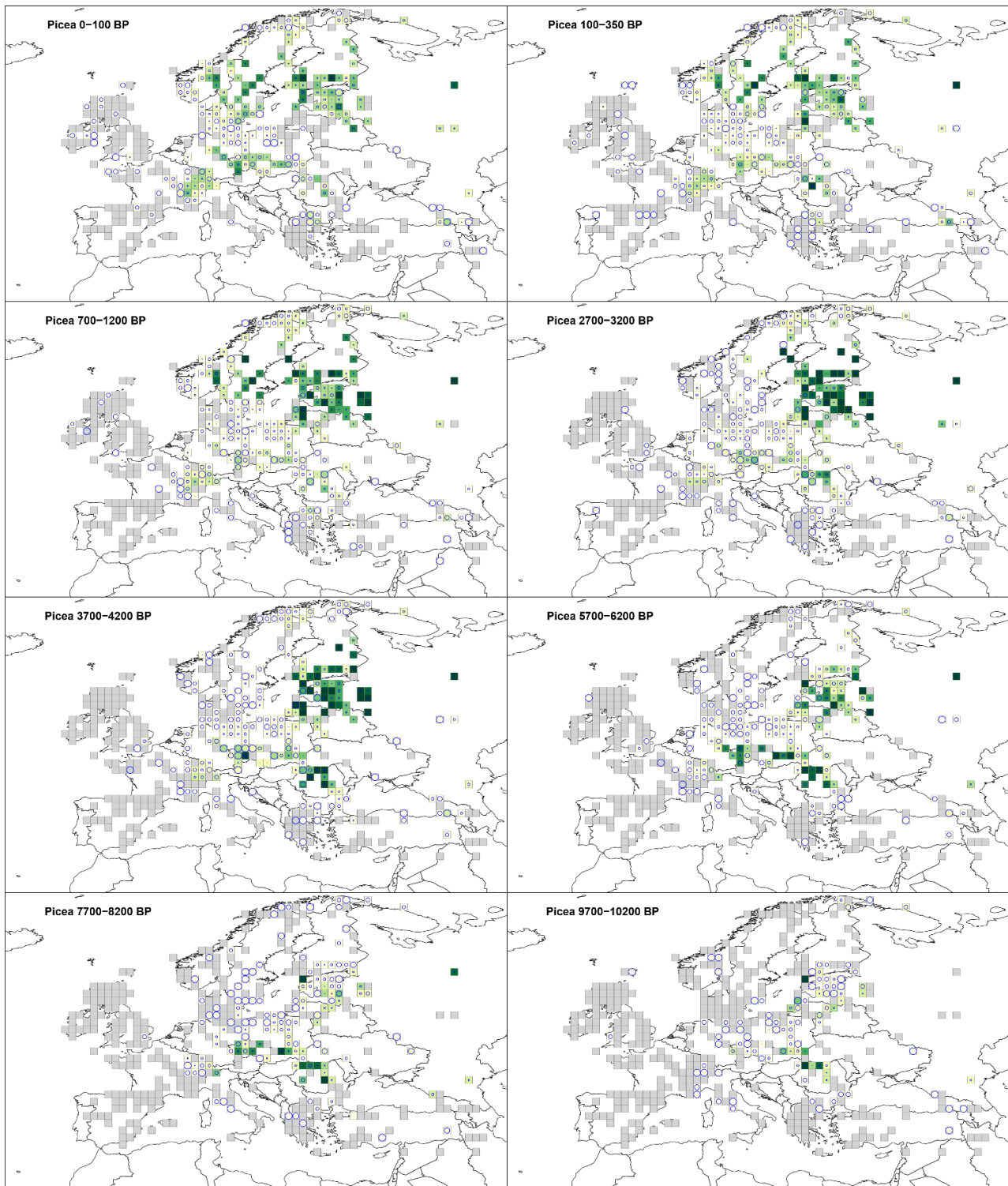
371 Cerealia-t. (Fig. 5) is recorded throughout the Holocene with 10-15% as the maximum cover. Cerealia-t. is present in southern
372 Europe at 9700-10200 BP with several grid cells recording >5 to 10%. Whilst scattered grid cells in central and western Europe
373 record the presence of Cerealia-t. at very low levels (0.5-1%), these values have high SE (greater than the REVEALS estimate)
374 and are therefore not different from zero; they correspond to single findings of Cerealia-t. By 5700-6200 BP, grid cells in
375 Estonia and France record 3-5% cover, and several regions within central and western Europe record 0-5% (0.5-1%), although
376 with high SEs. At 2700-3200 BP, Cerealia-t. is recorded across central and western Europe in the United Kingdom, France,
377 Germany, and Estonia with low values. In Norway, Sweden and Finland it has 0-1% cover with high SEs. The highest cover
378 (>5%) is observed across Europe from 1200 BP.



380 **Figure 5. Grid-based REVEALS estimates of Cerealia – t. cover for eight Holocene time windows. Percentage cover in 0.5% intervals**
381 **between 0 and 3%, 1% intervals between 3 and 5, and 5% interval between 5 and 10%. Intervals represented by increasingly darker**
382 **shades of green from 1-1.5%. Grey cells: cells without pollen data for the time window, but with pollen data in other time windows.**
383 **Circles in grid cells represent the coefficient of variation (CV; the standard error divided by the REVEALS estimate). When $SE \geq$**
384 **REVEALS estimate, the circle fills the entire grid cell and the REVEALS estimate is not different from zero. This occurs mainly**
385 **where REVEALS estimates are low.**

386 **3.2.2 *Picea abies***

387 *Picea abies* cover (Fig. 6) is low (1-2%) at 9700-10200 BP, although a number of grid cells in central and eastern Europe
388 record values between 30 and 50%. By 7700-8200 BP, grid cells recording 30-50% cover are observed in more regions of
389 central and eastern Europe than earlier (Russia, Estonia, Romania, Slovakia and Austria). At 5700-6200 BP, almost all of
390 central Europe has consistent but low cover of *Picea abies*; values are higher towards northeastern Europe (Russia, Estonia,
391 Latvia, Belarus and Lithuania), up to 30-50%. By 2700-3200 BP the cover of *Picea abies* has increased across central (ca.
392 10%) and northeastern Europe (>30%). From 1200 BP, *Picea abies* is recorded in northern Europe, particularly in Norway
393 and Sweden with some grid cells recording 25-50% cover.



no data 0 2 5 10 15 20 25 30 35 50 % estimated regional vegetation cover

395 **Figure 6. Grid-based REVEALS estimates of *Picea* cover for eight Holocene time windows. Percentage cover in 1% interval between**
396 **0 and 2%, 3% interval between 2 and 5%, 5% intervals between 5 and 30%, and 20% interval between 30 and 50%. Intervals**
397 **represented by increasingly darker shades of green from 5-10%. Grey cells: cells without pollen data for the time window, but with**
398 **pollen data in other time windows. Circles in grid cells represent the coefficient of variation (CV; the standard error divided by the**
399 **REVEALS estimate). When $SE \geq$ REVEALS estimate, the circle fills the entire grid cell and the REVEALS estimate is not different**
400 **from zero. This occurs mainly where REVEALS estimates are low.**

401 **3.2.3 *Calluna vulgaris***

402 During the Holocene, *Calluna vulgaris* cover (Fig. D1) peaks at 50%, and is largely distributed in a central European belt from
403 the United Kingdom across to the southern Baltic States. At 9700-10200 BP, it is recorded in only a few grid cells, mostly in
404 central and western Europe, and at levels <10%. Cover slowly increases and by 7700-8200 BP, there are several grid cells with
405 cover >25% within the United Kingdom, and with 10-20% cover within Denmark. At 5700-6200 BP, grid cells in coastal
406 locations in northwestern Europe (particularly France, Germany and Denmark) have 50% *Calluna vulgaris* cover. Cover
407 steadily increases within the same grid cells and by 2700-3200 BP, cover has increased in northern and eastern Europe e.g.
408 Norway, Estonia, with values up to 20% cover. The highest cover of *Calluna vulgaris* is recorded in the last two millennia.
409 Although some grid cells in southeast Europe record low cover values, these have high SE.

410 **3.2.4 Deciduous *Quercus* type (t.)**

411 Deciduous *Quercus* t. (Fig. D2) is recorded in central and western Europe at 9700-10200 BP at low levels (<10%), while in
412 southern Europe (Italy) several grid cells recording >20% cover. By 7700-8200 BP, cover in central and western Europe is
413 between 1-10% while in northern and eastern Europe grid cells it is <2% with high SEs. During the mid-Holocene (5700-6200
414 BP) most of Europe, with the exception of some grid cells at the northern and southeast extremes, record deciduous *Quercus*
415 t. cover values between 2-15%. By 2700-3200 BP, % cover in the same grid cells has decreased to values between 2-10%.
416 Thereafter, the number of grid cells recording deciduous *Quercus* t. cover remains similar; however, the percentage cover
417 slowly decreases and at 350-100 BP, the number of grid cells with deciduous *Quercus* t. cover above 5% is very low.

418 **3.2.5 Evergreen *Quercus* type (t.)**

419 The spatial distribution of evergreen *Quercus* t. (Fig. D3) remains the same throughout the Holocene. Cover of >30% is
420 restricted to only a few grid cells and time windows. At the start of the Holocene, evergreen *Quercus* t. is recorded with values
421 <15% in southern Europe (Spain, Italy, Greece and Turkey) with high SEs. Cover of evergreen *Quercus* t. does not exceed
422 15% until 6700-7200 BP (not shown), in grid cells located in Turkey, Greece and Italy. From 6700-7200 BP there is an increase
423 in the number of grid cells recording evergreen *Quercus* t. in southern Europe but most show low cover values (<15%), and
424 have high SEs.

425 4 Discussion

426 The results presented here are the first full-Holocene grid-based REVEALS estimates of land-cover change for Europe
427 spanning the Mediterranean, temperate and boreal biomes, which highlight the spatial and temporal dynamics of 31 plant taxa,
428 12 PFTs and 3 LCTs across Europe over the last 11700 years. Previous studies have demonstrated major differences between
429 REVEALS results and pollen percentages (Marquer et al., 2014; Trondman et al., 2015), and the differences between
430 REVEALS results and other methods used to transform pollen data, including pseudobiomisation, and MAT (Roberts et al.
431 2018). It is not the scope of this paper to evaluate the results in that context. This discussion focuses on the reliability and
432 potential of this “second generation” of REVEALS land cover reconstruction for Europe for use by the wider science
433 community.

434 4.1 Data reliability

435 The REVEALS results are reliant on the quality of the input datasets, namely pollen count data, chronological control for
436 sequences, and the number and reliability of RPP estimates used (see discussion on RPPs under 4.2). The standard errors (SEs)
437 can be considered a measure of the precision of the REVEALS results, and of reliability/quality (Trondman et al., 2015).
438 Where SEs are equal or greater than the REVEALS estimates (represented in the maps of Fig. 2-6 and D1-D3 as a circle that
439 fills the grid), caution should be applied in the use of the REVEALS estimates, as it implies that they are not different from
440 zero when taking the SEs into account. Whilst this is possible within an algorithmic approach that includes estimates of
441 uncertainty, it is conceptually impossible to have negative vegetation cover. If $SEs \geq \text{mean REVEALS value}$ it is therefore
442 uncertain whether the plant taxon has cover within the grid cell. Cover may either be very low or the taxon may be absent
443 within the region (grid cell in this case).

444 The size of pollen counts impacts on the size of REVEALS SEs (Sugita, 2007a); larger counts result in smaller SEs.
445 Aggregation of samples from pollen records to longer time windows results in larger count sizes and thus lower SEs (see
446 sections 2.2 above and 4.2 below). Our input dataset includes more than 59 million individual pollen identifications, organised
447 here into 16711 samples from 1128 sites, where a sample is an aggregated pollen count for RPP taxa for a time window at a
448 site. Seventy-seven percent of samples have count sizes in excess of 1000 which is deemed most appropriate for REVEALS
449 reconstructions (Sugita, 2007a). The mean count size across all samples is 3550. Samples with count sizes lower than 1000
450 are still used, but result in higher SEs. More than half of the pollen records used in the study were sourced from databases (see
451 section 2.2). Note that the EMBSecBIO taxonomy has been pre-standardised, and the data compilers have removed *Cerealia-*
452 *type* (t.). This means that for grid cells within the Eastern Mediterranean-Black Sea-Caspian-Corridor, caution is advised in
453 the interpretation of *Cerealia-type*. Nevertheless, pollen from ruderals are often related to agriculture, for example, *Artemisia*,
454 *Amaranthaceae/Chenopodiaceae*, and *Rumex acetosa* type are included in the land-cover type open land (OL); therefore,
455 changes in OL cover in the Eastern Mediterranean-Black Sea-Caspian-Corridor may be related to changes in agricultural land
456 (see also discussion below, re agricultural, section 4.3).

457 Aggregation of pollen counts to time windows depends on age-depth models. We have used the best age-depth models
458 available to us, based on the chronologies presented in Giesecke et al. (2014) for EPD sites, and through liaison with data
459 contributors. Nevertheless, future REVEALS runs may draw on improvements to age-depth modelling, which may result in
460 some original pollen count data being assigned to different time windows.

461 The REVEALS results presented here are provided for $1^\circ \times 1^\circ$ grid cells across Europe. The size and number of suitable pollen
462 records is an important factor in the quality of the REVEALS estimates for each grid cell. The REVEALS model was developed
463 for use with “large lakes” (≥ 50 ha; Sugita, 2007a) that represent regional vegetation. Grid cells with multiple large lakes will
464 thus provide results with the highest level of certainty and reflect the regional vegetation most accurately. These grid cell
465 results comprised of one or more large lakes, or several small sites (lake or bog) or a mix of large site(s) and small sites, are
466 considered “high quality” (dark grey grids in figure 1B). It has been shown both theoretically (Sugita, 2007a) and empirically
467 (Fyfe et al., 2013; Trondman et al., 2016) that pollen records from multiple smaller (<50 ha) lakes will also provide REVEALS
468 estimates that reflect regional vegetation. However, SEs may be larger if there is high variability in pollen composition between
469 records. We therefore also consider grid cells with multiple sites “high quality”. Application of REVEALS to pollen records
470 from large bogs violates assumptions of the model (see section 2.1 above). Therefore, REVEALS estimates for grid cells
471 including large bogs or single small sites (lake or bog) may not be representative of regional vegetation, particularly in areas
472 characterised by heterogeneous vegetation. We consider such estimates as “lower quality” (light grey grids in figure 1B),
473 although they may still provide first-order indications of vegetation cover, and represent an improvement on pollen percentage
474 data (Marquer et al., 2014). Our results provide REVEALS estimates for a maximum of 420 grid cells per time window. The
475 number and type of pollen records in a grid cell can change between time windows: not all pollen records cover the entire
476 Holocene. To assess the reliability of individual results it is important to consider not just the number and type of pollen records
477 in the total dataset, but how these changes between the time windows. Results for a maximum of 143 grid cells are based on
478 three or more sites, 65 on two sites, and a minimum of 212 grid cells on a single site. The results of a maximum of 67 grid
479 cells are based on single small bogs (<400 m radius), 68 on single small lakes (<400 m radius), and 82 on single large bogs.
480 This implies that about half the grid cells with REVEALS results should be considered as “lower quality” results.

481 **4.2 Role of RPPs and FSP in REVEALS results**

482 A key assumption of the REVEALS model is that RPP values are constant within the region of interest, and through time
483 (Sugita, 2007a). Nevertheless, it has been suggested that RPPs may vary between regions, with the variation caused by
484 environmental variability (climate, land use), vegetation structure, or methodological design differences (Broström et al., 2008;
485 Hellman et al., 2008a; Mazier et al., 2012; Li et al., 2020; Wiczorek and Herzsuh, 2020). Wiczorek and Herzsuh (2020)
486 have shown that inter-taxon variability in RPP values is generally lower than intra-taxon variability, lending support to
487 application of the approach we used in the new synthesis of RPPs for Europe (Appendix A-C), i.e. calculation of mean RPPs
488 using all available RPP values that can be considered as reliable. Nevertheless, some RPP taxa still present a challenge, for
489 example, Ericaceae, where Mediterranean tree forms have a greater number of inflorescences and hence may have a higher

490 RPP than low-growth form Ericaceae in central and northern Europe. As we have only unique RPP values for Ericaceae in
491 both boreal-temperate Europe and Mediterranean Europe, and therefore the large difference in RPP between the two biomes
492 remains to be confirmed with more RPP studies.

493 Currently there is higher confidence in the boreal and temperate RPP values that are based on a wider set of studies increasing
494 the spread of values and hence reliability of the mean RPP values used (Mazier et al., 2012; Wiczorek and Herschuh, 2020),
495 whilst RPP values for Mediterranean taxa are based on fewer empirical RPP studies. The new RPP datasets for Europe
496 produced for this study (Appendix A-C) can be used in different ways. The RPPs provided in Table A1 can be used for the
497 entire European region, including or excluding entomophilous taxa, and including all values from the Mediterranean area or
498 only the values for the strictly sub-Mediterranean and/or Mediterranean taxa. If one uses all RPPs from the Mediterranean
499 area, there will be taxa for which there is both a RPP value obtained in boreal/temperate Europe and a RPP value obtained in
500 Mediterranean Europe. Application of both RPP values in a single REVEALS reconstruction is not straightforward to achieve,
501 because the border between the two regions has shifted over the Holocene. In the REVEALS reconstruction presented in this
502 paper, we chose to use the RPPs from Mediterranean Europe only for the sub-Mediterranean and/or Mediterranean taxa
503 (including Ericaceae) (Table 1 and A1), and for all other taxa we used the RPPs from boreal/ temperate Europe. The major
504 issue with this choice is the RPP value of Ericaceae. Using only the large value from Mediterranean Europe may lead to an
505 under-representation of Ericaceae (*Calluna* excluded), in particular in boreal Europe, but perhaps also in temperate Europe.
506 Using only the small value from boreal/temperate Europe may lead to an over-representation of Ericaceae in Mediterranean
507 Europe.

508 Until we have more RPP values for each taxon, it is not possible to disentangle the effect of all factors influencing the
509 estimation of RPPs and to separate the effect of methodological factors from those of factors such as vegetation type, climate
510 and land use. The only way to evaluate the reliability of RPP datasets is to test them with modern or historical pollen
511 assemblages and related plant cover (Hellman et al., 2008a, 2008b). We argue that RPP values of certain taxa may not vary
512 substantially within some plant families or genera, while they might be variable within others, depending on the characteristics
513 of flowers and inflorescences that may be either very different or relatively constant within families or genera (see discussion
514 in Li et al. (2018)). Therefore, we advise to use compilations of RPPs at continental or sub-continental scales rather than
515 compilations at multi-continental scales as the northern Hemisphere dataset proposed by Wiczorek and Herzschuh (2020).
516 We consider the RPP selection used within this work as the most suitable for Europe to date, but expect revised and improved
517 RPP values as more RPP empirical studies are published. Moreover, experimentation in REVEALS applications will allow
518 future studies to evaluate the effects of using different RPP datasets on land-cover reconstructions (e.g. Mazier et al., 2012).
519 The role of FSP values in the pollen dispersal and deposition function ($g_i(z)$ in equation (1) of the REVEALS model, section
520 2.1) has been discussed by Theuerkauf et al. (2013). In this application of REVEALS we used the Gaussian Plume Model
521 (GPM) of dispersion and deposition as most existing RPP values have been estimated using this model. The GPM approximates
522 dispersal as a fast-declining curve with distance from the source plant, which implies short distances of transport for pollen
523 grain with high FSP compared to other models of dispersion and deposition (Theuerkauf et al., 2012). We have used the FSP

524 values obtained for deciduous *Quercus* type (t.) (0.035 m/s) and boreal-temperate Ericaceae (0.037 m/s) for evergreen *Quercus*
525 t. and Mediterranean Ericaceae, respectively, although the FSP values of those two taxa were estimated to 0.015 and 0.051 in
526 the Mediterranean study (Table 1 and A1). Whether using a lower FSP for evergreen *Quercus* t. (0.015 m/s) and a higher FSP
527 for Mediterranean Ericaceae (0.051 m/s) will have an effect on the REVEALS results is not known and requires further testing.

528 **4.3 Use of the REVEALS land cover reconstructions results**

529 This second generation dataset of pollen-based REVEALS land cover in Europe over the Holocene is currently used in two
530 major research projects: LandClim, and PAGES LandCover6k. LandClim is a Swedish Research Council project studying the
531 difference in the biogeophysical effect of land-cover change on climate at 6000, 2500 and 200 BP (Fyfe et al., 2022; Githumbi
532 et al., 2019; Strandberg et al., 2014; Trondman et al., 2015). PAGES LandCover6k focuses on providing datasets on past land-
533 cover/land-use for climate modelling studies (Dawson et al., 2018; Gaillard et al., 2018; Harrison et al., 2020). The first
534 generation REVEALS land-cover reconstruction (Marquer et al., 2014, 2017; Trondman et al., 2015) were used to evaluate
535 other pollen-based reconstructions of Holocene tree-cover changes in Europe (Roberts et al., 2018) and scenarios of
536 anthropogenic land-cover changes (ALCCs) (Kaplan et al., 2017) (see also section 1). The Trondman et al. (2015)
537 reconstructions were used to create continuous spatial datasets of past land cover using spatial statistical modelling
538 (Pirzamanbein et al., 2014, 2018, 2020).

539 Spatially explicit datasets/maps based on these second generation of REVEALS reconstructions are currently being produced
540 within PAGES LandCover6k and used to evaluate and revise the HYDE (Klein Goldewijk et al., 2017) and KK10 (Kaplan et
541 al., 2009) ALCC scenarios. Moreover, LandCover6k archaeology-based reconstructions of past land-use change (Morrison et
542 al., 2021) will be integrated with the datasets of REVEALS land-cover. Besides the uses listed above, the second generation
543 of REVEALS reconstruction for Europe offers great potential for use in a large range of studies on past European regional
544 vegetation dynamics and changes in biodiversity over the Holocene (Marquer et al., 2014, 2017) and the relationship between
545 regional plant cover, land use, and climate over millennial and centennial time scales. Since the reconstructions are of regional
546 plant cover they will have value in archaeological research when impacts are expected at the regional level (e.g. the impact of
547 early mining (Schauer et al., 2019)). Archaeological questions and research programmes that require information on local
548 vegetation cover will require the full application of the LRA (REVEALS and LOVE; Sugita, 2007a, b), such as the local
549 vegetation estimates presented from Norway focussing on cultural landscape development (Mehl et al., 2015). The same
550 approach of using the REVEALS results within the LOVE model is necessary for ecological questions that require local
551 vegetation estimates (Cui et al., 2013, 2014; Sugita et al., 2010).

552 Several papers have discussed in depth the issues that need to be taken into account when interpreting REVEALS
553 reconstructions of past plant cover, in particular Trondman et al. (2015) and Marquer et al. (2017). The interpretation in terms
554 of human-induced vegetation change is one of the major challenges. The cover of open land (OL) may be used to assess
555 landscape openness, but is not a precise measure of human disturbance, as OL will include plant taxa characterizing both
556 naturally-open land and agricultural land that has been created by humans through the course of the Holocene with the

557 domestication of plants and livestock. Natural openness can occur in arctic and alpine areas, in wet regions, in river deltas and
558 around large lakes, as well as in eastern steppe areas. It is a particular challenge in the Mediterranean region where natural
559 vegetation openness represents a larger fraction of the land cover than in temperate or boreal Europe (Roberts et al., 2019).
560 Agricultural Land (AL; Trondman et al., 2015 is the only PFT that includes cultivars; nevertheless, it is restricted to cereal
561 cropping, and many other cultivated crop types that can be identified through pollen analysis do not yet have RPP values (e.g.
562 *Linum usitatissimum* (common flax), *Cannabis* (hemp), *Fagopyrum* (buckwheat), beans, etc.). Moreover, the Cerealia-t. pollen
563 morphological type includes pollen from wild species of Poaceae, especially when identification relies essentially on
564 measurements of the pollen grain and its pore and does not consider exine structure and sculpture (Beug, 2004; Dickson, 1988).
565 The maps presented and described in section 3 as an illustration of the results show similar changes in spatial distributions and
566 quantitative cover of plant taxa and land-cover types through time, between 6000 BP and present, as the results published in
567 Trondman et al., (2015). The much greater potential of the new REVEALS reconstruction resides in its larger spatial extent,
568 covering not only boreal and temperate Europe but also southern and eastern Europe, and its contiguous time windows across
569 the entire Holocene, from 11700 BP to present. The quality of results is also higher in a number of grid cells in comparison to
570 Trondman et al (2015), where new pollen records have been included, which may in several cases decrease the standard error
571 on the REVEALS estimates.

572 **5. Data availability**

573 All data files reported in this work, which were used for calculations, and figure production are available for public download
574 at <https://doi.pangaea.de/10.1594/PANGAEA.937075> (Fyfe et al., 2022). The data and the DOI number are subject to future
575 updates and only refer to this version of the paper. The data available in Pangaea includes: 1) REVEALS reconstructions and
576 their associated SE for the 25 time windows; 2) Metadata of the 1128 pollen records used; 3) LandClimII contributors listing
577 the data contributors\collectors\databases. 4) The list of FSP and RPP values used for the reconstructions and 5) Grid cell
578 quality information (in terms of available pollen data, which influences the result quality: mean REVEALS estimate of plant
579 cover) for all grid cells. Pollen data were extracted from ALPADABA (<https://www.neotomadb.org/>), EMBSEC BIO
580 (<https://research.reading.ac.uk/palaeoclimate/embsecbio/>), EPD (<http://www.europeanpollendatabase.net/index.php>),
581 LandClimI, PALYCZ (<https://botany.natur.cuni.cz/palycz/>) and PALEOPYR (<http://paleopyr.univ-tlse2.fr/>).

582

583 **6. Code availability**

584 REVEALS was implemented using the REVEALS function within the LRA R-package (Abraham et al., 2014), available at
585 <https://github.com/petrkunes/LRA>.

586 Example code for data preparation and implementation of REVEALS, using two grid cells from SW Britain, is available at
587 <https://github.com/rmfyfe/landclimII>.

588 7. Conclusions

589 The application of the REVEALS model to 1128 pollen records distributed across Europe has produced the first full-Holocene
590 estimates of vegetation cover for 31 plant taxa in $1^\circ \times 1^\circ$ grid cells. These data are made available for use by the wider science
591 community, including aggregation of results to PFTs and LCTs. The REVEALS model assumptions are clearly stated to allow
592 interpretation and assessment of our results and several of the assumptions have been tested and validated. We can therefore
593 use the land-cover reconstructions to test the role of climate and humans on Holocene plant cover at regional scales. The
594 overview of land-cover change across Europe over the Holocene can be used to track the timing and rate of vegetation shifts.
595 We can also determine the effect of human-induced changes in regional vegetation cover on climate, i.e. study land use as a
596 climate forcing (Gaillard et al., 2010a, 2018; Harrison et al., 2020; Strandberg et al., 2014). Local reconstructions (LOVE) can
597 be a complementary approach to archaeological surveys as fine-scale human use of the landscape cannot be distinguished
598 using REVEALS (regional estimates). The LOVE model requires that regional plant cover is known: the REVEALS
599 reconstructions are therefore needed for this purpose as well, and gridded reconstructions may be a way to perform LOVE
600 reconstructions, although other strategies can be chosen (Cui et al., 2013; Mazier et al., 2015). Questions aiming to understand
601 the degree of vegetation openness through the Holocene in Europe, or regarding changes in the relationship between summer-
602 green and evergreen tree cover through time can now and in the future be answered and validated with fossil pollen data via
603 the REVEALS approach. We expect that, in the future, improved REVEALS estimates, as more pollen records are
604 incorporated, and work on RPPs develops.

605 Appendices

606 Appendix A - New RPP dataset for Europe

607 A.1 New RPP synthesis for Europe

608 The most common method to estimate RPPs involves the application of the Extended R-Value (ERV) model on datasets of
609 modern pollen assemblages and related vegetation cover. A summary of the ERV model and its assumptions, and an extensive
610 description of standardised field methods for the purpose of RPP studies are found in Bunting et al. (2013b). Estimation of
611 RPPs in Europe started with the studies by Sugita et al. (1999) and Broström et al. (2004) in southern Sweden, and Nielsen et
612 al. (2004) in Denmark. The first tests of the RPP in pollen-based reconstructions of plant cover using the LRA's REVEALS
613 (Regional Estimates of VEgetation Abundance from Large Sites) model (Sugita, 2007a) were published by Soepboer et al.
614 (2007) in Switzerland and Hellman et al. (2008a and b) in South Sweden. Over the last 15 years, a large number of RPP studies
615 have been undertaken in Europe North of the Alps, but it is only recently that RPP studies were initiated in the Mediterranean
616 area (Grindean et al., 2019; Mazier et al., unpublished). Two earlier syntheses of RPPs in Europe were published by Broström
617 et al. (2008) and Mazier et al. (2012). From 2012 onwards, these RPP values have been used in numerous applications of the
618 LRA's two models REVEALS and LOVE (LOcal VEgetation Estimates) (Sugita, 2007a and b) to reconstruct regional and
619 local plant cover in Europe (Cui et al., 2013; Fyfe et al., 2013; Marquer et al., 2020; Mazier et al., 2015; Nielsen et al., 2012;
620 Nielsen and Odgaard, 2010; Trondman et al., 2015). Recently, Wieczorek and Herzschuh (2020) published a synthesis of the
621 RPPs available for the northern Hemisphere; it includes new mean RPP values for Europe that were produced independently
622 from the synthesis we present here.

623 Table A1 is the result of the new synthesis of RPPs available in Europe that we have performed for the REVEALS
624 reconstruction presented in the paper. It includes RPPs for 39 plant taxa from studies in boreal and temperate Europe of which
625 22 (Poaceae included) are herbs or low shrubs, and for 22 plant taxa from studies in the Mediterranean area. The two regions
626 have RPP values for 7 plant taxa in common. These RPPs are compared to those from two syntheses published earlier, Mazier
627 et al. (2012) and Wieczorek and Herzschuh (2020). The number of selected RPP values (n) for Poaceae is larger than the total
628 number of RPP (tn), i.e. $n = tn + 1$. This is due to the fact that the study of Bunting et al. 2005 does not include a value for
629 Poaceae and the RPP values are related to *Quercus* (Bunting et al., 2005); therefore, RPPs related to Poaceae were calculated
630 by assuming the RPP value for *Quercus* (related to Poaceae; $Quercus_{(Poaceae)}$) was the same in this study region than the mean
631 of $Quercus_{(Poaceae)}$ RPPs from all other available studies.

632 The ranking of RPPs (relative to Poaceae, RPP=1) for 23 tree taxa (M: Mediterranean taxa), from the largest (13.56) to the
633 smallest (0.240), is as follows (Poaceae included for comparison): *Alnus*> evergreen *Quercus* t.(M)> *Abies alba*> *Pinus*>
634 *Fagus sylvatica*> *Picea abies*> Ericaceae (M)> *Betula*> deciduous *Quercus* t.> *Carpinus betulus*> *Populus*> *Juniperus*>
635 *Corylus avellana*> *Castanea sativa*> *Sambucus nigra*-t.> *Ulmus*> *Tilia*> *Salix*> *Fraxinus*> Poaceae (=1)> *Acer*> *Pistacia* (M)>
636 *Phillyrea* (M)> *Carpinus orientalis* (M). All tree taxa have mean RPPs larger than 1 except *Acer* (0.8), *Pistacia* (0.755),
637 *Phillyrea* (0.512) and *Carpinus orientalis* (0.240). The ranking of RPPs for 24 herb and low shrub taxa, from the largest (10.52)

638 to the smallest (0.10), is as follows: *Urtica*> Chenopodiaceae> *Secale*> *Artemisia*> Rubiaceae> *Rumex acetosa*-t.>
639 *Filipendula*> *Plantago lanceolata*> *Trollius*> Ranunculaceae (M)> *Ranunculus acris*-t.> Cerealia-t.> *Potentilla*-t.> *Plantago*
640 *media*> *Calluna vulgaris*> Poaceae (=1)> Cyperaceae> *Plantago montana*> Fabaceae (M)> Rosaceae (M)> Apiaceae>
641 Compositae SF. Cichorioideae> *Empetrum*> *Leucanthemum (Anthemis)*-t.. Of the taxa with RPPs larger than 3, only six taxa
642 are herbs while twelve are trees.

643 The two studies in the Mediterranean area provide single RPP values for 16 taxa, five herb taxa (Poaceae included) and 11 tree
644 taxa of which six are sub-Mediterranean and/or Mediterranean, and three include both temperate and Mediterranean taxa
645 (Cupressaceae, Ericaceae, *Fraxinus*) (Table B2). The RPP of herb taxa are significantly different between the study of
646 Grindean et al. (2019) from the forest-steppe zone and our synthesis, except for *Artemisia* (5.89 and 3, 94, respectively). The
647 RPP of *Corylus avellana* from the study of Mazier et al. (unpublished) (3.44) is double the mean RPP in our synthesis (1.71),
648 and the mean RPP of deciduous *Quercus* t. in our synthesis (4.54) is four times larger than the RPP from the study of Grindean
649 et al. (2019) (1.10).

650 **Table A1: New synthesis of European RPPs: mean RPPs with their SDs in brackets, and mean RPPs from the syntheses by Mazier**
651 **et al. (2012) (St2 values) and Wieczorek and Herzsuh (2020), for comparison. This synthesis: values in bold are new mean RPPs**
652 **compared to Mazier et al. (2012). The RPP values from studies in the Mediterranean area are indicated with “M” in the second**
653 **column. The values in cells emphasized by a thick rectangle are the mean RPPs used in the new REVEALS reconstruction for**
654 **Europe (this paper), values in bold are new values, values not in bold are the same values as in Mazier et al. (2012). The values of**
655 **fall speed of pollen (FSP) are from Mazier et al. (2012) except those in italic, i.e. FSPs for Amaranthaceae/Chenopodiaceae, *Urtica***
656 **and *Sambucus nigra*-t. (Abraham and Kozáková, 2012), and *Populus* (Wieczorek and Herzsuh, 2020) and the new FSPs for**
657 **Mediterranean taxa. For the three syntheses, the number of selected RPP values (n) included in the calculation of the mean RPP**
658 **estimate is indicated with the total number of available RPP values (tn) in brackets. The reason why the number of selected RPP**
659 **values (n) for Poaceae is larger than the total number of RPP (tn) is provided in section A.1. Abbreviations: Comp. Compositae**
660 **(=Asteraceae), Dec. deciduous, *Filipend Filipendula*, *Pot Potentilla*, SF. Subfamily, t. type, Symbols: * Separate mean RPP values for**
661 ***Calluna vulgaris*, *Empetrum*, and Ericaceae (*Calluna* and *Empetrum* excluded) in this synthesis, a single mean RPP values for all**
662 **Ericales in Wieczorek and Herzsuh (2020), ** Separate mean RPP values for Cerealia type (*Secale* excluded) and *Secale* in this**
663 **synthesis, a single mean RPP for all cereals in Wieczorek and Herzsuh (2020), *** Separate mean RPP values for Compositae SF**
664 **Cichorioideae and *Leucanthemum (Anthemis)* type in this synthesis, a single mean RPP for all Asteraceae in Wieczorek and**
665 **Herzsuh (2020). Note that there are no RPP for Asteraceae (Compositae SF Cichorioideae and *Leucanthemum (Anthemis)* type**
666 **excluded) in our synthesis, ^ Separate mean RPP values for *Filipendula* and *Potentilla* type in this synthesis, a single mean RPP for**
667 **all Rosaceae in Wieczorek and Herzsuh (2020); note that there are no RPP for Rosaceae (*Filipendula* and *Potentilla*-t. excluded)**
668 **in our synthesis; moreover *Filipendula* and *Potentilla*-t. are classified as herbs, while Rosaceae is classified as tree in Wieczorek and**
669 **Herzsuh (2020), ^^ Separate mean RPP values for *Plantago lanceolata*, *P. media* and *P. montana* in this synthesis, a single mean**
670 **RPP for all Plantaginaceae in Wieczorek and Herzsuh (2020); note that there are no RPP for Plantaginaceae (*Plantago lanceolata*,**
671 ***P. media* and *P. montana* excluded) in our synthesis, ^^ Separate mean RPP values for *Ranunculus acris* type and *Trollius* in this**
672 **synthesis, a single mean RPP for all Ranunculaceae in Wieczorek and Herzsuh (2020); note that there are no RPP for**
673 **Ranunculaceae (*Ranunculus acris*-t and *Trollius* excluded) in our synthesis.**

Study n (tn), FSP, RPP	This paper, synthesis			Mazier et al. 2012 St 3		Wieczorek & Herzschuh 2020 Europe version 2		
	n (tn)	FSP	RPP (SE)	n (tn)	RPP (SE)	n(tn)	RPP (SE)	Notes
HERB TAXA								
Poaceae (Reference taxon)	16(15)	0.035	1.00 (0.00)	9(8)	1.00 (0.00)	14(12)	1.00 (0.00)	
Herb taxa								
Amaranthaceae/Chenopodiaceae	1(1)	0.019	4.280 (0.270)	none	none	1(1)	<u>4.28 (0.27)</u>	Same value as in this synthesis
Apiaceae	1(1)	0.042	0.260 (0.010)	1(1)	0.26 (0.01)	3(3)	2.13 (0.41)	
Apiaceae	M 1(1)	0.042	5.910 (1.230)					
<i>Artemisia</i>	3(3)	0.025	3.937 (0.146)	1(1)	3.48 (0.20)	2(2)	4.33 (1.59)	
<i>Artemisia</i>	M 1(1)	0.014	5.890 (3.160)					
Comp. <i>Leucanth. (Anthemis)t.</i> ***	1(1)	0.029	0.100 (0.010)	1(1)	0.10 (0.01)			see Asteraceae all***
Comp. SF. Cichorioideae***	3(3)	0.051	0.160 (0.020)	3(3)	0.16 (0.02)	8(10)	0.22 (0.02)	Asteraceae all***
Comp. SF. Cichorioideae	M 1(1)	0.061	1.162 (0.075)					
Comp. (Asteroideae + Cichorioideae)	M 1(1)	0.029	0.160 (0.100)					
<i>Calluna vulgaris</i> *	2(4)	0.038	1.085 (0.029)	2(4)	1.09 (0.03)			see Ericales all*
Cerealia t.**	3(7)	0.060	1.850 (0.380)	2(4)	1.18 (0.04)	4(6)	2.36 (0.42)	Cereals all**
Cerealia t. (<i>Triticum</i> ., <i>Secale</i> , <i>Zea</i>)	M 1(1)	0.060	0.220 (0.120)					
Cyperaceae	4(6)	0.035	0.962 (0.050)	4(6)	0.83 (0.04)	6(8)	0.56 (0.02)	
<i>Empetrum</i> *	1(2)	0.038	0.110 (0.030)	1(2)	0.11 (0.03)			see Ericales all*
Ericaceae*	1(1)	0.038	0.070 (0.040)	1(1)	0.07 (0.04)	7(9)	0.44 (0.02)	Ericales all*
Fabaceae	M 1(1)	0.021	0.400 (0.070)					
<i>Filipendula</i> ^	3(3)	0.006	3.000 (0.285)	2(3)	2.81 (0.43)	4(6)	0.97 (0.11)	Rosaceae all ^
<i>Plantago lanceolata</i> ^^	4(6)	0.029	2.330 (0.201)	3(4)	1.04 (0.09)	8(10)	2.49 (0.11)	Plantaginaceae all^^
<i>Plantago lanceolata</i>	M 1(1)	0.029	0.580 (0.320)					
<i>Plantago media</i> ^^	1(1)	0.024	1.270 (0.180)	1(1)	1.27 (0.18)			see Plantaginaceae all^^
<i>Plantago montana</i> ^^	1(1)	0.030	0.740 (0.130)	1(1)	0.74 (0.13)			see Plantaginaceae all^^
<i>Potentilla</i> t.^	2(3)	0.018	1.720 (0.200)	2(3)	1.72 (0.20)			see Rosaceae all^
Ranunculaceae	M 1(1)	0.020	2.038 (0.335)					
<i>Ranunculus acrist.</i> ^^^	2(2)	0.014	1.960 (0.360)	2(2)	1.96 (0.36)	3(5)	0.99 (0.12)	Ranunculaceae all^^^

Rosaceae (<i>Filipend.</i> , <i>Pot. t.</i> , <i>Sanguisorba</i>)	M	1(1)	0.018	0.290 (0.120)		3.71			
Rubiaceae		2(3)	0.019	3.710 (0.340)	2(3)	(0.34)	3(5)	1.56 (012)	
Rubiaceae	M	1(1)	0.019	0.400 (0.070)					
<i>Rumex acetosat.</i>		3(4)	0.018	3.020 (0.278)	3(3)	0.85 (0.05)	3(4)	0.58 (0.03)	
<i>Secale**</i>		3(3)	0.060	3.990 (0.320)	1(1)	3.02 (0.05)			see Cereals all**
<i>Trollius^^^</i>		1(1)	0.013	2.290 (0.360)	1(1)	2.29 (0.36)			see Ranunculaceae all^^^
<i>Urtica</i>		1(1)	0.007	10.520 (0.310)	none	none	1(1)	<u>10.52 (0.31)</u>	Same value as in this synthesis
TREE TAXA									
<i>Abies alba</i>		2(2)	0.120	6.875 (1.442)	2(2)	6.88 (1.44)	2(2)	<u>6.88 (1.44)</u>	Same value as in this synthesis
<i>Acer</i>		2(2)	0.056	0.800 (0.230)	2(2)	0.80 (0.23)	3(3)	0.23 (0.04)	
<i>Acer</i>	M	1(1)	0.056	0.300 (0.090)					
<i>Alnus</i>		5(7)	0.021	13.562 (0.293)	3(3)	9.07 (0.10)	4(6)	8.49 (0.22)	
<i>Betula</i> (mainly <i>B. pubescens</i> , <i>B. pendula</i>)		7(9)	0.024	5.106 (0.303)	6(6)	3.99 (0.17)	6(8)	4.94 (0.44)	
<i>Buxus sempervirens</i>	M	1(1)	0.032	1.890 (0.068)					
<i>Carpinus betulus</i>		2(4)	0.042	4.520 (0.425)	2(2)	3.55 (0.43)	3(5)	3.09 (0.28)	
<i>Carpinus orientalis</i>	M	1(1)	0.042	0.240 (0.070)					
<i>Castanea sativa</i>	M	1(1)	0.010	3.258 (0.059)					
<i>Corylus avellana</i>		4(4)	0.025	1.710 (0.100)	3(3)	1.99 (0.20)	3(4)	1.05 (0.33)	
<i>Corylus avellana</i>	M	1(1)	0.025	3.440 (0.890)					
Cupressaceae (<i>Juniperus</i> 3 species)	M	1(1)	0.020	1.618 (0.161)					See <i>Juniperus</i>
Ericaceae (<i>Arbutus unedo</i> , <i>Erica</i> 3 species)	M	1(1)	0.051	4.265 (0.094)					
<i>Fagus sylvatica</i>		3(6)	0.057	5.863 (0.176)	4(4)	3.43 (0.09)	3(3)	2.35 (0.11)	
<i>Fraxinus excelsior</i>		5(6)	0.022	1.044 (0.048)	3(3)	1.03 (0.11)	5(5)	2.97 (0.25)	
<i>Fraxinus</i> (<i>F. excelsior</i> , <i>F. ornus</i>)	M	1(1)	0.022	2.990 (0.880)					
<i>Juniperus communis</i>		1(2)	0.016	2.070 (0.040)	1(2)	2.07 (0.04)	1(1)	7.94 (1.28)	
<i>Phillyrea</i>	M	1(1)	0.015	0.512 (0.076)					
<i>Pistacia</i>	M	1(1)	0.030	0.755 (0.201)					
<i>Picea abies</i>		4(8)	0.056	5.437 (0.097)	4(6)	2.62 (0.12)	4(6)	1.65 (0.15)	
<i>Pinus</i> (mainly <i>P. sylvestris</i>)		6(9)	0.031	6.058 (0.237)	3(5)	6.38 (0.45)	4(6)	10.86 (0.80)	
<i>Populus</i>		1(1)	0.025	2.660 (1.250)	none	none	1(1)	3.42 (1.60)	

Dec. <i>Quercust.</i> (mainly <i>Q. robur</i> , <i>Q. petraea</i>)		6(8)	0.035	4.537 (0.086)	4(4)	5.83 (0.15)	5(7)	2.42 (0.10)	Same value as in this synthesis
Dec. <i>Quercust.</i> (mainly <i>Q. peduncularis</i>)	M	1(1)	0.035	1.100 (0.350)					
Evegreen <i>Quercust.</i> (<i>Q. ilex</i> , <i>Q. coccifera</i>)	M	1(1)	0.015	11.043 (0.261)					
<i>Salix</i>		5(5)	0.022	1.182 (0.077)	3(4)	1.79 (0.16)	3(4)	0.39 (0.06)	
<i>Sambucus nigra</i> t.		1(1)	0.013	1.300 (0.120)	none	none	1(1)	<u>1.30 (0.12)</u>	
<i>Tilia</i>		4(5)	0.032	1.210 (0.116)	1(1)	0.80 (0.03)	3(4)	0.93 (0.09)	
<i>Ulmus</i>		1(2)	0.032	1.270 (0.050)	1(1)	1.27 (0.05)	none		

675

676 A.2 Comparison of the current synthesis with two previous syntheses (Table A1)

677 Of the 39 plant taxa for which we have a mean RPP in our new synthesis (New), 21 have a new mean RPP value compared to
678 the earlier synthesis of Mazier et al. (2012) (Maz), 18 taxa have the same mean RPPs in both syntheses. There are three new
679 taxa for which there were no RPP in Maz, i.e. Amaranthaceae/Chenopodiaceae, *Sambucus nigra*-t. and *Urtica*. The mean RPPs
680 are comparable between the two syntheses New and Maz, except for *Plantago lanceolata* (2.33 in New/1.04 in Maz), *Alnus*
681 (13.56/9.07), *Betula* (5.11/3.09), *Carpinus betulus* (4.52/3.55), *Fagus* (5.86/3.43), *Picea* (5.44/2.62) and *Quercus* (4.54/5.83).
682 *Abies alba* has the same RPP in all three syntheses. Amaranthaceae/Chenopodiaceae, *Sambucus nigra*-t. and *Urtica* have the
683 same single RPP values in the synthesis of Wiczorek and Herzsuh (2020) (W&H) and New. New and W&H also have
684 comparable mean RPP values for *Artemisia*, Cereals (Cereals, *Secale* excluded in New, all Cereals in W&H), Compositae (SF
685 Cichorioideae in N, all Compositae (=Asteraceae) in W&H), Cyperaceae, *Plantago* (*P. lanceolata* in New, all Plantaginaceae
686 in W&H), *Betula*, *Corylus*, *Populus* and *Tilia*. There are relatively large differences in mean RPPs in W&H and New for 16
687 plant taxa, although the ranking of the plant taxa in terms of their mean RPPs is almost the same. Mean RPP is larger in W&H
688 than in New for Apiaceae (2.13/0.26), Ericales (0.44 in W&H) – *Empetrum* (0.11) and Ericaceae (0.07) in New, *Fraxinus*
689 (2.97/1.04), *Juniperus* (7.94/2.07), *Pinus* (10.86/6.06). Mean RPP is smaller in W&H than in New for *Filipendula* (0.97/3.00),
690 Rubiaceae (1.56/3.71), *Rumex acetosa* (0.58/2.02), *Acer* (0.23/0.80), *Alnus* (8.49/13.56), *Carpinus* (3.09/4.52), *Fagus*
691 (2.35/5.86)), *Picea* (1.65/5.44), *Quercus* (2.42/4.54) and *Salix* (0.39/1.18).

692 The larger differences between the mean RPPs in New and W&H than between New and Maz have not been examined in
693 detail. It is due to a slightly different selection of studies, i.e. the study of Theuerkauf et al. (2013) is not included in W &H
694 and we did not include in New (boreal and temperate Europe, Mediterranean area excluded) the studies of Bunting et al.
695 (2013a), Kuneš et al. (2019) and Grindean et al. (2019). Another important influencing factor is the selection of RPP values
696 for calculation of the mean RPP. Although the rules used to select RPP values are very similar between the syntheses, there
697 are obvious differences between New and W&H that are sometimes very significant (e.g. *Juniperus*).

698 A.3 Comparison of the new synthesis with three additional individual studies (Table A2)

699 The RPPs from Twiddle et al. (2012) (Twi) for *Pinus*, *Betula* and *Calluna* are considerably larger than the mean RPPs in our
700 synthesis (New). This is probably due to the assumption made on the RPP of *Picea* related to Poaceae. The RPP of *Picea*
701 varies greatly between the selected studies in New, from 0.57 to 8.43 (eight values available). If we assumed that the RPP of
702 *Picea* related to Poaceae in the study region of Twi was the mean RPP of the five smallest RPPs, i.e. 1.57, the RPP of the three
703 taxa would be 4.8 for *Pinus*, 3.4 for *Betula*, and 3.3 for *Calluna*, which is more comparable to the mean RPPs in New.
704 Three taxa in Bunting et al. (2013a) (Bun) have a RPP comparable to the mean RPP in New, i.e. for Cyperaceae, *Ranunculus*
705 *acris*-t., and *Rumex acetosa*-t. (*R. acetosa* in Bun). The other taxa have a RPP in Bun smaller than the mean RPP in New,
706 except *Plantago maritima* that has a larger RPP (5.8) in Bun than the mean RPP for *P. lanceolata* in New.
707 Of nine taxa, three have a RPP in Kuneš et al. (2019) (Kun) that is comparable to the mean RPP in New, i.e. for *Plantago*
708 *lanceolata*, *Ranunculus acris*-t. and *Rumex acetosa*-t.. The other six taxa have a RPP larger than the mean RPP in New
709 (Compositae SF Cichorioideae, Cyperaceae and *Leucanthemum (Anthemis)*-t., or smaller (Amaranthaceae/Chenopodiaceae,
710 Rubiaceae) to considerably smaller (*Urtica*). Of the 14 tree taxa, only four have a RPP in Kun comparable to the mean RPP in
711 New, i.e. for *Corylus*, *Fraxinus*, *Salix*, and *Ulmus*. For the other 10 tree taxa, the RPP in K is much smaller than the mean RPP
712 in N for *Abies alba*, *Alnus*, *Carpinus*, *Fagus*, *Picea*, *Pinus*, smaller for *Quercus*, and larger for *Acer* and *Tilia*.
713 Most of the RPP values of the three studies Twi, Bun and Kun are in the range of the values selected from the studies included
714 in our synthesis (New) except for *Urtica*, *Abies alba*, *Carpinus*, and *Pinus* in Kun. The Lagrangian Stochastic Model is used
715 in Kun instead of the Gaussian Plume Model in New, which may be one of the factors behind the lower RPPs in Kun, in
716 particular (but not only) for taxa with heavy pollen grains.

717

718 Table A2: Comparison of the mean RPPs in this synthesis with the RPP estimates from Britain (Twiddle et al., 2012), Greenland
719 (Bunting et al., 2013a) and Czech Republic (Kuneš et al., 2019). Explanations for symbols in the taxa list, see caption Table A1. The
720 values in cells emphasized by a thick rectangle are the mean RPPs used in the new REVEALS reconstruction for Europe (this paper),
721 values in bold are new values, values not in bold are the same values as in Mazier et al. (2012). Underlined values are values from
722 the three published studies that are close to the values of the synthesis in this paper. Other symbols: + The original paper does not
723 provide a RPP for Poaceae and values of standard deviations (SDs) for the RPPs. We extracted the RPP values related to *Picea* from
724 Table 5 in Twiddle et al. (2012). RPPs related to Poaceae (1.00+) were then calculated by assuming that the RPP of *Picea* was equal
725 to the mean RPP of *Picea* in Europe (this synthesis) (in bold). ++ The RPPs and their SDs are not listed in the original paper, we
726 therefore extracted the values from Figure 4 in Bunting et al. (2013a) and the decimals are approximate. +++ Kuneš et al. (2019):
727 we chose the RPP values that were considered best by the authors, i.e. using the lake dataset (pollen from lake sediment), ERV sub-
728 model 1 and the Lagrangian Stochastic Model (for details, see Discussion section, this paper). # value for *Plantago maritima* and ##
729 two values for *Rumex acetosa* and *Rumex acetosella*, respectively (Bunting et al., 2013a), for comparison with *Plantago* spp. and
730 *Rumex acetosa-t.* (this paper). Underlined RPPs are close to mean RPPs (this synthesis).

731

Study	This paper synthesis RPP (SE)	Twiddle et al. (2012)+ RPP - ERV3 random GPM	Bunting et al. (2013)++ RPP (SE) - ERV1 GPM	Kunes et al (2019)+++ RPP (SE) - R ERV1 LSM
Information on analysis				
HERB TAXA				
Poaceae (Reference taxon)	1.000 (0.000)	1.00+	1.00 (0.00)	1.00 (0.00)
Herb taxa				
Amaranthaceae/Chenopodiaceae	4.280 (0.270)			1.58 (0.74)
<i>Calluna vulgaris</i> *	1.085 (0.029)	11.42		
Comp. <i>Leucanthemum</i> (<i>Anthemis</i>)t.***	0.10 (0.01)			0.94 (0.43)
Comp. SF. Cichorioideae***	0.160 (0.020)			1.04 (0.64)
Cyperaceae	0.962 (0.050)		0.95 (0.05)	2.10 (0.88)
<i>Plantago lanceolata</i> ^^	2.330 (0.201)		5.8 (0.3)#	2.24 (0.71)
<i>Potentilla</i> t.^	1.720 (0.200)		0.4 (0.03)	
<i>Ranunculus acrist.</i> ^^^	1.960 (0.360)		2.0 (0.1)	1.38 (1.13)
Rubiaceae	3.710 (0.340)			1.03 (0.74)
<i>Rumex acetosat.</i>	3.020 (0.278)		3.5 (0.3)/2.0 (0.1)##	1.94 (1.35)
<i>Urtica</i>	10.520 (0.310)			1.16 (0.52)
TREE TAXA				
<i>Abies alba</i>	6.875 (1.442)			1.08 (0.99)
<i>Acer</i>	0.800 (0.230)			1.25 (0.75)
<i>Alnus</i>	13.562 (0.293)			2.44 (0.73)
<i>Betula</i> (mainly <i>B. pubescens</i> , <i>B. pendula</i>)	5.106 (0.303)	13.16	3.75 (0.4)	2.53 (0.91)
<i>Carpinus betulus</i>	4.520 (0.425)			1.36 (0.36)
<i>Corylus avellana</i>	1.710 (0.100)			2.31 (1.13)
<i>Fagus sylvatica</i>	5.863 (0.176)			0.88 (0.25)
<i>Fraxinus excelsior</i>	1.044 (0.048)			0.79 (0.37)
<i>Picea abies</i>	5.437 (0.097)	5.44		2.39 (0.93)
<i>Pinus</i> (mainly <i>P. sylvestris</i>)	6.058 (0.237)	16.32		1.55 (0.44)
Dec. <i>Quercust.</i> (mainly <i>Q. robur</i> , <i>Q. petraea</i>)	4.537 (0.086)			2.08 (0.46)
<i>Salix</i>	1.182 (0.077)		0.7 (0.03)	1.43 (0.62)
<i>Tilia</i>	1.210 (0.116)			2.30 (1.24)
<i>Ulmus</i>	1.270 (0.050)			0.96 (0.77)

734 Appendix B - Selection of RPP values and calculation of the mean RPPs and their SDs

735 B.1 Methods

736 Tables B1 (Boreal and Temperate Europe) and B2 (Mediterranean Europe) list the RPP values from the 16 selected studies
737 according to the information on models used provided in Appendix C (Table C1) with further explanations on selection of
738 RPP studies. We followed similar procedures and rules as Mazier et al. (2012) and Li et al. (2018) to produce a new standard
739 RPP dataset for Europe. We consider that there are still too few RPP values per taxon to disentangle variability in the RPP
740 values for a particular taxon due to methodological issues, landscape characteristics, land use, or climate. We therefore use the
741 mean of selected RPP values for each taxon in the new standard RPP dataset, following Broström et al. (2008) and Mazier et
742 al. (2012). In boreal and temperate Europe, the number of RPP values per taxon varies between one and nine (*Betula*) (Table
743 B1), and in Mediterranean Europe, there is only one value per taxon (Table B2). In general, all three sub-models of the ERV
744 model were used in the RPP studies. We selected the RPP values obtained with the ERV sub-model considered by the authors
745 to have provided the best results (following the approach of Li et al., 2018). This is usually evaluated from the shape of the
746 curve of likelihood function scores (LFS), or log likelihood (LL) (Twiddle et al., 2012) and the LFS and LL values themselves.
747 All RPPs selected for this synthesis are expressed relative to Poaceae (RPP=1). In studies that used another reference taxon
748 and calculated a RPP for Poaceae, the RPPs were recalculated relative to Poaceae. In studies that did not include a RPP value
749 for Poaceae, it was assumed that the reference taxon had a RPP related to Poaceae equal to the mean of the RPP values for that
750 taxon in the other studies (Mazier et al., 2012). For simplicity, we used the value of *Quercus* (5.83) calculated by Mazier et al.
751 (2012) for the study by Bunting et al. (2005) (*Quercus* as reference taxon, no RPP value for Poaceae). We could also have
752 used the new mean RPP for *Quercus* (4.54) using our selected RPPs (five values, instead of three in Mazier et al. (2012)). The
753 latter would not have changed our results significantly; the mean RPP for *Quercus* would have been 4.28 instead of 4.54 (Table
754 A4). For the study by Baker et al. (2016), we used the RPP values obtained with Poaceae as the reference taxon, given that the
755 RPPs relative to *Quercus* or *Pinus* were almost identical when ERV submodel 3 was used. The selection of RPP values in
756 boreal and temperate Europe for the calculation of the mean RPP values of each taxon (values in bold and emphasized by a
757 thick rectangle in Table B1, (A) and (B)) is based on the following rules:

- 758 1. We excluded the RPP values that were not significantly different from zero considering the lower bound of its SE,
759 and values that were considered as uncertain by the authors of the original publications (e.g., *Vaccinium* for Finland
760 (Räsänen et al., 2007), *Pinus* for Central Sweden (von Stedingk et al., 2008)). Moreover, some RPP values were
761 excluded as they were assumed to be outliers or unreliable based on experts' knowledge on the plants involved, the
762 pollen-vegetation dataset, and the field characteristics of the related studies. For example, the RPPs for Cyperaceae,
763 *Potentilla-t* and Rubiaceae obtained in SW Norway (Hjelle, 1998) and those for *Salix* and *Calluna vulgaris* from
764 Central Sweden (von Stedingk et al., 2008) were assumed to be too low compared to the values obtained in other
765 study areas (Mazier et al., 2012).

766 2. (i) when five or more RPP estimates of pollen productivity ($N \geq 5$) were available for a pollen type, the largest and the
767 smallest RPP values (generally outlier values) were excluded, and the mean was calculated using the remaining three
768 or more RPP estimates; (ii) when $N=4$, the most deviating value was excluded, and the mean calculated using the
769 other three RPP values; (iii) when $N=3$, the mean was based on all values available except if one value was strongly
770 deviating from the other two; and (iv) when $N=2$, the mean was based on the two values available; an exception is
771 *Ulmus* for which we excluded the value from Germany (Theuerkauf et al. 2013) given that several of the RPPs in this
772 study are considerably higher than most values in the other available studies, i.e. for *Betula* (18.7), *Quercus* (17.85)
773 and *Tilia* (12.38). The latter values were also excluded from the mean RPP, as well as the unusually high values found
774 by Baker et al. (2016) for *Betula* (13.94), *Pinus* (23.12) and *Quercus* (18.47). Baker et al. (2016) argue that the high
775 RPP values might be characteristic of temperate deciduous forests that were little impacted by human activities. More
776 studies in this type of wooded environments would be needed to confirm this assumption. In the absence of such
777 studies we consider these values as outliers.

778 The SDs for the mean RPP values were calculated using the delta method (Stuart. and Ord., 1994), a mathematical solution to
779 the problem of calculating the mean of individual SDs (see Li et al. 2020 for more details).

780 Table B1: Europe (Mediterranean area excluded): RPP estimates and their SDs (in brackets) with the total number of taxa per study
781 indicated and in brackets the number of taxa with selected RPP estimates. (A) Studies using moss pollsters as pollen samples. (B)
782 Studies using surface lake sediments as pollen samples. Values in bold emphasized by thick rectangle: selected RPP estimates to be
783 included in the mean RPP values. Values in bold emphasized by thin rectangle: RPP estimates excluded because of a too large
784 difference with the other available estimates and their mean (less than half or more than double the mean RPP). Values not
785 emphasized by a rectangle: RPP estimates excluded due to its extreme high value compared to the other available estimates (much
786 over double the mean of the other RPPs), i.e. from the study at Bialowice forest (Poland, Baker et al., 2016) for *Betula*, *Pinus* and
787 *Quercus*, Central Sweden (von Stedingk et al., 2008) for *Pinus*, and Germany**** (Theuerkauf et al., 2013) for *Betula*, *Quercus*,
788 *Tilia*, and *Ulmus*. Values in italic: RPP estimates excluded because $SE \geq RPP$. Abbreviations: t. type, C central, Comp. Compositae
789 (= Asteraceae), ERV Extended R-Value model, Medit Mediterranean region, Rep Republic, S southern, SF. Subfamily. Symbols: #
790 RPPs for herbs from Broström et al. (2004); RPPs for trees from Sugita et al. (1999) (reference taxon *Juniperus*), converted to
791 Poaceae as reference taxon by Broström et al. (2004). ## Bunting et al. (2005), reference taxon *Quercus* and no RPP for Poaceae;
792 RPPs relative to Poaceae calculated by Mazier et al. (2012) assuming that the RPP of *Quercus* relative to Poaceae is the same as the
793 mean RPP of *Quercus* from three other studies in NW Europe. * New RPPs from the Czech Republic (Abraham and Kozáková,
794 2012). ** New RPPs from Poland. Poaceae as reference taxa (see text for more details). *** New RPPs from Germany (Matthias et
795 al., 2012), reference taxon *Pinus*. RPPs converted to Poaceae as reference taxon. We selected the RPP estimates obtained with the
796 dataset of vegetation cover including only the trees that had reached their flowering age (allFIDage) (for more information, see
797 Matthias et al., 2012). **** New RPPs from Germany (Theuerkauf et al., 2013); in the original publication, the ERV analysis was
798 performed with the Lagrangian Stochastic Model (LSM) for dispersal of pollen and with *Pinus* as reference taxon. For this synthesis,
799 Martin Theuerkauf redid the analysis with the Gaussian Plume Model for dispersal of pollen (Parsons and Prentice, 1981; Prentice
800 and Parsons, 1983) and with Poaceae as reference taxon.

801

Type of pollen sample Region ERV submodel	Moss polsters							
	Finland	C Sweden	S Sweden#	Norway	England ##	Swiss Jura	Czech Rep*	Poland* *
	ERV 3	ERV 3	ERV 3	ERV 1	ERV 1	ERV 1	ERV 1	ERV 3
HERB TAXA								
Poaceae (Reference taxon)	1.00 (0.00)	1.00 (0.00)	1.00 (0.00)	1.00 (0.00)	1.00 (0.00)	1.00 (0.00)	1.00 (0.00)	1.00 (0.00)
Amaranthaceae/Chenopodiaceae							4.28 (0.27)	
Apiaceae				0.26 (0.009)				
<i>Artemisia</i>							2.77 (0.39)	
<i>Calluna vulgaris</i>		0.30 (0.03)	4.70 (0.69)	1.07 (0.03)				
Cerealia t.			3.20 (1.14)				0.0462 (0.0018)	
Comp. <i>Leucanthemum(Anthemis) t.</i>				0.10 (0.008)				
Comp. SF. Cichorioideae			0.24 (0.06)	0.06 (0.004)				
Cyperaceae	0.002 (0.0022)	0.89 (0.03)	1.00 (0.16)	0.29 (0.01)			0.73 (0.08)	
<i>Empetrum</i>	0.07 (0.06)	0.11 (0.03)						
Ericaceae		0.07 (0.04)						
<i>Filipendula</i>			2.48 (0.82)	3.39 (0.00)				
<i>Plantago lanceolata</i>			12.76 (1.83)	1.99 (0.04)			3.70 (0.77)	
<i>Plantago media</i>							1.27 (0.18)	
<i>Plantago montana</i>							0.74 (0.13)	
<i>Potentilla</i>			2.47 (0.38)	0.14 (0.005)			0.96 (0.13)	
<i>Ranunculus acrist.</i>			3.85 (0.72)	0.07 (0.004)				
Rubiaceae			3.95 (0.59)	0.42 (0.01)			3.47 (0.35)	
<i>Rumex acetosat.</i>			4.74 (0.83)	0.13 (0.004)				
<i>Secale</i>			3.02 (0.05)					
<i>Trollius</i>							2.29 (0.36)	
<i>Urtica</i>							10.52 (0.31)	
<i>Vaccinium</i>	0.01 (0.01)							

TREE TAXA								
<i>Abies</i>						3.83 (0.37)		
<i>Acer</i>			1.27 (0.45)			0.32 (0.10)		
<i>Alnus</i>			4.20 (0.14)		8.74 (0.35)		2.56 (0.32)	15.95 (0.6622)
<i>Betula</i>	4.6 (0.70)	2.24 (0.20)	8.87 (0.13)		6.18 (0.35)			13.94 (0.2293)
<i>Carpinus</i>			2.53 (0.07)					4.48 (0.0301)
<i>Corylus</i>			1.40 (0.04)		1.51 (0.06)			1.35 (0.0512)
<i>Fagus</i>			6.67 (0.17)			1.20 (0.16)		
<i>Fraxinus</i>			0.67 (0.03)		0.70 (0.06)		1.11 (0.09)	
<i>Juniperus</i>		0.11 (0.45)	2.07 (0.04)					
<i>Picea</i>		2.78 (0.21)	1.76 (0.00)			8.43 (0.30)		
<i>Pinus</i>	8.40 (1.34)	21.58 (2.87)	5.66 (0.00)				6.17 (0.41)	23.12 (0.2388)
Deciduous <i>Quercust.</i>			7.53 (0.08)		5.83 (0.00)##		1.76 (0.20)	18.47 (0.1032)
<i>Salix</i>		0.09 (0.03)	1.27 (0.31)		1.05 (0.17)		1.19 (0.12)	
<i>Sambucus nigrat.</i>							1.30 (0.12)	
<i>Tilia</i>			0.80 (0.03)				1.36 (0.26)	0.98 (0.0263)
<i>Ulmus</i>			1.27 (0.05)					
Total number of taxa 39 (38)	6 (4)	10 (7)	26 (25)	12 (8)	7 (7)	11(10)	13(12)	8 (5)

804

Type of pollen sample Region ERV submodel	lake surface sediment				
	Estonia	Denmark	Swiss Plateau	Germany** *	Germany ****
	ERV 3	ERV 1		ERV 3	
HERB TAXA					
Poaceae (Reference taxon)	1.00 (0.00)	1.00 (0.00)	1.00 (0.00)	1.00 (0.00)	1.00 (0.00)
<i>Artemisia</i>	3.48 (0.20)				5.56 (0.020)
<i>Calluna vulgaris</i>		1.10 (0.05)	0.00076 (0.0019)		
Cerealia t.	1.60 (0.07)	0.75 (0.04)	0.17 (0.03)	9.00 (1.92)	0.08 (0.001)
Compositae <i>Leucanthemum</i> (<i>Anthemis</i>) t.			0.24 (0.15)		
Cyperaceae	1.23 (0.09)				
<i>Filipendula</i>	3.13 (0.24)				
<i>Plantago lanceolata</i>		0.90 (0.23)			2.73 (0.043)
<i>Rumex acetosa</i> t.		1.56 (0.09)			2.76 (0.022)
<i>Secale</i>				4.08 (0.96)	4.87 (0.006)
TREE TAXA					
			9.92 (2.86)		
<i>Alnus</i>	13.93 (0.15)		2.42 (0.39)	15.51 (1.25)	13.68 (0.049)
<i>Betula</i>	1.81 (0.02)		4.56 (0.85)	9.62 (1.92)	19.70 (0.117)
<i>Carpinus</i>			2.58 (0.39)	9.45 (0.51)	
<i>Corylus</i>			0.76 (0.17)		
<i>Fagus</i>		5.09 (0.22)	1.39 (0.21)	5.83 (0.45)	9.63 (0.008)
<i>Fraxinus</i>				6.74 (0.68)	1.35 (0.012)
<i>Juniperus</i>			0.57 (0.16)		
<i>Picea</i>	4.73 (0.13)	1.19 (0.42)	1.35 (0.45)	1.58 (0.28)	5.81 (0.007)
<i>Pinus</i>	5.07 (0.06)			5.66 (0.00)	5.39 (0.222)
<i>Populus</i>			2.56 (0.39)	2.66 (1.25)	
Deciduous <i>Quercust.</i>	7.39 (0.20)			2.15 (0.17)	17.85 (0.049)
<i>Salix</i>	2.31 (0.08)				
<i>Tilia</i>				1.47 (0.23)	12.38 (0.101)
<i>Ulmus</i>					11.51 (0.101)
Total number of taxa (selected values) 23 (22)	11 (11)	7 (7)	13 (9)	13 (10)	15 (11)

807 **Table B2: Mediterranean area: RPP estimates and their SDs from two available studies, and mean RPPs for northern and temperate**
808 **Europe (Table A1, Appendix A), for comparison. RPPs and FSPs emphasized in bold are those used in the REVEALS reconstruction**
809 **for Europe (this paper), single RPP values from the Mediterranean region within thick rectangles, and mean RPPs from Europe**
810 **(Mediterranean region excluded) within thin rectangles. The plant taxa emphasized in bold are sub-Mediterranean and/or**
811 **Mediterranean plant species and genera. FSP values: from Mazier et al. (2012) except (‘) new values from Mazier et al. (unpubl.),**
812 **(‘’) value from Abraham and Kózáková (2012), (‘’’) value from (Commerford et al., 2013). *, **FSP from Mazier et al. (2012) used**
813 **in the REVEALS reconstruction (this study) for Ericaceae (Medit)* and evergreen *Quercus* t. ** instead of the new FSP values from**
814 **Mazier et al. (unpubl.); for more explanations, see Discussion section, this paper. Abbreviations: Comp. Compositae (= Asteraceae),**
815 **ERV Extended R-Value model, Medit Mediterranean region, SF. Subfamily.**

816

Region	France Medit. (ERV3)			Romania (ERV3)			Europe, Medit. excluded		
Study reference	Mazier et al. (unpubl.)			Grindean et al. (2019)			This paper (Tables A1)		
	RPP	SD	FSP	RPP	SD	FSP	RPP	SD	FSP
HERB TAXA									
Poaceae (reference taxon)	1.000	0.000	0.035	1.00	0.00	0.035	1.00	0.00	0.035
Apiaceae				5.91	1.23	0.042	0.26	0.01	0.042
<i>Artemisia</i>				<u>5.89</u>	3.16	0.014"	3.937	0.146	0.014"
Compositae (Asteroideae + Cichorioideae)				<u>0.16</u>	0.10	0.029			
Comp. SF. Asteroideae (<i>Anthemis</i> t., <i>Leucanthemum</i>)							<u>0.10</u>	0.01	0.029
Comp. SF. Cichorioideae	1.162	0.675	0.061'				<u>0.16</u>	0.02	0.05
Cerealia (Cerealia t. + <i>Triticum</i> t. + <i>Secale</i> + <i>Zea</i>)				0.22	0.12	0.060			
Cerealia t. (Cerealia t., <i>Secale</i> excluded)							1.85	0.38	0.060
Cerealia - <i>Secale cereale</i>							3.99	0.33	0.060
Fabaceae				0.40	0.07	0.021'''			
<i>Plantago lanceolata</i>				0.58	0.32	0.029	2.33	0.20	0.029
Ranunculaceae	<u>2.038</u>	0.335	0.020'						
Ranunculaceae - <i>Ranunculus acris</i> t.							<u>1.96</u>	0.36	0.014
Ranunculaceae - <i>Trollius</i>							<u>2.29</u>	0.36	0.013
Rosaceae (<i>Filipendula</i> , <i>Potentilla</i> t., <i>Sanguisorba</i>)				0.29	0.12	0.018			
Rosaceae - <i>Filipendula</i>							3.00	0.28	0.006
Rosaceae - <i>Potentilla</i> t.							1.72	0.20	0.018
Rubiaceae				0.40	0.07	0.019	3.71	0.34	0.019
TREE/SHRUB TAXA									
<i>Acer</i>				<u>0.30</u>	0.09	0.056	<u>0.80</u>	0.23	0.056
<i>Buxus sempervirens</i>	1.890	0.068	0.032'						
<i>Carpinus betulus</i>							4.52	0.43	0.042
<i>Carpinus orientalis</i>				0.24	0.07	0.042			
<i>Castanea sativa</i>	3.258	0.059	0.010'						
<i>Corylus avellana</i>	3.440	0.890	0.025				1.71	0.10	0.025
Cupressaceae (<i>Juniperus communis</i> , <i>J. phoenica</i> , <i>J. oxycedrus</i>)	<u>1.618</u>	0.161	0.020'						
Cupressaceae - <i>Juniperus communis</i>							2.07	0.04	0.016
Ericaceae (<i>Arbutus unedo</i> , <i>Erica arborea</i> , <i>E. cinerea</i> , <i>E. multiflora</i>)	4.265	0.094	0.051'						

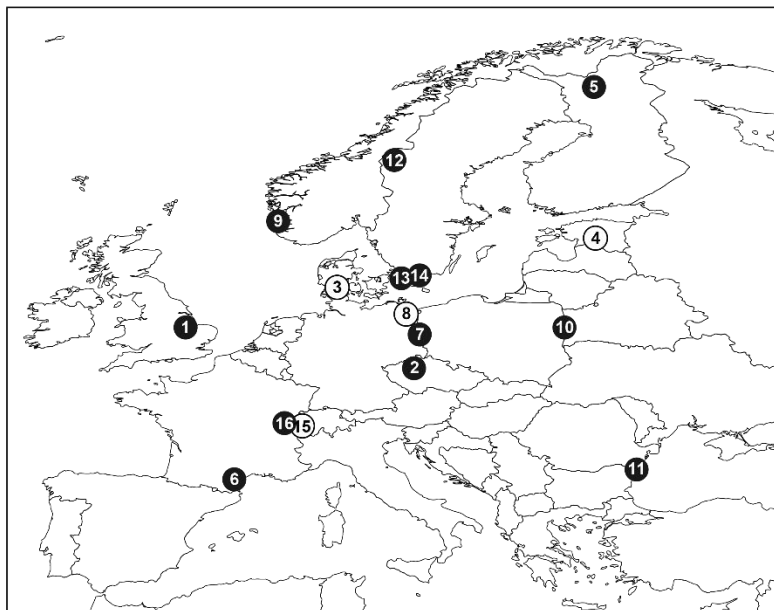
Ericaceae (<i>Vaccinium</i> dominant, <i>Calluna</i> excluded)					0.07	0.04	0.038*
<i>Fraxinus excelsior</i>					1.04	0.02	0.022
<i>Fraxinus</i> (<i>F. excelsior</i> , <i>F. ornus</i>)		2.99	0.88	0.022			
<i>Phillyrea</i>	0.512	0.076	0.015'				
<i>Pistacia</i>	0.755	0.201	0.030'				
Evergreen <i>Quercus</i> t. (<i>Q. ilex</i> , <i>Q. coccifera</i>)	11.04						
Deciduous <i>Quercus</i> t. (<i>Q. spp.</i> , <i>Q. peduncularis</i> dominant)	3	0.261	0.015'				
Deciduous <i>Quercus</i> t. (<i>Q. petraea</i> + <i>Q. rubra</i>)				1.10	0.35	0.035	
					4.54	0.09	0.035**
Total number of taxa	11			13			

817

818 Appendix C - Selection of RPP studies

819 The synthesis of mean RPPs presented here was produced in 2018 and applied in REVEALS reconstructions 2018-2020. Of
820 nineteen RPP studies available (in July 2021), we selected fifteen published between 1998 and 2018 and one unpublished
821 study in 2018 (Grindean et al., 2019). The sixteen study regions are distributed in twelve European countries (Figure C1) and
822 detailed in Table C1. Three studies are not included in our synthesis: Britain (Twiddle et al., 2012) because of the absence of
823 Poaceae in the calculated RPPs, curves of likelihood function scores exhibiting departures from theoretically correct curves,
824 and doubts expressed by the authors on the reliability of the values; Greenland (Bunting et al., 2013a) because this land area
825 was not included in the REVEALS reconstruction of Holocene plant cover in Europe presented in this paper; and Czech
826 Republic (Kuneš et al., 2019) because the study was not ready when we finalized our synthesis. However, we compare the
827 RPP values from these three studies with the mean RPP values in this synthesis (Appendix A, Table A2).

828 All studies used the ERV model to calculate RPPs, and all but one study used modern pollen assemblages and vegetation; only
829 Nielsen et al. (2004; Denmark) used historical pollen and vegetation data. Eleven studies used pollen assemblages from moss
830 pollsters, five studies from lake sediments. Grindean et al. (2019; Romania) also used some pollen assemblages from surface



831

832 **Figure C1: Location of the selected studies of relative pollen productivities (RPP) in Europe. 1. Britain, (Bunting et al., 2005); 2.**
833 **Czech Republic, (Abraham and Kozáková, 2012); 3. Denmark, (Nielsen, 2004); 4. Estonia, (Poska et al., 2011); 5. Finland, (Räsänen**
834 **et al., 2007); 6. France, Mazier et al. unpublished; 7. Germany, (Matthias et al., 2012); 8. Germany, (Theuerkauf et al., 2013); 9.**
835 **Norway, (Hjelle, 1998); 10. Poland, (Baker et al., 2016); 11. Romania, (Grindean et al., 2019); 12. Sweden, (von Stedingk et al., 2008);**
836 **13. Sweden, (Sugita et al., 1999); 14. Sweden, (Broström et al., 2004); 15. Switzerland, (Soepboer et al., 2007); 16. Switzerland,**
837 **(Mazier et al., 2008).**

838 soil samples. All studies used distance-weighted vegetation except two, Hjelle et al. (1998; SW Norway) and Sugita et al.
839 (1999; S Sweden). The Gaussian Plume Model (GPM) was used for pollen dispersal and deposition to distance-weight
840 vegetation, i.e. the Prentice's bog model (Parsons and Prentice, 1981; Prentice and Parsons, 1983) in studies using pollen from
841 moss pollsters, and the Sugita's lake model (Sugita, 1993) in studies using pollen from lake sediments (see also caption of
842 Table C1). In the case of the study by Theuerkauf et al. (2013), the published RPP values were calculated using the Lagrangian
843 Stochastic Model. For the purpose of this synthesis, Theuerkauf recalculated the RPPs using the GPM bog model in the
844 application of the ERV model. The distribution of sites for collection of pollen samples and vegetation data within the study
845 regions is random or random stratified in seven of the eleven studies using moss pollsters; the five remaining studies used
846 selected sites (or systematic distribution). Studies using lake sediments normally result in a systematic site distribution. Earlier
847 studies (Broström et al., 2005; Twiddle et al., 2012) showed that random distribution of sites provided better estimates of
848 "relevant source area of pollen" (RSAP; *sensu* Sugita, 1994) and thus of RPPs, given that the reliable RPPs are those obtained
849 at the RSAP distance and beyond. Both studies indicated that systematic distribution of sites have the tendency to result in
850 curves of likelihood function scores that do not follow the theoretical behaviour, i.e. an increase of the scores with distance
851 until the values reach an asymptote. However, the difference in RPPs between systematic and random sampling is generally
852 not very large. Nonetheless, systematic sampling may lead to uncertainty in terms of reliability of RPPs and random
853 distribution of sites is recommended and has generally been used in studies using moss pollsters or soil samples published
854 from 2008 and onwards.

855 **Table C1: Selection of studies for the synthesis of relative pollen productivity (RPP) estimates. Emphasized in bold: additional, new**
856 **studies compared to the studies included in the synthesis of Mazier et al. (2012). Symbols: ¹L=lakes; M=moss pollsters; S=surface**
857 **soil; ²Other distance-weighting models were used in most studies, including the Gaussian Plume Model (GPM), 1/d, 1/d² (d=distance)**
858 **and the Lagrangian Stochastic Model (LSM). The GPM is used in both the model developed for bogs (Parsons and Prentice, 1981;**
859 **Prentice and Parsons, 1983) and lakes (Sugita, 1993). For this RPP synthesis, we chose the results from the analyses using GPM**
860 **rather than 1/d or 1/d². Note: In the study of Theuerkauf et al. (2013) the LSM was used. For this synthesis, Theuerkauf recalculated**
861 **his RPPs using the lake model developed by Sugita (1993); ³Number of plant taxa for which RPP was estimated, including the**
862 **reference taxon. Note: In the study by Theuerkauf et al. (2013) RPPs were estimated for 17 taxa using LSM. The RPPs were**
863 **recalculated using the lake model (Sugita, 1993) for 15 taxa (see note under ² above) for this synthesis. In the study of Sugita et al.**
864 **(1999) RPPs were calculated for 14 trees and 3 herbs. We used only the values for the 14 trees in this synthesis, following the syntheses**
865 **by Broström et al. (2008) and Mazier et al. (2012); [^] Britain: the study includes two areas (a and b) in which RPP estimates were**
866 **calculated for different sets of taxa and the two areas have different numbers of sites: a. Calthorpe (34), 5 taxa; b. Wheatfen (17),**
867 **same 5 taxa and *Corylus* (6 taxa in total); ^{^^} random distribution restricted to areas of the study region with existing vegetation**
868 **maps (therefore no sites outside these areas); i.e. study region including separate areas (Mazier et al., 2008). ⁺ Vegetation data from**
869 **historical maps around 1800 CE; ⁺⁺ lake sediments dated to ca. 1800; ^{*} The reference taxon used in the original study is different**
870 **from Poaceae. For this synthesis the RPPs were converted to values relative to Poaceae; ^{**} The study of Bunting et al. (2005) does**
871 **not include a RPP for Poaceae. In order to calculate the RPPs relative to Poaceae, it was assumed that the RPP of *Quercus* was equal**
872 **to the mean of RPPs from three other studies in Europe (see Mazier et al., 2012 for details). Although we have included new RPP**
873 **values for *Quercus* in this synthesis, we did not recalculate the RPPs from Bunting et al. (2005) with a new mean value for *Quercus*,**
874 **but used the same values as in Mazier et al. (2012). For comparison, the mean value for *Quercus* using the RPPs of the additional**
875 **studies included in this synthesis is 4.28 (instead of 5.83 in Mazier et al., 2012). This would imply slightly lower RPPs in Britain also**
876 **for *Alnus*, *Betula*, *Corylus*, *Fraxinus* and *Salix*. # no distance weighting used for vegetation data because there was no information**
877 **about vegetation with increasing distance from the pollen sample (Hjelle et al., 1998; Sugita et al., 1999). In the Swedish study,**
878 **vegetation data within a 10² m² (herb taxa) and 10³ m² quadrat (tree taxa) centred on the pollen sample was used (Sugita et al., 1999).**
879

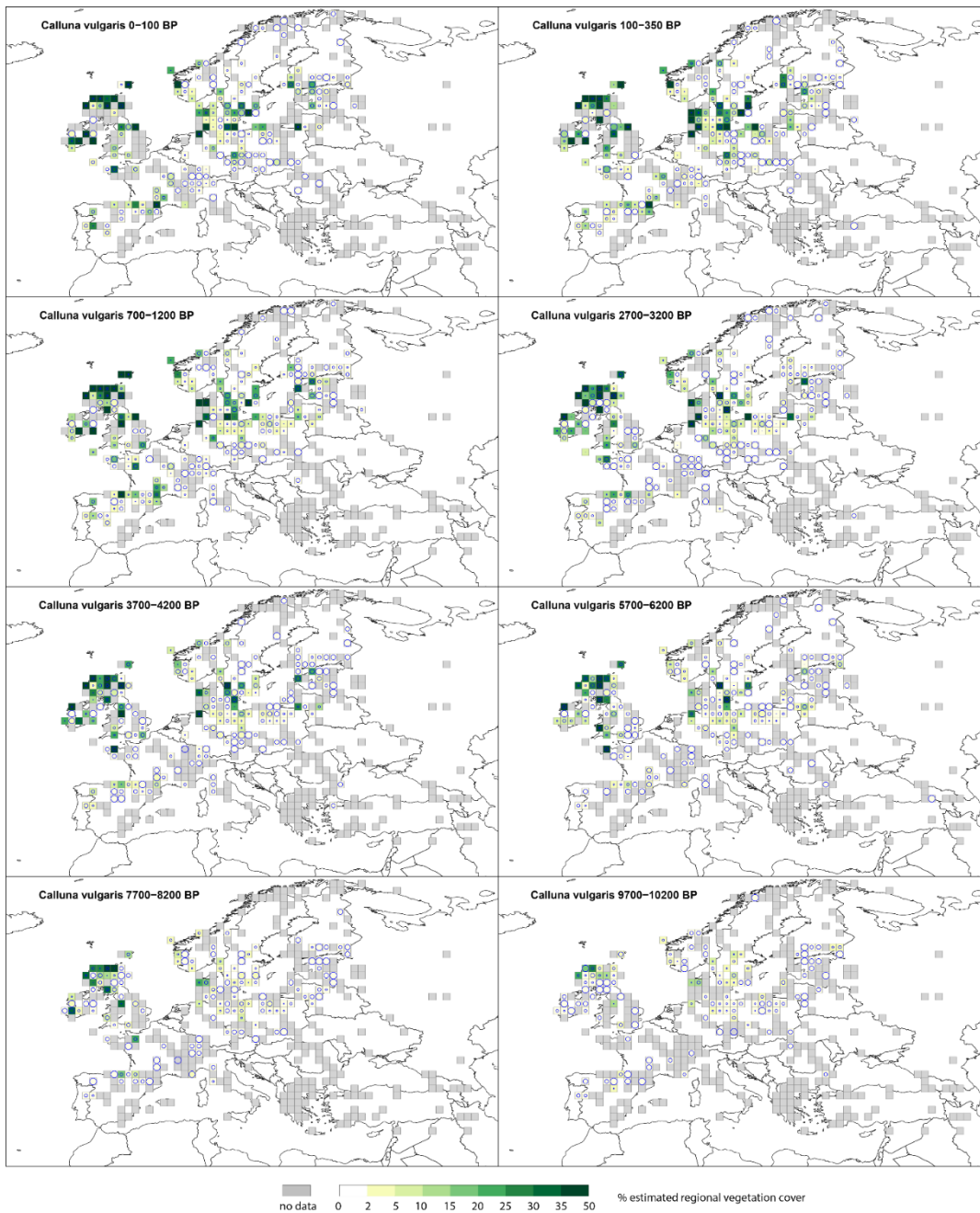
880

Country	Region	No sites	Site distrib.	Pollen sample ¹	ERV sub-model	Distance weighting model ²	Reference taxon	No taxa ³	Reference
Britain	East Anglian: Norfolk woodlands	(34 + 19) [^]	selected	M	1	GPM Prentice's bog	<i>Quercus</i> Poaceae**	6	Bunting et al. 2005
Czech Republic	Central Bohemia: agricultural landscape	54	stratified random	M	1	GPM Prentice's bog	Poaceae	13	Abraham & Kóžaková 2012
Denmark	Ancient agricultural landscape ⁺	30	selected	L ⁺⁺	1	GPM Sugita's lake	Poaceae	7	Nielsen et al. 2004
Estonia	Hemiboreal forest zone: mixed woodland - agricultural landscape	40	selected	L	3	GPM Sugita's lake	Poaceae	10	Poska et al. 2011
Finland	N Finland	24	stratified random	M	3	GPM Prentice's bog	Poaceae	6	Räsänen et al. 2007
France	Mediterranean region	23	random	M	3	GPM Prentice's bog	Poaceae	11	Mazier et al. unpubl.
Germany	Eastern Germany: Brandenburg, agricultural landscape	49	selected	L	3	GPM Sugita's lake	<i>Pinus</i> Poaceae*	16	Matthias et al. 2012
	NE Germany: agricultural landscape	27	selected	L	3	LSM GPM Sugita's Lake ²	<i>Pinus</i> Poaceae*	11 (15) ³	Theuerkauf et al. 2013
Norway	SW Norway: Hordaland and Sogn og Fjordane, mown or grazed grass-land and heath	39	selected	M	1	None [#]	Poaceae	17	Hjelle 1998
Poland	NE Poland: Bialowieza Forest	18	stratified random	M	3	GPM Prentice's bog	Poaceae	8	Baker et al. 2016
Romania	SE Romania: Forest-steppe region	26	random	M & S	3	GPM Prentice's bog	Poaceae	13	Grindean et al. 2019
Sweden	West- Central Sweden: Forest-tundra ecotone	30	random	M	3	GPM Prentice's bog	Poaceae	10	von Stedingk et al. 2008
	S Sweden: ancient cultural landscapes	114	selected	M	3	None [#]	<i>Juniperus</i> Poaceae*	14 (17) ³	Sugita et al. 1999
	S Sweden: unfertilized mown or grazed grasslands	42	selected	M	3	GPM Prentice's bog	Poaceae	11	Broström et al. 2004

Switzerland	Lowland: agricultural landscape	20	selected	L	3	GPM Prentice's bog	Poaceae	13	Soepboer et al. 2007
	Jura Mountain: pasture woodlands	20	(stratified) random^^	M	1	GPM Prentice's bog	Poaceae	11	Mazier et al. 2008

881

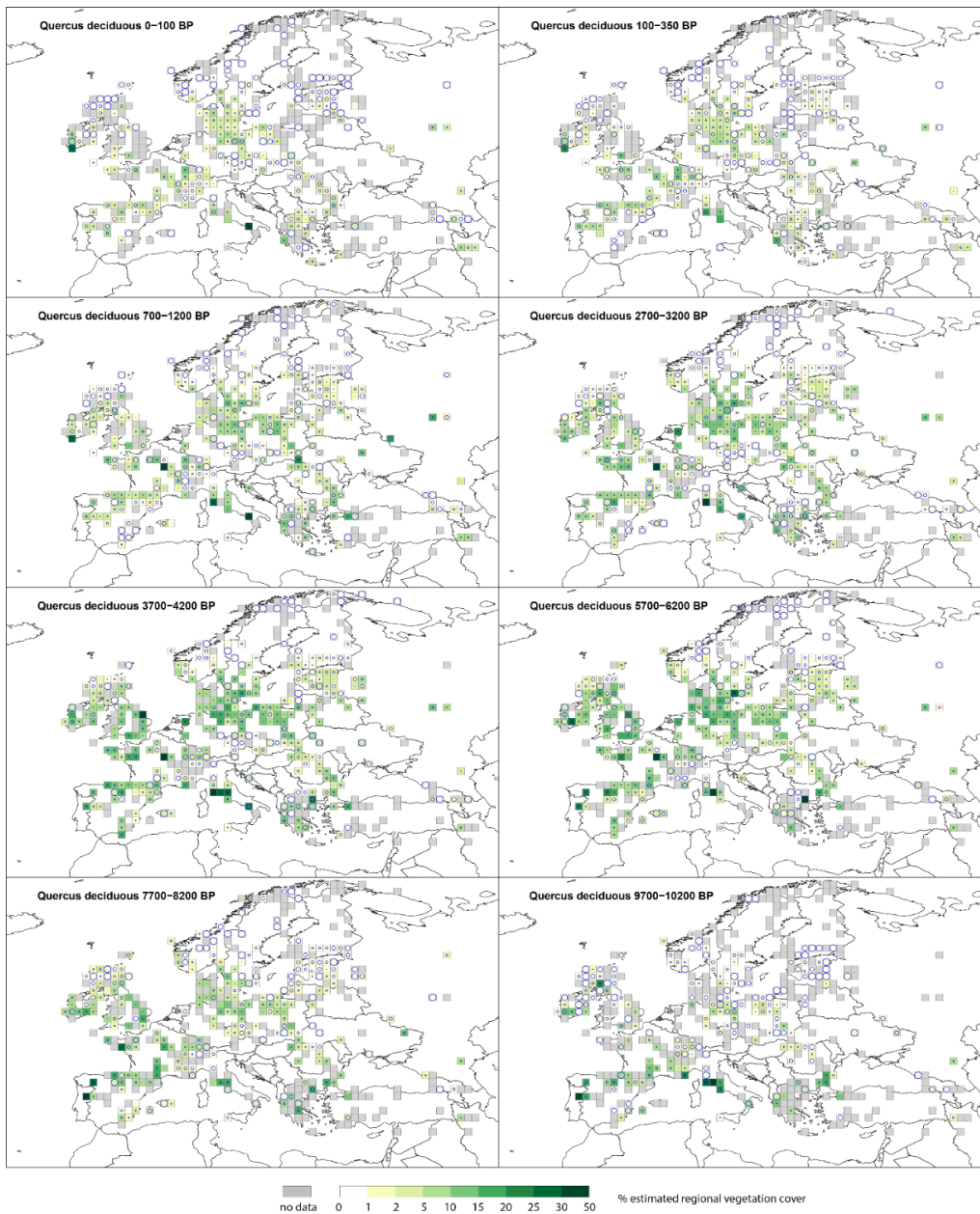
882 **Appendix D Maps of REVEALS cover for three plant taxa (*Calluna vulgaris*, deciduous *Quercus* type (t.) and evergreen**
883 ***Quercus* t.)**



884

885 **Figure D1.** Grid-based REVEALS estimates of *Calluna vulgaris* cover for eight Holocene time windows. Percentage cover in 2%
 886 interval between 0 and 2%, 3% interval between 2 and 5%, 5% intervals between 5 – 35% and 15% interval between 35 and 50%.
 887 Intervals represented by increasingly darker shades of green from 5-10%. Grey grid cells have no data (pollen) for *Calluna vulgaris*
 888 in the mapped time window. The circles represent the coefficient of variation (CV; the standard error divided by the REVEALS
 889 estimate). When $SE \geq REVEALS$ estimate, the circle fills the entire grid cell and the REVEALS estimate is not different from zero.
 890 This occurs mainly where REVEALS estimates are low.

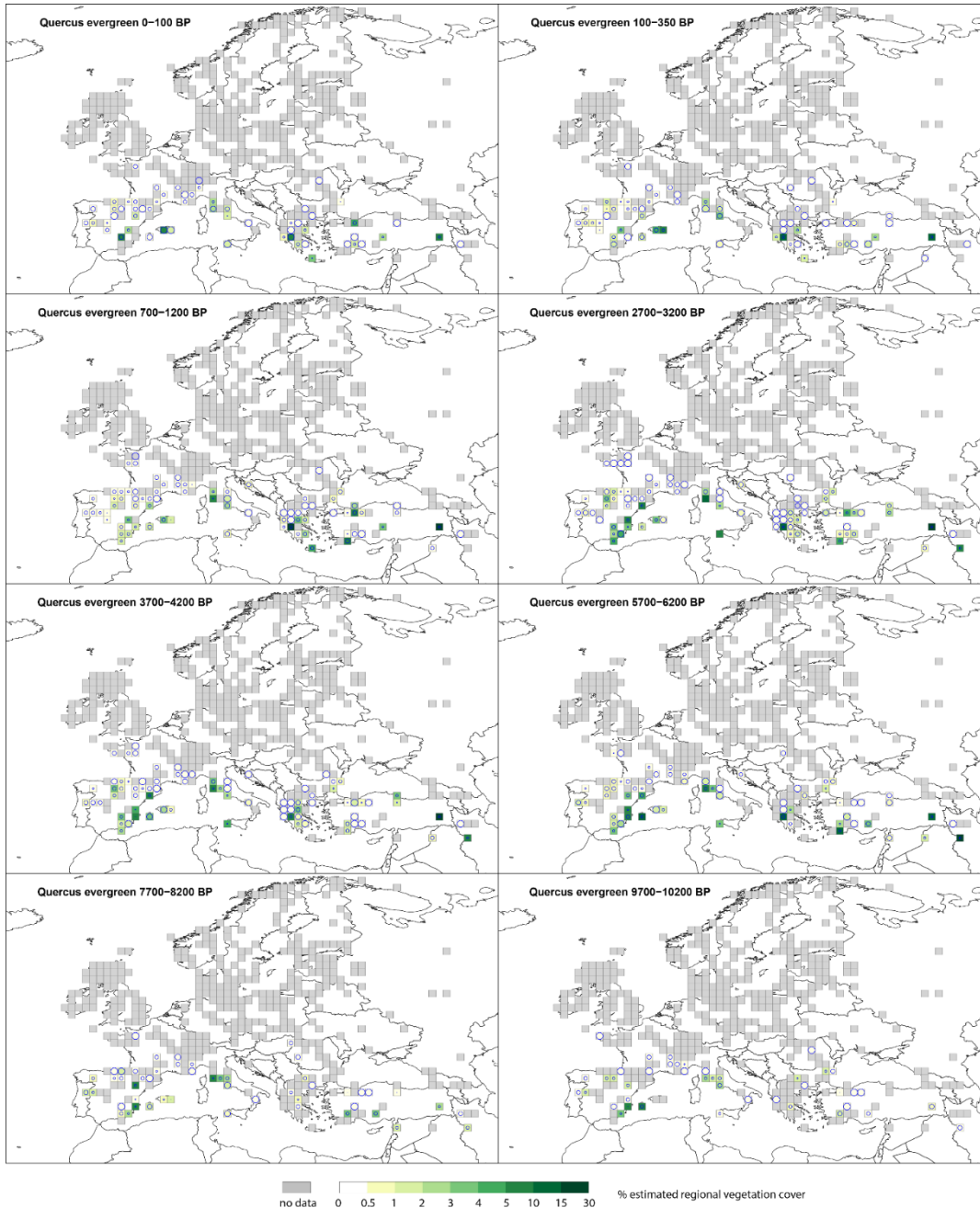
891



893

894

895 **Figure D2. Grid-based REVEALS estimates of deciduous *Quercus* cover in eight Holocene time windows. Percentage**
 896 **cover in 1% interval between 0 and 2%, 3% interval between 2 and 5%, 5% intervals between 5 and 30% and 20%**
 897 **interval between 30 and 50%. Intervals represented by increasingly darker shades of green from 2-5%. Grey grid**
 898 **cells have no data (pollen) for *Calluna vulgaris* in the mapped time window. The circles represent the coefficient of**
 899 **variation (CV; the standard error divided by the REVEALS estimate). When $SE \geq$ REVEALS estimate, the circle**
 900 **fills the entire grid cell and the REVEALS estimate is not different from zero. This occurs mainly where REVEALS**
 901 **estimates are low.**



903

904 **Figure D3. Grid-based REVEALS estimates of evergreen *Quercus* cover for eight Holocene time windows. Percentage**
 905 **cover in 0.5% intervals between 0 and 1%, 1% intervals between 1 and 5%, 5% intervals between 5 and 15 and 15%**
 906 **interval between 15 and 30%. See caption of Figure A1 for more explanations. Intervals represented by increasingly**
 907 **darker shades of green from 1-2%. Grey grid cells have no data (pollen) for *Calluna vulgaris* in the mapped time**
 908 **window. The circles represent the coefficient of variation (CV; the standard error divided by the REVEALS**
 909 **estimate). When $SE \geq REVEALS$ estimate, the circle fills the entire grid cell and the REVEALS estimate is not**
 910 **different from zero. This occurs mainly where REVEALS estimates are low.**

911 **+Team list**

912 Åkesson Christine (School of Geography & Sustainable Development, University of St. Andrews, UK), Balakauskas Lauras
913 (Department of Geology and Mineralogy, Vilnius University, Vilnius, Lithuania), Batalova Vlada (Lomonosov Moscow State
914 University, Department of Physical geography and Landscape science, Moscow, Russia), Birks H.J.B. (Department of
915 Biological Sciences and Bjerknes Centre for Climate Research, University of Bergen, Norway), Bjune Anne. E. (Department
916 of Biological Sciences and Bjerknes Centre for Climate Research, University of Bergen, Norway), Borisova Olga (Institute of
917 Geography, Russian Academy of Sciences, Moscow, Russia), Bozilova Elissaveta (Department of Botany, Sofia University
918 St. Kliment Ohridski, Sofia, Bulgaria), Burjachs Francesc (ICREA Barcelona, Catalonia, Spain; Rovira i Virgili University
919 (URV), Tarragona, Catalonia, Spain; Institut Català de Paleoecologia Humana i Evolució Social (IPHES), Campus Sescelades
920 URV, W3, 43007 Tarragona, Spain), Cheddadi Rachid (Institut des Sciences de l'Evolution de Montpellier, Université de
921 Montpellier, CNRS-UM-IRD, Montpellier, France), Christiansen Jörg (Department of Palynology and Climate Dynamics,
922 Georg-August University, Göttingen, Germany), David Remi (Archeosciences Laboratory, UMR 6566 CReAAH, CNRS,
923 Rennes1 University, Rennes, France), de Klerk Pim (State Museum of Natural History, Karlsruhe, Germany), Di Rita Federico
924 (Dipartimento di Biologia Ambientale, Università di Roma "La Sapienza", Piazzale Aldo Moro, 5, 00185, Roma, Italia),
925 Dörfler Walter (Institute für Ur- und Frühgeschichte, Christian-Albrechts University, Kiel, Germany), Doyen Elise
926 (Paleobotanab, Bureau d'étude spécialisé en reconstitution des paléoenvironnements à partir de vestiges botaniques, 01300
927 Nattages), Eastwood Warren (School of Geography, Earth and Environmental Sciences, University of Birmingham B15 2TT,
928 UK), Etienne David (Savoie Mont Blanc University, Chambéry, France), Feeser Ingo (Institut für Ur- und Frühgeschichte,
929 Christian-Albrechts University, Kiel, Germany), Filipova-Marinova Mariana (Museum of Natural History, Varna, Bulgaria),
930 Fischer E. (Institute für Ur- und Frühgeschichte, Christian-Albrechts University, Kiel, Germany), Galop Didier (GEODE UMR
931 5602, Toulouse University, Toulouse, France), Garcia Jose Sebastian Carrion (Departamento de Biología Vegetal, Facultad
932 de Biología, Universidad de Murcia, 30100 Murcia, Spain), Gauthier Emilie (Laboratoire Chrono-Environnement, UMR 6249
933 CNRS-Franche-Comté University, Besançon, France), Giesecke Thomas (Department of Physical Geography, Utrecht
934 University, Utrecht, The Netherlands), Herking Christa (Institute of Botany and Landscape Ecology, EMAU, Greifswald,
935 Germany), Herzschuh Ulrike (Alfred-Wegener-Institut Potsdam, Germany), Jouffroy-Bapicot Isabelle (Laboratoire Chrono-
936 Environnement, UMR 6249 CNRS, Franche-Comté University, Besançon, France), Kasianova Alisa (Department of
937 Palynology and Climate Dynamics, Georg-August-University, Göttingen, Germany), Kouli Katerina (Department of Geology
938 and Geoenvironment, National and Kapodistrian University of Athens, Panepistimioupolis, 15784 Ilissia, Greece), Kuneš Petr
939 (Department of Botany, Charles University, Prague, Czech RepublicCzech), Lagerås Per (The Archaeologists, National
940 Historical Museums, Lund, Sweden), Latałowa Małgorzata (Department of Plant Ecology, University of Gdansk, Poland),
941 Lechterbeck Jutta (State Office for Cultural Heritage Baden-Wuerttemberg, Germany), Leroyer Chantal (Archeosciences
942 Laboratory, UMR 6566 CReAAH, CNRS, Rennes1 University, Rennes, France), Leydet Michelle (European Pollen Database,

943 IMBE, Aix-Marseille Université, Avignon Université, IRD, Aix-en-Provence, France), Lisystina Olga (Department of
944 Geology, Tallinn University of Technology, 19086 Tallinn, Estonia), Lukanina Ekaterina (Department of Palynology and
945 Climate Dynamics, Georg-August-University, Göttingen, Germany), Magyari Enikő (Department of Environmental and
946 Landscape Geography, Eötvös Loránd University, Budapest, Hungary), Marguerie Dominique (UMR 6553 ECOBIO / Thème
947 PaysaBio, Université de Rennes 1, 35042 RENNES Cedex France), Mariotti Lippi Marta (Dipartimento di Biologia,
948 Università di Firenze, Via G. La Pira, 4, 50121 Firenze, Italy), Mensing Scott (Department of Geography, University of
949 Nevada, Reno, NV 89557, USA), Mercuri Anna Maria (Laboratorio di Palinologia e Paleobotanica, Dipartimento di Scienze
950 della Vita, Università di Modena e Reggio Emilia, Italy), Miebach Andrea (Steinmann Institute for Geology, Mineralogy, and
951 Paleontology, University of Bonn, Bonn, Germany), Milburn Paula (College of Science and Engineering, University of
952 Edinburgh, Edinburgh, Scotland), Miras Yannick (CNRS HNHP UMR 7194, Museum National d'Histoire Naturelle, Paris,
953 France), Morales del Molino César (Alpine Pollen Database, Institute of Plant Sciences, Bern University, Switzerland),
954 Mrotzek Almut (Institute of Botany and Landscape Ecology, EMAU, Greifswald, Germany), Nosova Maria (Main Botanical
955 Garden, Russian Academy of Sciences, Moscow, Russia), Odgaard Bent Vad (Department of Geoscience, Aarhus University,
956 Denmark). Overballe-Petersen Mette (Forest & Landscape, Faculty of Life Sciences, University of Copenhagen,
957 Frederiksberg, Denmark), Panajiotidis Sampson (Aristotle University of Thessaloniki, Department of Forestry and Natural
958 Environment, PO Box: 270, GR54124 Thessaloniki, Greece), Pavlov Danail (Society of Innovative Ecologists of Bulgaria,
959 Varna, Bulgaria), Persson Thomas[†] (Department of Geology, Lund University, Lund, Sweden), Pinke Zsolt (Department of
960 Physical Geography, Eötvös Loránd University, Budapest, Hungary), Ruffaldi Pascale (Laboratoire Chrono-Environnement,
961 UMR 6249 CNRS, Franche-Comté University, Besançon, France), Sapelko Tatyana (Institute of Limnology, Russian
962 Academy of Sciences, St. Petersburg, Russia), Schmidt Monika (Department of Palynology and Climate Dynamics, Georg-
963 August-University, Göttingen, Germany), Schult Manuela (Institute of Botany and Landscape Ecology, EMAU, Greifswald,
964 Germany), Stivrins Normunds (Department of Geography, Faculty of Geography and Earth Sciences, University of Latvia,
965 Jelgavas iela 1, Riga, 1004, Latvia), Tarasov Pavel E. (Institute of Geological Sciences, Free University of Berlin, Germany),
966 Theuerkauf Martin (Institute of Botany and Landscape Ecology, EMAU Greifswald, 1748 Greifswald, Germany), Veski Siim
967 (Department of Geology, Tallinn University of Technology, Tallinn, Estonia), Wick Lucia (IPNA, University of Basel, Basel,
968 Switzerland), Wiethold Julian (INRAP, Direction interrégionale Grand-Est Nord, Laboratoire archéobotanique, Metz, France),
969 Woldring Henk (Groningen Institute of Archaeology, University of Groningen, The Netherlands), Zernitskaya Valentina
970 (Institute for Nature Management, National Academy of Sciences of Belarus, Minsk, Republic of Belarus).

971 **Author Contribution**

972 MJG coordinated the study as part of LandClim II and PAGES LandCover6k, two research projects for which she is the overall
973 coordinator and administrator. MJG, AKT, EG, FM, RF, ABN, AP and SS conceptualised the study and methodology. SS
974 developed the REVEALS model and helped with all issues related to the application of the model and interpretation of results.

975 EG, AKT, RF, FM, ABN, and AP collected new pollen records from individual authors. JW provided part of the pollen records
976 from the Mediterranean area (collected earlier for a separate project). LS, MS and ST provided unpublished pollen records.
977 EG and AKT had the major responsibility of handling the pollen data files and collecting all related metadata. AKT collected
978 new values of relative pollen productivity estimates (RPPs) in Europe. FM provided unpublished RPP values for the
979 Mediterranean area. FM, JA, VL, LM, and NNC were all involved in the unpublished RPP study in southern France, and AF,
980 RG, ABN and IT performed the RPP study in Romania. MJG performed the selection of RPP values for the new RPP synthesis
981 used in this paper, EG made the calculations of mean RPPs, and MJG wrote Appendices A, B, and C, and prepared the Figures
982 and Tables therein. RF performed the REVEALS model runs and created Figure 1 and the maps of REVEALS-based plant
983 cover (Figures 2-6 and D1-D3). EG, RF and MJG designed the manuscript, EG prepared the first draft of the manuscript and
984 all Tables, and the final manuscript for submission, RF and MJG wrote parts of the text and edited the full manuscript. All the
985 co-authors, including the data contributors in the Team List (LandClim II data contributors), were involved in commenting
986 and revising the manuscript.

987 **Competing interests**

988 The authors declare that they have no conflict of interest.

989 **Figures entirely compiled by the manuscript authors:** Since such figures are part of the manuscript, they will receive the
990 same distribution licence as the entire manuscript, namely a CC BY License. No citation is needed and no reproduction rights
991 must be obtained.

992 **Acknowledgements**

993 This study was funded by a research project financed by the Swedish Research Council VR (Vetenskapsrådet) on
994 “Quantification of the bio-geophysical and biogeochemical forcings from anthropogenic de-forestation on regional Holocene
995 climate in Europe, LandClim II”. Financial support from the Linnaeus University’s Faculty of Health and Life Science is
996 acknowledged for Marie-José Gaillard, Anna-Kari Trondman, and Esther Githumbi. This is a contribution to the Swedish
997 Strategic Research Area (SRA) MERGE (Modelling the Regional and Global Earth system; www.merge.lu.se) and to the Past
998 Global Change (PAGES) project and its working group LandCover6k (<http://pastglobalchanges.org/landcover6k>) that in turn
999 received support from the Swiss National Science Foundation, the Swiss Academy of Sciences, the US National Science
1000 Foundation, and the Chinese Academy of Sciences. Anneli Poska was supported by the ESF project number PRG323. We
1001 thank Sandy Harrison (University of Reading, UK) for providing the pollen records from the EMBSeCBIO project. The work
1002 of the data contributors to - and the database managers of ALPADABA (<https://www.neotomadb.org/>), EMBSECBIO
1003 (<https://research.reading.ac.uk/palaeoclimate/embsecbio/>), EPD (<http://www.europeanpollendatabase.net/index.php>),
1004 LandClimI (Trondman et al., 2015), PALY CZ (<https://botany.natur.cuni.cz/palycz/>), and PALEOPYR ([http://paleopyr.univ-](http://paleopyr.univ-tlse2.fr/)
1005 [tlse2.fr/](http://paleopyr.univ-tlse2.fr/)) is gratefully acknowledged.

1006 **References**

- 1007 Abraham, V. and Kozáková, R.: Relative pollen productivity estimates in the modern agricultural landscape of Central
1008 Bohemia (Czech Republic), *Rev. Palaeobot. Palynol.*, 179, 1–12, doi:10.1016/j.revpalbo.2012.04.004, 2012.
- 1009 Abraham, V., Oušková, V. and Kuneš, P.: Present-Day Vegetation Helps Quantifying Past Land Cover in Selected Regions of
1010 the Czech Republic, edited by B. Bond-Lamberty, *PLoS One*, 9(6), e100117, doi:10.1371/journal.pone.0100117, 2014.
- 1011 Andersen, S. T.: The relative pollen productivity and pollen representation of north European trees, and correction factors for
1012 tree pollen spectra, *Danmarks Geol. Undersogelse II*, 96, 99, 1970.
- 1013 Baker, A. G., Zimny, M., Keczyński, A., Bhagwat, S. A., Willis, K. J. and Latałowa, M.: Pollen productivity estimates from
1014 old-growth forest strongly differ from those obtained in cultural landscapes: Evidence from the Białowieża National Park,
1015 Poland, *The Holocene*, 26(1), 80–92, doi:10.1177/0959683615596822, 2016.
- 1016 Barnosky, A. D., Hadly, E. A., Bascombe, J., Berlow, E. L., Brown, J. H., Fortelius, M., Getz, W. M., Harte, J., Hastings, A.,
1017 Marquet, P. A., Martinez, N. D., Mooers, A., Roopnarine, P., Vermeij, G., Williams, J. W., Gillespie, R., Kitzes, J., Marshall,
1018 C., Matzke, N., Mindell, D. P., Revilla, E. and Smith, A. B.: Approaching a state shift in Earth’s biosphere, *Nature*, 486(7401),
1019 52–58, doi:10.1038/nature11018, 2012.
- 1020 Beug, H. J.: Leitfaden der Pollenbestimmung für Mitteleuropa und angrenzende Gebiete (Guide to pollen determination for
1021 Central Europe and neighboring areas)., Verlag Dr. Friedrich Pfeil., 2004.
- 1022 Broström, A., Sugita, S. and Gaillard, M.-J.: Pollen productivity estimates for the reconstruction of past vegetation cover in
1023 the cultural landscape of southern Sweden, *The Holocene*, 14(3), 368–381, doi:10.1191/0959683604hl713rp, 2004.

1024 Broström, A., Sugita, S., Gaillard, M.-J. and Pilesjö, P.: Estimating the spatial scale of pollen dispersal in the cultural landscape
1025 of southern Sweden, *The Holocene*, 15(2), 252–262, doi:10.1191/0959683605hl790rp, 2005.

1026 Broström, A., Nielsen, A. B., Gaillard, M.-J., Hjelle, K., Mazier, F., Binney, H., Bunting, J., Fyfe, R., Meltsov, V., Poska, A.,
1027 Räsänen, S., Soepboer, W., von Stedingk, H., Suutari, H. and Sugita, S.: Pollen productivity estimates of key European plant
1028 taxa for quantitative reconstruction of past vegetation: a review, *Veg. Hist. Archaeobot.*, 17(5), 461–478, doi:10.1007/s00334-
1029 008-0148-8, 2008.

1030 Bunting, M. J., Armitage, R., Binney, H. A. and Waller, M.: Estimates of ‘relative pollen productivity’ and ‘relevant source
1031 area of pollen’ for major tree taxa in two Norfolk (UK) woodlands, *The Holocene*, 15(3), 459–465,
1032 doi:10.1191/0959683605hl821rr, 2005.

1033 Bunting, M. J., Schofield, J. E. and Edwards, K. J.: Estimates of relative pollen productivity (RPP) for selected taxa from
1034 southern Greenland: A pragmatic solution, *Rev. Palaeobot. Palynol.*, 190, 66–74, doi:10.1016/j.revpalbo.2012.11.003, 2013a.

1035 Bunting, M. J., Farrell, M., Broström, A., Hjelle, K. L., Mazier, F., Middleton, R., Nielsen, A. B., Rushton, E., Shaw, H. and
1036 Twiddle, C. L.: Palynological perspectives on vegetation survey: a critical step for model-based reconstruction of Quaternary
1037 land cover, *Quat. Sci. Rev.*, 82, 41–55, doi:10.1016/j.quascirev.2013.10.006, 2013b.

1038 Commerford, J. L., McLauchlan, K. K. and Sugita, S.: Calibrating Vegetation Cover and Grassland Pollen Assemblages in the
1039 Flint Hills of Kansas, USA, *Am. J. Plant Sci.*, 04(07), 1–10, doi:10.4236/ajps.2013.47A1001, 2013.

1040 Cui, Q.-Y., Gaillard, M.-J., Lemdahl, G., Sugita, S., Greisman, A., Jacobson, G. L. and Olsson, F.: The role of tree composition
1041 in Holocene fire history of the hemiboreal and southern boreal zones of southern Sweden, as revealed by the application of the
1042 Landscape Reconstruction Algorithm: Implications for biodiversity and climate-change issues, *The Holocene*, 23(12), 1747–
1043 1763, doi:10.1177/0959683613505339, 2013.

1044 Cui, Q., Gaillard, M., Lemdahl, G., Stenberg, L., Sugita, S. and Zernova, G.: Historical land-use and landscape change in
1045 southern Sweden and implications for present and future biodiversity, *Ecol. Evol.*, 4(18), 3555–3570, doi:10.1002/ece3.1198,
1046 2014.

1047 Davis, B. A. S., Collins, P. M. and Kaplan, J. O.: The age and post-glacial development of the modern European vegetation: a
1048 plant functional approach based on pollen data, *Veg. Hist. Archaeobot.*, 24(2), 303–317, doi:10.1007/s00334-014-0476-9,
1049 2015.

1050 Davis, M. B.: On the theory of pollen analysis, *Am. J. Sci.*, 261(10), 897–912, doi:10.2475/ajs.261.10.897, 1963.

1051 Dawson, A., Cao, X., Chaput, M., Hopla, E., Li, F., Edwards, M., Fyfe, R., Gajewski, K., Goring, S. J., Herzsuh, U., Mazier,
1052 F., Sugita, S., Williams, J. W., Xu, Q. and Gaillard, M.-J.: Finding the magnitude of human-induced Northern Hemisphere
1053 land-cover transformation between 6 and 0.2 ka BP, *Past Glob. Chang. Mag.*, 26(1), 34–35, doi:10.22498/pages.26.1.34, 2018.

1054 Dickson, C.: Distinguishing cereal from wild grass pollen: some limitations, *Circaea*, 5, 67–71, 1988.

1055 Downs, P. W. and Piégay, H.: Catchment-scale cumulative impact of human activities on river channels in the late
1056 Anthropocene: implications, limitations, prospect, *Geomorphology*, 338, 88–104, doi:10.1016/j.geomorph.2019.03.021, 2019.

1057 Edwards, K. J., Fyfe, R. and Jackson, S. T.: The first 100 years of pollen analysis, *Nat. Plants*, 3(2), 17001,

1058 doi:10.1038/nplants.2017.1, 2017.

1059 Ellis, E. C.: Ecology in an anthropogenic biosphere, *Ecol. Monogr.*, 85(3), 287–331, doi:10.1890/14-2274.1, 2015.

1060 Feurdean, A., Vanni re, B., Finsinger, W., Warren, D., Connor, S. C., Forrest, M., Liakka, J., Panait, A., Werner, C., Andri ,

1061 M., Bobek, P., Carter, V. A., Davis, B., Diaconu, A.-C., Dietze, E., Feeser, I., Florescu, G., Ga ka, M., Giesecke, T., Jahns, S.,

1062 Jamrichova, E., Kajuka o, K., Kaplan, J., Karpi nska-Ko aczek, M., Ko aczek, P., Kune , P., Kupriyanov, D., Lamentowicz,

1063 M., Lemmen, C., Magyari, E. K., Marcisz, K., Marinova, E., Niamir, A., Novenko, E., Obremaska, M., P dziszewska, A.,

1064 Pfeiffer, M., Poska, A., R sch, M., S owi nski, M., Stan kai t , M., Szal, M.,  wi ta-Musznicka, J., Tan au, I., Theuerkauf, M.,

1065 Tonkov, S., Valk , O., Vassiljev, J., Veski, S., Vincze, I., Wacnik, A., Wiethold, J. and Hickler, T.: Fire hazard modulation by

1066 long-term dynamics in land cover and dominant forest type in eastern and central Europe, *Biogeosciences*, 17(5), 1213–1230,

1067 doi:10.5194/bg-17-1213-2020, 2020.

1068 Foley, J. A.: Global Consequences of Land Use, *Science* (80-.), 309(5734), 570–574, doi:10.1126/science.1111772, 2005.

1069 Fyfe, R., de Beaulieu, J.-L., Binney, H., Bradshaw, R. H. W., Brewer, S., Le Flao, A., Finsinger, W., Gaillard, M.-J., Giesecke,

1070 T., Gil-Romera, G., Grimm, E. C., Huntley, B., Kunes, P., K hl, N., Leydet, M., Lotter, A. F., Tarasov, P. E. and Tonkov, S.:

1071 The European Pollen Database: past efforts and current activities, *Veg. Hist. Archaeobot.*, 18(5), 417–424,

1072 doi:10.1007/s00334-009-0215-9, 2009.

1073 Fyfe, R., Roberts, N. and Woodbridge, J.: A pollen-based pseudobiomisation approach to anthropogenic land-cover change,

1074 *The Holocene*, 20(7), 1165–1171, doi:10.1177/0959683610369509, 2010.

1075 Fyfe, R., Twiddle, C., Sugita, S., Gaillard, M. J., Barratt, P., Caseldine, C. J., Dodson, J., Edwards, K. J., Farrell, M., Froyd,

1076 C., Grant, M. J., Huckerby, E., Innes, J. B., Shaw, H. and Waller, M.: The Holocene vegetation cover of Britain and Ireland:

1077 Overcoming problems of scale and discerning patterns of openness, *Quat. Sci. Rev.*, 73, 132–148,

1078 doi:10.1016/j.quascirev.2013.05.014, 2013.

1079 Fyfe, R. M., Woodbridge, J. and Roberts, N.: From forest to farmland: pollen-inferred land cover change across Europe using

1080 the pseudobiomization approach, *Glob. Chang. Biol.*, 21(3), 1197–1212, doi:10.1111/gcb.12776, 2015.

1081 Fyfe, R. M., Woodbridge, J. and Roberts, C. N.: Trajectories of change in Mediterranean Holocene vegetation through

1082 classification of pollen data, *Veg. Hist. Archaeobot.*, 27(2), 351–364, doi:10.1007/s00334-017-0657-4, 2018.

1083 Fyfe, R. M., Githumbi, E., Trondmann, A.-K., Mazier, F., Nielsen, A. B., Poska, A., Sugita, S., Woodbridge, J., Contributors,

1084 L. and Gaillard, M.-J.: A full Holocene record of transient gridded vegetation cover in Europe, *Pangaea*,

1085 doi:https://doi.pangaea.de/10.1594/PANGAEA.937075, 2022.

1086 Gaillard, M.-J., Sugita, S., Bunting, M. J., Middleton, R., Brostr m, A., Caseldine, C., Giesecke, T., Hellman, S. E. V., Hicks,

1087 S., Hjelle, K., Langdon, C., Nielsen, A.-B., Poska, A., von Stedingk, H. and Veski, S.: The use of modelling and simulation

1088 approach in reconstructing past landscapes from fossil pollen data: a review and results from the POLLANDCAL network,

1089 *Veg. Hist. Archaeobot.*, 17(5), 419–443, doi:10.1007/s00334-008-0169-3, 2008.

1090 Gaillard, M.-J., Sugita, S., Mazier, F., Trondman, A.-K., Brostr m, A., Hickler, T., Kaplan, J. O., Kjellstr m, E., Kokfelt, U.,

1091 Kune , P., Lemmen, C., Miller, P., Olofsson, J., Poska, A., Rundgren, M., Smith, B., Strandberg, G., Fyfe, R., Nielsen, A. B.,

1092 Alenius, T., Balakauskas, L., Barnekow, L., Birks, H. J. B. B., Bjune, A., Björkman, L., Giesecke, T., Hjelle, K., Kalnina, L.,
1093 Kangur, M., van der Knaap, W. O., Koff, T., Lagerås, P., Latałowa, M., Leydet, M., Lechterbeck, J., Lindbladh, M., Odgaard,
1094 B., Peglar, S., Segerström, U., von Stedingk, H. and Seppä, H.: Holocene land-cover reconstructions for studies on land cover-
1095 climate feedbacks, *Clim. Past*, 6(4), 483–499, doi:10.5194/cp-6-483-2010, 2010a.

1096 Gaillard, M.-J., Kleinen, T., Samuelsson, P., Nielsen, A. B., Bergh, J., Kaplan, J. O., Poska, A., Sandström, C., Strandberg,
1097 G., Trondman, A.-K. and Wramneby, A.: Second Assessment of Climate Change for the Baltic Sea Basin, edited by The
1098 BACC II Author Team, Springer International Publishing, Cham., 2015.

1099 Gaillard, M. J., Sugita, S., Rundgren, M., Smith, B., Mazier, F., Trondman, A.-K., Fyfe, R., Kokfelt, U., Nielsen, A.-B.,
1100 Strandberg, G. and Team, L. members: Pollen-inferred quantitative reconstructions of Holocene land-cover in NW Europe for
1101 the evaluation of past climate-vegetation feedbacks - The Swedish LANDCLIM project and the NordForsk LANDCLIM
1102 network, *Geophys. Res. Abstr.*, 12(April 2010), 3–4, 2010b.

1103 Gaillard, M. J., Morrison, K. D., Madella, M. and Whitehouse, N.: Editorial: Past land-use and land-cover change: the
1104 challenge of quantification at the subcontinental to global scales, *Past Glob. Chang. Mag.*, 26(1), 3–3,
1105 doi:10.22498/pages.26.1.3, 2018.

1106 Giesecke, T., Davis, B., Brewer, S., Finsinger, W., Wolters, S., Blaauw, M., de Beaulieu, J.-L., Binney, H., Fyfe, R. M.,
1107 Gaillard, M.-J., Gil-Romera, G., van der Knaap, W. O., Kuneš, P., Kühl, N., van Leeuwen, J. F. N. N., Leydet, M., Lotter, A.
1108 F., Ortu, E., Semmler, M. and Bradshaw, R. H. W. W.: Towards mapping the late Quaternary vegetation change of Europe,
1109 *Veg. Hist. Archaeobot.*, 23(1), 75–86, doi:10.1007/s00334-012-0390-y, 2014.

1110 Gilgen, A., Wilkenskjeld, S., Kaplan, J. O., Kühn, T. and Lohmann, U.: Effects of land use and anthropogenic aerosol
1111 emissions in the Roman Empire, *Clim. Past*, 15(5), 1885–1911, doi:10.5194/cp-15-1885-2019, 2019.

1112 Githumbi, E., Fyfe, R., Kjellström, E., Lindström, J., Lu, Z., Mazier, F., Nielsen, A. B., Poska, A., Smith, B., Strandberg, G.,
1113 Sugita, S., Zhang, Q. and Gaillard, M.-J.: Holocene quantitative pollen-based vegetation reconstructions in Europe for climate
1114 modelling: LandClim II, in INQUA 2019: Life on the Edge, Dublin. [online] Available from:
1115 [https://portal.research.lu.se/portal/en/publications/holocene-quantitative-pollenbased-vegetation-reconstructions-in-europe-](https://portal.research.lu.se/portal/en/publications/holocene-quantitative-pollenbased-vegetation-reconstructions-in-europe-for-climate-modelling-landclim-ii(46cc8471-f51c-4117-a7c6-ccff00638e82)/export.html)
1116 [for-climate-modelling-landclim-ii\(46cc8471-f51c-4117-a7c6-ccff00638e82\)/export.html](https://portal.research.lu.se/portal/en/publications/holocene-quantitative-pollenbased-vegetation-reconstructions-in-europe-for-climate-modelling-landclim-ii(46cc8471-f51c-4117-a7c6-ccff00638e82)/export.html) (Accessed 9 August 2021), 2019.

1117 Gregory, P.: Spores: their properties and sedimentation in still air. *Microbiology of the atmosphere. A plant science*
1118 *monograph*, 1973.

1119 Grindean, R., Nielsen, A. B., Tanțău, I. and Feurdean, A.: Relative pollen productivity estimates in the forest steppe landscape
1120 of southeastern Romania, *Rev. Palaeobot. Palynol.*, 264, 54–63, doi:10.1016/j.revpalbo.2019.02.007, 2019.

1121 Guiry, E., Beglane, F., Szpak, P., Schulting, R., McCormick, F. and Richards, M. P.: Anthropogenic changes to the Holocene
1122 nitrogen cycle in Ireland, *Sci. Adv.*, 4(6), eaas9383, doi:10.1126/sciadv.aas9383, 2018.

1123 Harrison, S. P., Gaillard, M. J., Stocker, B. D., Vander Linden, M., Klein Goldewijk, K., Boles, O., Braconnot, P., Dawson,
1124 A., Fluet-Chouinard, E., Kaplan, J. O., Kastner, T., Pausata, F. S. R., Robinson, E., Whitehouse, N. J., Madella, M. and
1125 Morrison, K. D.: Development and testing scenarios for implementing land use and land cover changes during the Holocene

1126 in Earth system model experiments, *Geosci. Model Dev.*, 13(2), 805–824, doi:10.5194/gmd-13-805-2020, 2020.

1127 He, F., Vavrus, S. J., Kutzbach, J. E., Ruddiman, W. F., Kaplan, J. O. and Krumhardt, K. M.: Simulating global and local
1128 surface temperature changes due to Holocene anthropogenic land cover change, *Geophys. Res. Lett.*, 41(2), 623–631,
1129 doi:10.1002/2013GL058085, 2014.

1130 Hellman, S., Gaillard, M.-J., Broström, A. and Sugita, S.: The REVEALS model, a new tool to estimate past regional plant
1131 abundance from pollen data in large lakes: validation in southern Sweden, *J. Quat. Sci.*, 23(1), 21–42, doi:10.1002/jqs.1126,
1132 2008a.

1133 Hellman, S. E. V., Gaillard, M., Broström, A. and Sugita, S.: Effects of the sampling design and selection of parameter values
1134 on pollen-based quantitative reconstructions of regional vegetation: a case study in southern Sweden using the REVEALS
1135 model, *Veg. Hist. Archaeobot.*, 17(5), 445–459, doi:10.1007/s00334-008-0149-7, 2008b.

1136 Hibbard, K., Janetos, A., van Vuuren, D. P., Pongratz, J., Rose, S. K., Betts, R., Herold, M. and Feddema, J. J.: Research
1137 priorities in land use and land-cover change for the Earth system and integrated assessment modelling, *Int. J. Climatol.*, 30(13),
1138 2118–2128, doi:10.1002/joc.2150, 2010.

1139 Hjelle, K. L.: Herb pollen representation in surface moss samples from mown meadows and pastures in western Norway, *Veg.*
1140 *Hist. Archaeobot.*, 7(2), 79–96, doi:10.1007/BF01373926, 1998.

1141 Hofman-Kamińska, E., Bocherens, H., Drucker, D. G., Fyfe, R. M., Gumiński, W., Makowiecki, D., Pacher, M., Piličiauskienė,
1142 G., Samojlik, T., Woodbridge, J. and Kowalczyk, R.: Adapt or die—Response of large herbivores to environmental changes
1143 in Europe during the Holocene, *Glob. Chang. Biol.*, 25(9), 2915–2930, doi:10.1111/gcb.14733, 2019.

1144 Huntley, B.: European vegetation history: Palaeovegetation maps from pollen data - 13 000 yr BP to present, *J. Quat. Sci.*,
1145 5(2), 103–122, doi:10.1002/jqs.3390050203, 1990.

1146 Kaplan, J., Krumhardt, K., Gaillard, M.-J., Sugita, S., Trondman, A.-K., Fyfe, R., Marquer, L., Mazier, F. and Nielsen, A.:
1147 Constraining the Deforestation History of Europe: Evaluation of Historical Land Use Scenarios with Pollen-Based Land Cover
1148 Reconstructions, *Land*, 6(4), 91, doi:10.3390/land6040091, 2017.

1149 Kaplan, J. O., Krumhardt, K. M. and Zimmermann, N.: The prehistoric and preindustrial deforestation of Europe, *Quat. Sci.*
1150 *Rev.*, 28(27–28), 3016–3034, doi:10.1016/j.quascirev.2009.09.028, 2009.

1151 Kaplan, J. O., Krumhardt, K. M., Ellis, E. C., Ruddiman, W. F., Lemmen, C. and Goldewijk, K. K.: Holocene carbon emissions
1152 as a result of anthropogenic land cover change, *The Holocene*, 21(5), 775–791, doi:10.1177/0959683610386983, 2011.

1153 Klein Goldewijk, K., Beusen, A., Doelman, J. and Stehfest, E.: Anthropogenic land use estimates for the Holocene – HYDE
1154 3.2, *Earth Syst. Sci. Data*, 9(2), 927–953, doi:10.5194/essd-9-927-2017, 2017.

1155 Kuneš, P., Abraham, V., Kovářik, O., Kopecký, M., Břízová, E., Dudová, L., Jankovská, V., Knipping, M., Kozšková, R.,
1156 Nováková, K., Petr, L., Pokorný, P., Roszková, A., Rybničková, E., Svobodová-Svitavská, H. and Wacnik, A.: Czech
1157 quaternary palynological Database - Palycz: review and basic statistics of the data, *Preslia*, 81(3), 209–238, 2009.

1158 Kuneš, P., Abraham, V., Werchan, B., Plesková, Z., Fajmon, K., Jamrichová, E. and Roleček, J.: Relative pollen productivity
1159 estimates for vegetation reconstruction in central-eastern Europe inferred at local and regional scales, *The Holocene*, 29(11),

1160 1708–1719, doi:10.1177/0959683619862026, 2019.

1161 Lerigoleur, E., Mazier, F., Jégou, L., Perret, M. and Galop, D.: PALEOPYR: un système d'information pour la gestion et
1162 l'exploitation de données palaeoenvironnementales sur le massif nord-pyrénéen. *Ingénierie des Systèmes d'Information* 3.
1163 [online] Available from: <http://paleopyr.univ-tlse2.fr/%0A>, 2015.

1164 Li, F., Gaillard, M.-J., Xu, Q., Bunting, M. J., Li, Y., Li, J., Mu, H., Lu, J., Zhang, P., Zhang, S., Cui, Q., Zhang, Y. and Shen,
1165 W.: A Review of Relative Pollen Productivity Estimates From Temperate China for Pollen-Based Quantitative Reconstruction
1166 of Past Plant Cover, *Front. Plant Sci.*, 9(September), doi:10.3389/fpls.2018.01214, 2018.

1167 Li, F., Gaillard, M.-J., Cao, X., Herzsuh, U., Sugita, S., Tarasov, P. E., Wagner, M., Xu, Q., Ni, J., Wang, W., Zhao, Y., An,
1168 C., Beusen, A. H. W., Chen, F., Feng, Z., Goldewijk, C. G. M. K., Huang, X., Li, Y., Li, Y., Liu, H., Sun, A., Yao, Y., Zheng,
1169 Z. and Jia, X.: Towards quantification of Holocene anthropogenic land-cover change in temperate China: A review in the light
1170 of pollen-based REVEALS reconstructions of regional plant cover, *Earth-Science Rev.*, 203(February), 103119,
1171 doi:10.1016/j.earscirev.2020.103119, 2020.

1172 Marinova, E., Harrison, S. P., Bragg, F., Connor, S., Laet, V., Leroy, S. A. G., Mudie, P., Atanassova, J., Bozilova, E., Caner,
1173 H., Cordova, C., Djamali, M., Filipova-Marinova, M., Gerasimenko, N., Jahns, S., Kouli, K., Kotthoff, U., Kvavadze, E.,
1174 Lazarova, M., Novenko, E., Ramezani, E., Röpke, A., Shumilovskikh, L., Tanțău, I. and Tonkov, S.: Pollen-derived biomes
1175 in the Eastern Mediterranean–Black Sea–Caspian–Corridor, *J. Biogeogr.*, 45(2), 484–499, doi:10.1111/jbi.13128, 2018.

1176 Marquer, L., Gaillard, M.-J., Sugita, S., Trondman, A.-K., Mazier, F., Nielsen, A. B., Fyfe, R., Odgaard, B. V., Alenius, T.,
1177 Birks, H. J. B., Bjune, A. E., Christiansen, J., Dodson, J., Edwards, K. J., Giesecke, T., Herzsuh, U., Kangur, M., Lorenz,
1178 S., Poska, A., Schult, M. and Seppä, H.: Holocene changes in vegetation composition in northern Europe: why quantitative
1179 pollen-based vegetation reconstructions matter, *Quat. Sci. Rev.*, 90, 199–216, doi:10.1016/j.quascirev.2014.02.013, 2014.

1180 Marquer, L., Gaillard, M.-J., Sugita, S., Poska, A., Trondman, A.-K., Mazier, F., Nielsen, A. B., Fyfe, R., Jönsson, A. M.,
1181 Smith, B., Kaplan, J. O., Alenius, T., Birks, H. J. B. J. B., Bjune, A. E., Christiansen, J., Dodson, J., Edwards, K. J., Giesecke,
1182 T., Herzsuh, U., Kangur, M., Koff, T., Latałowa, M., Lechterbeck, J., Olofsson, J. and Seppä, H.: Quantifying the effects of
1183 land use and climate on Holocene vegetation in Europe, *Quat. Sci. Rev.*, 171, 20–37, doi:10.1016/j.quascirev.2017.07.001,
1184 2017.

1185 Marquer, L., Mazier, F., Sugita, S., Galop, D., Houet, T., Faure, E., Gaillard, M.-J., Haunold, S., de Munnik, N., Simonneau,
1186 A., De Vleeschouwer, F. and Le Roux, G.: Pollen-based reconstruction of Holocene land-cover in mountain regions:
1187 Evaluation of the Landscape Reconstruction Algorithm in the Vicdessos valley, northern Pyrenees, France, *Quat. Sci. Rev.*,
1188 228, 106049, doi:10.1016/j.quascirev.2019.106049, 2020.

1189 Matthias, I., Nielsen, A. B. and Giesecke, T.: Evaluating the effect of flowering age and forest structure on pollen productivity
1190 estimates, *Veg. Hist. Archaeobot.*, 21(6), 471–484, doi:10.1007/s00334-012-0373-z, 2012.

1191 Mazier, F., Broström, A., Gaillard, M.-J., Sugita, S., Vittoz, P. and Buttler, A.: Pollen productivity estimates and relevant
1192 source area of pollen for selected plant taxa in a pasture woodland landscape of the Jura Mountains (Switzerland), *Veg. Hist.*
1193 *Archaeobot.*, 17(5), 479–495, doi:10.1007/s00334-008-0143-0, 2008.

1194 Mazier, F., Gaillard, M. J., Kunes, P., Sugita, S., Trondman, A.-K. and Brostrom, A.: Testing the effect of site selection and
1195 parameter setting on REVEALS-model estimates of plant abundance using th Czech Quaternary Palynological database
1196 Testing the effect of site selection and parameter setting on REVEALS-model estimates of plant abunda, *Rev. Palaeobot.*
1197 *Palynol.*, 187, 38–49 [online] Available from: <https://halshs.archives-ouvertes.fr/halshs-00959845>, 2012.

1198 Mazier, F., Broström, A., Bragée, P., Fredh, D., Stenberg, L., Thiere, G., Sugita, S. and Hammarlund, D.: Two hundred years
1199 of land-use change in the South Swedish Uplands: comparison of historical map-based estimates with a pollen-based
1200 reconstruction using the landscape reconstruction algorithm, *Veg. Hist. Archaeobot.*, 24(5), 555–570, doi:10.1007/s00334-
1201 015-0516-0, 2015.

1202 McLauchlan, K. K., Williams, J. J., Craine, J. M. and Jeffers, E. S.: Changes in global nitrogen cycling during the Holocene
1203 epoch, *Nature*, 495(7441), 352–355, doi:10.1038/nature11916, 2013.

1204 Mehl, I. K., Overland, A., Berge, J. and Hjelle, K. L.: Cultural landscape development on a west–east gradient in western
1205 Norway – potential of the Landscape Reconstruction Algorithm (LRA), *J. Archaeol. Sci.*, 61, 1–16,
1206 doi:10.1016/j.jas.2015.04.015, 2015.

1207 Morrison, K. D., Hammer, E., Boles, O., Madella, M., Whitehouse, N., Gaillard, M.-J., Bates, J., Vander Linden, M., Merlo,
1208 S., Yao, A., Popova, L., Hill, A. C., Antolin, F., Bauer, A., Biagetti, S., Bishop, R. R., Buckland, P., Cruz, P., Dreslerová, D.,
1209 Dusseldorp, G., Ellis, E., Filipovic, D., Foster, T., Hannaford, M. J., Harrison, S. P., Hazarika, M., Herold, H., Hilpert, J.,
1210 Kaplan, J. O., Kay, A., Klein Goldewijk, K., Kolář, J., Kyazike, E., Laabs, J., Lancelotti, C., Lane, P., Lawrence, D., Lewis,
1211 K., Lombardo, U., Lucarini, G., Arroyo-Kalin, M., Marchant, R., Mayle, F., McClatchie, M., McLeester, M., Mooney, S.,
1212 Moskal-del Hoyo, M., Navarrete, V., Ndiema, E., Góes Neves, E., Nowak, M., Out, W. A., Petrie, C., Phelps, L. N., Pinke, Z.,
1213 Rostain, S., Russell, T., Sluyter, A., Styring, A. K., Tamanaha, E., Thomas, E., Veerasamy, S., Welton, L. and Zanon, M.:
1214 Mapping past human land use using archaeological data: A new classification for global land use synthesis and data
1215 harmonization, edited by J. Freeman, *PLoS One*, 16(4), e0246662, doi:10.1371/journal.pone.0246662, 2021.

1216 Nielsen, A. B.: Modelling pollen sedimentation in Danish lakes at c.ad 1800: an attempt to validate the POLLSCAPE model,
1217 *J. Biogeogr.*, 31(10), 1693–1709, doi:10.1111/j.1365-2699.2004.01080.x, 2004.

1218 Nielsen, A. B. and Odgaard, B. V.: Quantitative landscape dynamics in Denmark through the last three millennia based on the
1219 Landscape Reconstruction Algorithm approach, *Veg. Hist. Archaeobot.*, 19(4), 375–387, doi:10.1007/s00334-010-0249-z,
1220 2010.

1221 Nielsen, A. B., Giesecke, T., Theuerkauf, M., Feeser, I., Behre, K.-E., Beug, H.-J., Chen, S.-H., Christiansen, J., Dörfler, W.,
1222 Endtmann, E., Jahns, S., de Klerk, P., Kühl, N., Latałowa, M., Odgaard, B. V., Rasmussen, P., Stockholm, J. R., Voigt, R.,
1223 Wiethold, J. and Wolters, S.: Quantitative reconstructions of changes in regional openness in north-central Europe reveal new
1224 insights into old questions, *Quat. Sci. Rev.*, 47, 131–149, doi:10.1016/j.quascirev.2012.05.011, 2012.

1225 Nosova, M. B., Novenko, E. Y., Severova, E. E. and Volkova, O. A.: Vegetation and climate changes within and around the
1226 Polistovo-Lovatskaya mire system (Pskov Oblast, north-western Russia) during the past 10,500 years, *Veg. Hist. Archaeobot.*,
1227 28(2), 123–140, doi:10.1007/s00334-018-0693-8, 2018.

1228 Palmisano, A., Woodbridge, J., Roberts, C. N., Bevan, A., Fyfe, R., Shennan, S., Cheddadi, R., Greenberg, R., Kaniewski, D.,
1229 Langgut, D., Leroy, S. A. G., Litt, T. and Miebach, A.: Holocene landscape dynamics and long-term population trends in the
1230 Levant, *The Holocene*, 29(5), 708–727, doi:10.1177/0959683619826642, 2019.

1231 Parsons, R. W. and Prentice, I. C.: Statistical approaches to R-values and the pollen—vegetation relationship, *Rev. Palaeobot.*
1232 *Palynol.*, 32(2–3), 127–152, doi:10.1016/0034-6667(81)90001-4, 1981.

1233 Pinhasi, R., Fort, J. and Ammerman, A. J.: Tracing the origin and spread of agriculture in Europe, *PLoS Biol.*, 3(12), 1–9,
1234 doi:10.1371/journal.pbio.0030410, 2005.

1235 Pirzamanbein, B., Lindström, J., Poska, A., Sugita, S., Trondman, A.-K., Fyfe, R., Mazier, F., Nielsen, A. B., Kaplan, J. O.,
1236 Bjune, A. E., Birks, H. J. B., Giesecke, T., Kangur, M., Latałowa, M., Marquer, L., Smith, B. and Gaillard, M.-J.: Creating
1237 spatially continuous maps of past land cover from point estimates: A new statistical approach applied to pollen data, *Ecol.*
1238 *Complex.*, 20, 127–141, doi:10.1016/j.ecocom.2014.09.005, 2014.

1239 Pirzamanbein, B., Lindström, J., Poska, A. and Gaillard, M. J.: Modelling Spatial Compositional Data: Reconstructions of past
1240 land cover and uncertainties, *Spat. Stat.*, 24, 14–31, doi:10.1016/j.spasta.2018.03.005, 2018.

1241 Pirzamanbein, B., Poska, A. and Lindström, J.: Bayesian Reconstruction of Past Land Cover From Pollen Data: Model
1242 Robustness and Sensitivity to Auxiliary Variables, *Earth Sp. Sci.*, 7(1), doi:10.1029/2018EA000547, 2020.

1243 Poska, A., Meltsov, V., Sugita, S. and Vassiljev, J.: Relative pollen productivity estimates of major anemophilous taxa and
1244 relevant source area of pollen in a cultural landscape of the hemi-boreal forest zone (Estonia), *Rev. Palaeobot. Palynol.*, 167(1–
1245 2), 30–39, doi:10.1016/j.revpalbo.2011.07.001, 2011.

1246 Prentice, C.: Records of vegetation in time and space: the principles of pollen analysis, in *Vegetation history*, pp. 17–42,
1247 Springer Netherlands, Dordrecht., 1988.

1248 Prentice, C., Guiot, J., Huntley, B., Jolly, D. and Cheddadi, R.: Reconstructing biomes from palaeoecological data: a general
1249 method and its application to European pollen data at 0 and 6 ka, *Clim. Dyn.*, 12(3), 185–194, doi:10.1007/BF00211617, 1996.

1250 Prentice, I. C.: Pollen Representation, Source Area, and Basin Size: Toward a Unified Theory of Pollen Analysis, *Quat. Res.*,
1251 23(1), 76–86, doi:10.1016/0033-5894(85)90073-0, 1985.

1252 Prentice, I. C. and Parsons, R. W. A.: Maximum Likelihood Linear Calibration of Pollen Spectra in Terms of Forest
1253 Composition, *Biometrics*, 39(4), 1051–1057, doi:10.2307/2531338, 1983.

1254 Prentice, I. C. and Webb III, T.: BIOME 6000: reconstructing global mid-Holocene vegetation patterns from palaeoecological
1255 records, *J. Biogeogr.*, 25(6), 997–1005, doi:10.1046/j.1365-2699.1998.00235.x, 1998.

1256 Räsänen, S., Suutari, H. and Nielsen, A. B.: A step further towards quantitative reconstruction of past vegetation in
1257 Fennoscandian boreal forests: Pollen productivity estimates for six dominant taxa, *Rev. Palaeobot. Palynol.*, 146(1–4), 208–
1258 220, doi:10.1016/j.revpalbo.2007.04.004, 2007.

1259 Roberts, C. N., Woodbridge, J., Palmisano, A., Bevan, A., Fyfe, R. and Shennan, S.: Mediterranean landscape change during
1260 the Holocene: Synthesis, comparison and regional trends in population, land cover and climate, *The Holocene*, 29(5), 923–
1261 937, doi:10.1177/0959683619826697, 2019.

1262 Roberts, N., Fyfe, R. M., Woodbridge, J., Gaillard, M.-J., Davis, B. A. S. S., Kaplan, J. O., Marquer, L., Mazier, F., Nielsen,
1263 A. B., Sugita, S., Trondman, A.-K. and Leydet, M.: Europe's lost forests: a pollen-based synthesis for the last 11,000 years,
1264 *Sci. Rep.*, 8(1), 716, doi:10.1038/s41598-017-18646-7, 2018.

1265 Ruddiman, W. F.: The Anthropogenic Greenhouse Era Began Thousands of Years Ago, *Clim. Change*, 61(3), 261–293,
1266 doi:10.1023/B:CLIM.0000004577.17928.fa, 2003.

1267 Ruddiman, W. F., Fuller, D. Q., Kutzbach, J. E., Tzedakis, P. C., Kaplan, J. O., Ellis, E. C., Vavrus, S. J., Roberts, C. N., Fyfe,
1268 R., He, F., Lemmen, C. and Woodbridge, J.: Late Holocene climate: Natural or anthropogenic?, *Rev. Geophys.*, 54(1), 93–
1269 118, doi:10.1002/2015RG000503, 2016.

1270 Schauer, P., Shennan, S., Bevan, A., Cook, G., Edinborough, K., Fyfe, R., Kerig, T. and Parker Pearson, M.: Supply and
1271 demand in prehistory? Economics of Neolithic mining in northwest Europe, *J. Anthropol. Archaeol.*, 54, 149–160,
1272 doi:10.1016/j.jaa.2019.03.001, 2019.

1273 Shennan, S.: *The First Farmers of Europe An Evolutionary Perspective*, Cambridge University Press, Cambridge. [online]
1274 Available from: [https://www-cambridge-org.proxy.lnu.se/se/academic/subjects/archaeology/archaeology-europe-and-near-](https://www-cambridge-org.proxy.lnu.se/se/academic/subjects/archaeology/archaeology-europe-and-near-and-middle-east/first-farmers-europe-evolutionary-perspective?format=HB&isbn=9781108422925)
1275 [and-middle-east/first-farmers-europe-evolutionary-perspective?format=HB&isbn=9781108422925](https://www-cambridge-org.proxy.lnu.se/se/academic/subjects/archaeology/archaeology-europe-and-near-and-middle-east/first-farmers-europe-evolutionary-perspective?format=HB&isbn=9781108422925), 2018.

1276 Smith, P., Davis, S. J., Creutzig, F., Fuss, S., Minx, J., Gabrielle, B., Kato, E., Jackson, R. B., Cowie, A., Kriegler, E., van
1277 Vuuren, D. P., Rogelj, J., Ciais, P., Milne, J., Canadell, J. G., McCollum, D., Peters, G., Andrew, R., Krey, V., Shrestha, G.,
1278 Friedlingstein, P., Gasser, T., Grübler, A., Heidug, W. K., Jonas, M., Jones, C. D., Kraxner, F., Littleton, E., Lowe, J., Moreira,
1279 J. R., Nakicenovic, N., Obersteiner, M., Patwardhan, A., Rogner, M., Rubin, E., Sharifi, A., Torvanger, A., Yamagata, Y.,
1280 Edmonds, J. and Yongsung, C.: Biophysical and economic limits to negative CO₂ emissions, *Nat. Clim. Chang.*, 6(1), 42–50,
1281 doi:10.1038/nclimate2870, 2016.

1282 Soepboer, W., Sugita, S., Lotter, A. F., van Leeuwen, J. F. N. and van der Knaap, W. O.: Pollen productivity estimates for
1283 quantitative reconstruction of vegetation cover on the Swiss Plateau, *The Holocene*, 17(1), 65–77,
1284 doi:10.1177/0959683607073279, 2007.

1285 Soepboer, W., Sugita, S. and Lotter, A. F.: Regional vegetation-cover changes on the Swiss Plateau during the past two
1286 millennia: A pollen-based reconstruction using the REVEALS model, *Quat. Sci. Rev.*, 29(3–4), 472–483,
1287 doi:10.1016/j.quascirev.2009.09.027, 2010.

1288 von Stedingk, H., Fyfe, R. M. and Allard, A.: Pollen productivity estimates from the forest—tundra ecotone in west-central
1289 Sweden: implications for vegetation reconstruction at the limits of the boreal forest, *The Holocene*, 18(2), 323–332,
1290 doi:10.1177/0959683607086769, 2008.

1291 Stephens, L., Fuller, D., Boivin, N., Rick, T., Gauthier, N., Kay, A., Marwick, B., Armstrong, C. G., Barton, C. M., Denham,
1292 T., Douglass, K., Driver, J., Janz, L., Roberts, P., Rogers, J. D., Thakar, H., Altaweel, M., Johnson, A. L., Sampietro Vattuone,
1293 M. M., Aldenderfer, M., Archila, S., Artioli, G., Bale, M. T., Beach, T., Borrell, F., Braje, T., Buckland, P. I., Jiménez Cano,
1294 N. G., Capriles, J. M., Diez Castillo, A., Çilingiroğlu, Ç., Negus Cleary, M., Conolly, J., Coutros, P. R., Covey, R. A.,
1295 Cremaschi, M., Crowther, A., Der, L., di Lernia, S., Doershuk, J. F., Doolittle, W. E., Edwards, K. J., Erlandson, J. M., Evans,

1296 D., Fairbairn, A., Faulkner, P., Feinman, G., Fernandes, R., Fitzpatrick, S. M., Fyfe, R., Garcea, E., Goldstein, S., Goodman,
1297 R. C., Dalpoim Guedes, J., Herrmann, J., Hiscock, P., Hommel, P., Horsburgh, K. A., Hritz, C., Ives, J. W., Junno, A., Kahn,
1298 J. G., Kaufman, B., Kearns, C., Kidder, T. R., Lanoë, F., Lawrence, D., Lee, G.-A., Levin, M. J., Lindsoug, H. B., López-
1299 Sáez, J. A., Macrae, S., Marchant, R., Marston, J. M., McClure, S., McCoy, M. D., Miller, A. V., Morrison, M., Motuzaite
1300 Matuzeviciute, G., Müller, J., Nayak, A., Noerwidi, S., Peres, T. M., Peterson, C. E., Proctor, L., Randall, A. R., Renette, S.,
1301 Robbins Schug, G., Ryzewski, K., Saini, R., Scheinsohn, V., Schmidt, P., Sebillaud, P., Seitsonen, O., Simpson, I. A.,
1302 Sołtysiak, A., Speakman, R. J., Spengler, R. N., Steffen, M. L., et al.: Archaeological assessment reveals Earth's early
1303 transformation through land use, *Science* (80-.), 365(6456), 897–902, doi:10.1126/science.aax1192, 2019.
1304 Strandberg, G., Kjellström, E., Poska, A., Wagner, S., Gaillard, M.-J., Trondman, A.-K., Mauri, A., Davis, B. A. S. S., Kaplan,
1305 J. O., Birks, H. J. B. B., Bjune, A. E., Fyfe, R., Giesecke, T., Kalnina, L., Kangur, M., van der Knaap, W. O., Kokfelt, U.,
1306 Kuneš, P., Latašová, M., Marquer, L., Mazier, F., Nielsen, A. B., Smith, B., Seppä, H. and Sugita, S.: Regional climate
1307 model simulations for Europe at 6 and 0.2 k BP: sensitivity to changes in anthropogenic deforestation, *Clim. Past*, 10(2), 661–
1308 680, doi:10.5194/cp-10-661-2014, 2014.
1309 Stuart, A. and Ord, J. K.: *Kendall's advanced theory of statistics*, *Distrib. theory*, 1 [online] Available from:
1310 <https://ci.nii.ac.jp/naid/10004597057> (Accessed 2 July 2021), 1994.
1311 Sugita, S.: A Model of Pollen Source Area for an Entire Lake Surface, *Quat. Res.*, 39(2), 239–244,
1312 doi:10.1006/qres.1993.1027, 1993.
1313 Sugita, S.: Theory of quantitative reconstruction of vegetation I: pollen from large sites REVEALS regional vegetation
1314 composition, *The Holocene*, 17(2), 229–241, doi:10.1177/0959683607075837, 2007a.
1315 Sugita, S.: Theory of quantitative reconstruction of vegetation II: all you need is LOVE, *The Holocene*, 17(2), 243–257,
1316 doi:10.1177/0959683607075838, 2007b.
1317 Sugita, S., Gaillard, M.-J. and Broström, A.: Landscape openness and pollen records: a simulation approach, *The Holocene*,
1318 9(4), 409–421, doi:10.1191/095968399666429937, 1999.
1319 Sugita, S., Parshall, T., Calcote, R. and Walker, K.: Testing the Landscape Reconstruction Algorithm for spatially explicit
1320 reconstruction of vegetation in northern Michigan and Wisconsin, *Quat. Res.*, 74(2), 289–300,
1321 doi:10.1016/j.yqres.2010.07.008, 2010.
1322 Sun, A., Luo, Y., Wu, H., Chen, X., Li, Q., Yu, Y., Sun, X. and Guo, Z.: An updated biomization scheme and vegetation
1323 reconstruction based on a synthesis of modern and mid-Holocene pollen data in China, *Glob. Planet. Change*, 192(May 2019),
1324 103178, doi:10.1016/j.gloplacha.2020.103178, 2020.
1325 Sutton, O. .: *Micrometeorology*, *Q. J. R. Meteorol. Soc.*, 79(341), 457–457, doi:10.1002/qj.49707934125, 1953.
1326 Theuerkauf, M., Kuparinen, A. and Joosten, H.: Pollen productivity estimates strongly depend on assumed pollen dispersal,
1327 *The Holocene*, 23(1), 14–24, doi:10.1177/0959683612450194, 2012.
1328 Theuerkauf, M., Couwenberg, J., Kuparinen, A. and Liescher, V.: A matter of dispersal: REVEALSinR introduces state-of-
1329 the-art dispersal models to quantitative vegetation reconstruction, *Veg. Hist. Archaeobot.*, 25(6), doi:10.1007/s00334-016-

1330 0572-0, 2016.

1331 Trondman, A.-K., Gaillard, M.-J., Sugita, S., Björkman, L., Greisman, A., Hultberg, T., Lagerås, P., Lindbladh, M. and Mazier,
1332 F.: Are pollen records from small sites appropriate for REVEALS model-based quantitative reconstructions of past regional
1333 vegetation? An empirical test in southern Sweden, *Veg. Hist. Archaeobot.*, 25(2), 131–151, doi:10.1007/s00334-015-0536-9,
1334 2016.

1335 Trondman, A. K., Gaillard, M. J., Mazier, F., Sugita, S., Fyfe, R., Nielsen, A. B., Twiddle, C., Barratt, P., Birks, H. J. B.,
1336 Bjune, A. E., Björkman, L., Broström, A., Caseldine, C., David, R., Dodson, J., Dörfler, W., Fischer, E., van Geel, B., Giesecke,
1337 T., Hultberg, T., Kalnina, L., Kangur, M., van der Knaap, P., Koff, T., Kuneš, P., Lagerås, P., Latalowa, M., Lechterbeck, J.,
1338 Leroyer, C., Leydet, M., Lindbladh, M., Marquer, L., Mitchell, F. J. G., Odgaard, B. V., Peglar, S. M., Persson, T., Poska, A.,
1339 Rösch, M., Seppä, H., Veski, S. and Wick, L.: Pollen-based quantitative reconstructions of Holocene regional vegetation cover
1340 (plant-functional types and land-cover types) in Europe suitable for climate modelling, *Glob. Chang. Biol.*, 21(2), 676–697,
1341 doi:10.1111/gcb.12737, 2015.

1342 Twiddle, C. L., Jones, R. T., Caseldine, C. J. and Sugita, S.: Pollen productivity estimates for a pine woodland in eastern
1343 Scotland: The influence of sampling design and vegetation patterning, *Rev. Palaeobot. Palynol.*, 174, 67–78,
1344 doi:10.1016/j.revpalbo.2011.12.006, 2012.

1345 de Vareilles, A., Pelling, R., Woodbridge, J. and Fyfe, R.: Archaeology and agriculture: plants, people, and past land-use,
1346 *Trends Ecol. Evol.*, 36(10), 943–954, doi:10.1016/j.tree.2021.06.003, 2021.

1347 Wiczorek, M. and Herzschuh, U.: Compilation of relative pollen productivity (RPP) estimates and taxonomically harmonised
1348 RPP datasets for single continents and Northern Hemisphere extratropics, *Earth Syst. Sci. Data*, 12(4), 3515–3528,
1349 doi:10.5194/essd-12-3515-2020, 2020.

1350 Wolf, A., Callaghan, T. V. and Larson, K.: Future changes in vegetation and ecosystem function of the Barents Region, *Clim.*
1351 *Change*, 87(1–2), 51–73, doi:10.1007/s10584-007-9342-4, 2008.

1352 Woodbridge, J., Fyfe, R. M. and Roberts, N.: A comparison of remotely sensed and pollen-based approaches to mapping
1353 Europe’s land cover, edited by M. Bush, *J. Biogeogr.*, 41(11), 2080–2092, doi:10.1111/jbi.12353, 2014.

1354 Woodbridge, J., Fyfe, R., Roberts, C., Trondman, A., Mazier, F. and Davis, B.: European forest cover since the start of
1355 Neolithic agriculture: a critical comparison of pollen-based reconstructions, *Past Glob. Chang. Mag.*, 26(1), 10–11,
1356 doi:10.22498/pages.26.1.10, 2018.

1357 Zanon, M., Davis, B. A. S. S., Marquer, L., Brewer, S. and Kaplan, J. O.: European Forest Cover During the Past 12,000
1358 Years: A Palynological Reconstruction Based on Modern Analogs and Remote Sensing, *Front. Plant Sci.*, 9(March), 1–25,
1359 doi:10.3389/fpls.2018.00253, 2018.

1360